May 2017

Accelerated Quantum Dynamics

Morgan Henry Lynch
University of Wisconsin-Milwaukee

ACCELERATED QUANTUM DYNAMICS

by

Morgan H. Lynch

A Dissertation Submitted in

Partial Fulfillment of the

Requirements for the Degree of

Doctor of Philosophy

in Physics

at

The University of Wisconsin-Milwaukee

May 2017

ABSTRACT

ACCELERATED QUANTUM DYNAMICS

by

Morgan H. Lynch

The University of Wisconsin-Milwaukee, 2017
Under the Supervision of Professor Valerică Raicu

In this dissertation we develop a formalism for the computation of observables due to acceleration-induced particle physics processes. By using the spacetime structure produced by acceleration, we examine the properties of accelerated particle detectors as well as accelerated fields. General expressions for the transition rate, multiplicity, power, spectra, and displacement law of particles undergoing time-dependent acceleration and transitioning into a final state of arbitrary particle number are obtained. The transition rate, power, and spectra are characterized by unique polynomials of multiplicity and thermal distributions of both bosonic and fermionic statistics. The acceleration-dependent multiplicities are computed in terms of the branching fractions of the associated inertial processes. The displacement law of the spectra predicts that the energy of the emitted particles is directly proportional to the accelerated temperature.

TABLE OF CONTENTS

LIST OF FIGURES

ACKNOWLEDGEMENTS

A personal thanks goes to the UW-Milwaukee physics department. I transferred to Milwaukee hoping to pursue research in quantum field theory in curved spacetime and I am incredibly grateful that I was given the opportunity to do so. I was also surprised to learn that I was not the first to come here to study these things, and I am honored to be one of many physicists whose interests have brought them along this same path.

I am grateful to my committee for overseeing the progress of my research and for their support during the chaos leading up to my defense. I would like to thank my advisor, Valerică Raicu, for all of his help and advocacy during my time in graduate school. In particular, I am thankful for him allowing me the freedom to pursue my research interests and for assuming the responsibility of taking me as his student. I am also grateful for access to his laboratory to explore self-accelerating particles. I am indebted to Phil Chang for his advocacy as well. He has, with his own money, provided me with financial support and was instrumental in me getting my fellowship to work with Niayesh Afshordi at the Perimeter Institute. John Friedman helped me get started on my research and has been incredibly supportive throughout the entirety of my time at Milwaukee. Our many discussions on the Unruh effect helped me understand better the ideas necessary to complete my dissertation and I thank him for his interest and insight. I owe Kate Valerius, the gate keeper, thanks for all the work she did in getting me here and for keeping me on track to graduate. I would also

like to thank my undergraduate advisor, David Bixler, for his mentorship and for helping lay the foundation of my understanding of physics.

A special thanks goes to my parents for supporting me throughout my time in university and for raising me to think for myself. Without their help I would not have been successful. I would like to thank all of my friends from Angelo State, Stony Brook, Waterloo, and Milwaukee; We did righteous battle together indeed. Finally, I would like to thank Emily for all of her support and guidance while I navigated my way through grad school.

I say we take off and nuke the entire site from orbit. It's the only way to be sure...

-Lieutenant 1st Class Ellen Ripley

Chapter 1

Introduction

The formalism of quantum field theory in curved spacetime [1, 2, 3] (QFTCST) is used to describe particle dynamics in the geometric backgrounds of general relativity. The combination of these resoundingly successful theories produces the current, and most complete, description of nature we have. The chief accomplishment of this theory is the fact that the three pillars of physics (quantum mechanics, gravitation, and thermodynamics) are all incorporated into one unified framework. In fact, in QFTCST, thermodynamics is not even present in the initial formulation but emerges as a by-product of extending quantum theory to incorporate curved spacetimes. What makes this even more incredible is how the thermodynamics emerges by a process involving the incredibly exotic phenomena of event horizons and vacuum fluctuations. Event horizons such as those found around black holes are able to create particles using vacuum fluctuations that occur near the horizon. Incredibly, the particles produced via this process have a thermal distribution determined by a temperature that is determined by the surface gravity of the event horizon. Moreover, there is even an entropy associated with the area of the event horizon. The emergence of these thermodynamic phenomena was surprising in that rather than unifying the forces of physics, it "unified the fields" by bringing gravitation, quantum mechanics, and thermodynamics under the same theoretical structure. Of all the possible spacetimes that can be analyzed using QFTCST,

there are three that are of particular importance: FRW cosmologies which model the expanding universe, Schwarzschild spacetimes which model black holes, and Rindler spacetime which model uniform accelerated motion.

In his PhD thesis, Leonard Parker established the formalism within QFTCST for analyzing particle creation and applied it to the expanding universe [4]. By using the Bogoliubov transformation he developed the technique to compute, among many other things, the number of particles produced by changing between two spacetimes [5]. Then, he applied this formalism to compute the number of particles created by starting with an initial vacuum Minkowski space, allowing it to expand, and ending with a final Minkowski space, see Figure 1.1 below. The thermal particles produced in this way are now a leading candidate for the cause of density perturbations seen in the cosmic microwave background and the techniques to analyze them are used routinely in probing the properties of inflationary cosmology [6, 7]. Experimentally, cosmology currently provides an active area to investigate these cosmological aspects of QFTCST. There is even an active search for "smoking gun" evidence for this particle production mechanism currently underway [8, 9]. The fact that there is an ongoing, very active, and fully funded research program devoted to studying the application of QFTCST to cosmology shows how it can be used to probe fundamental physics.

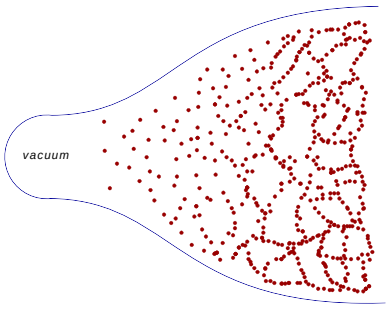

Figure 1.1: Cosmological particle creation.

The Bogoliubov transformation again found a particular important application in analyzing the formation of black holes. By comparing the spacetimes before and after a distribution

of matter collapses into a black hole, Stephen Hawking was able to show that black holes radiate thermal particles [10], see Figure 1.2 below. Even more interesting is the fact that the temperature of these particles is given by the surface gravity at the horizon. Using thermodynamics, this temperature was then used to compute the associated entropy predicted by Jacob Bekenstein [11]. The presence of this entropy, and the fact that it decreases, while a black hole evaporates has lead to the famous information loss paradox. The resolution of this paradox has been at the forefront of theoretical physics since its discovery. It is currently possible to study the classical properties of astrophysical black holes [12, 13], and there are analogue systems that can study quantum mechanical aspects of black holes in both analogue water experiments and condensed matter systems using Bose-Einstein condensation [14, 15]. Quantum properties of black holes, including thermal particle emission, have been experimentally verified in these analogue systems and appear to be in complete agreement with Hawkings prediction.

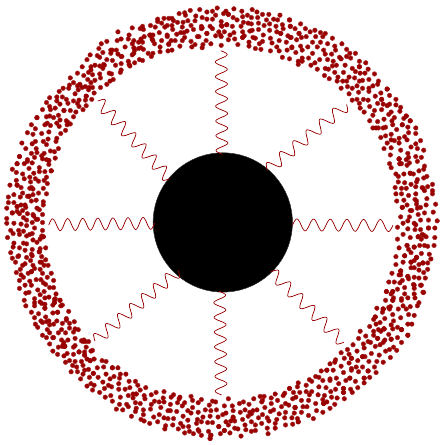

Figure 1.2: Black hole radiation.

In an attempt to understand the nature of black hole evaporation, Bill Unruh exploited a similarity in the spacetime structure near the black hole horizon and the spacetime structure seen by an observer in vacuum and under constant acceleration [16, 17, 18]. Then, by computing the number of particles after moving into an accelerated reference frame he found that even there a thermal distribution of particles is created. This time the temperature is

determined by the acceleration. In order to verify this effect, one needs to impart on particles an incredibly high acceleration. This is technologically difficult but there are many candidate systems which may have the ability to reach the necessary acceleration scales in the near future [19, 20, 21]. As such, this situation is different from the others in that there are still no experimental settings capable of probing this effect. It is in anticipation of experiments that are capable of probing the Unruh effect that I have written this dissertation. In short, my dissertation is devoted to developing the "particle physics" that one would expect to see in the presence of the Unruh effect.

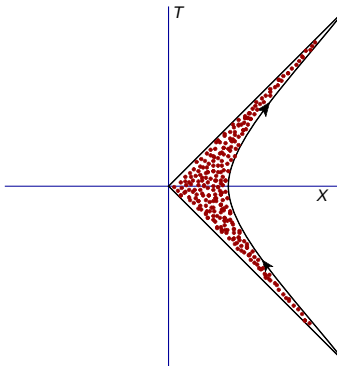

Figure 1.3: Radiation due to acceleration.

Since the discoveries of Parker [4], Hawking [10], and Unruh [16], namely cosmological particle creation, black hole evaporation, and accelerated radiation, respectively, a general notion has emerged that the particle content of spacetime is an observer-dependent quantity. For example, with the Unruh effect an observer undergoing uniform acceleration a will find the Minkowski vacuum state to be a thermalized bath of particles at temperature $t = a/2\pi$. Directly measuring this, or related phenomena, has remained outside the reach of our current experimental capabilities. Indirect measurements, such as the acceleration-dependent lifetime of particles, could provide a better avenue for verifying these effects. Muller [22] first calculated how acceleration affects the decay rates of muons, pions, and protons using scalar fields. A more detailed calculation of the accelerated decay of protons and neutrons, and related processes, using fermions coupled to semiclassical vector currents was carried

out by Matsas and Vanzella [23, 24, 25]. Here, we utilize scalar fields to develop a formalism which encompasses transitions with arbitrary final state multiplicity and compute both the power and the spectra. We also import certain relevant inertial quantities, such as the branching fractions of various decays, into the formalism and compute the acceleration scale to select the relevant decay pathway, i.e. multiplicity. We carry out the branching fraction analysis for the electron-muon system and also gives a first estimate for the lifetime of an accelerated electron using a scalar field approximation. Moreover, with the Planckian spectra obtained, we compute the peak energy of the emitted particles via a generalization of Wien's displacement law. This establishes that the most probable energy of the emitted particles is peaked about the accelerated temperature. These results are punctuated by the entire analysis being carried out using a newly developed time-dependent formalism which agrees with the previous developments of Obadia and Milgrom [26], Kothawala and Padmanabhan [27], and Barbado and Visser [28]. The time-dependence and ability to compute a wide class of observables developed in this dissertation establish a basic foundation for an acceleration-induced particle physics phenomenology with applications to highly accelerated systems. The matter contained in this dissertation is based off of the following two publications [29, 30]. All calculations are performed using the natural units $\hbar = c = k_B = 1$.

Chapter 2

Transition Rate of Accelerated Fields

In this chapter we determine the probability per unit time that a massive scalar particle will decay into n_M massless scalar particles using the method of field operators. Denoting the massive initial state by Ψ and the massless final states by ϕ_i, the process we are concerned with is given by

$$\Psi \rightarrow_a \phi_1\phi_2\phi_3\cdots\phi_{n_M}. \tag{2.1}$$

It should be noted that there may be symmetry factors associated with the final state products if there are more than one of the same particle species in the final state. For the current considerations we ignore any symmetry factors which may arise since we will have an arbitrary coupling constant which may be rescaled to take into account any degeneracy, statistical, or color factors. In order to describe this decay process, we work in the interaction picture and consider the following action [31, 32],

$$\hat{S}_I = \int d^4x\sqrt{-g}\sqrt{\frac{2}{\sigma\kappa}}G\hat{\Psi}\prod_{\ell=1}^{n_M}\hat{\phi}_\ell. \tag{2.2}$$

The coupling constant G will be determined by the specific interaction and, for the eventual concern of this paper, will be related to the Fermi coupling G_f. The additional

factor of $\sqrt{\frac{2}{\sigma\kappa}}$ will be used for the later convenience of absorbing the Jacobian of a proper time reparametrization σ and normalization constant κ. Note that we are modeling decay processes at tree level and provided the energy scale, i.e. the proper acceleration, remains below the $W^{\pm}$ and Z boson masses we need not worry about the nonrenormalizability of this effective Fermi interaction. All fields under consideration are assumed to be real and thus so is the interaction action. Note, all interactions, fields, trajectories, and thus the transition rate will eventually be evaluated in the Rindler coordinate chart. The probability amplitude for the acceleration induced decay of our massive initial state into n_M massless particles is given by

$$\mathcal{A} = \langle \prod_{m=1}^{n_M} \mathbf{k}_m | \otimes \langle 0 | \, \hat{S}_I \, | \Psi_i \rangle \otimes | 0 \rangle \, . \tag{2.3}$$

That is, the initial fock state $|\Psi_i\rangle$ of our massive field Ψ decays into the n_M-particle momentum eigenstate $|\prod_{i=1}^{n_M} \mathbf{k}_i\rangle$ of our massless fields ϕ_i under the influence of the interaction $\hat{S}_I$. Note we have used the shorthand notation $|\prod_{i=1}^{n_M} \mathbf{k}_i\rangle = |\mathbf{k}_1, \mathbf{k}_2, \ldots, \mathbf{k}_{n_M}\rangle$ to denote our final state. Defining $\prod_{j=1}^{n_M} d^3k_j = D^3_{n_M} k$, we can set up the differential probability, i.e. the magnitude squared of the probability amplitude per unit final state momenta, via

$$
\begin{aligned}
\frac{d\mathcal{P}}{D^3_{n_M}k} &= |\mathcal{A}|^2 \\
&= \left| \langle \prod_{m=1}^{n_M} \mathbf{k}_m | \otimes \langle 0 | \, \hat{S}_I \, | \Psi_i \rangle \otimes | 0 \rangle \right|^2 \\
&= G^2 \frac{2}{\sigma\kappa} \int d^4x \sqrt{-g} \int d^4x' \sqrt{-g'} \times \\
&\quad \left| \langle \prod_{m=1}^{n_M} \mathbf{k}_m | \otimes \langle 0 | \, \hat{\Psi}(x) \prod_{\ell=1}^{n_M} \hat{\phi}_\ell(x) \, | \Psi_i \rangle \otimes | 0 \rangle \right|^2 \\
&= G^2 \frac{2}{\sigma\kappa} \int d^4x \sqrt{-g} \int d^4x' \sqrt{-g'} \times \\
&\quad \left| \langle 0 | \, \hat{\Psi}(x) \, | \Psi_i \rangle \right|^2 \left| \langle \prod_{m=1}^{n_M} \mathbf{k}_m | \prod_{\ell=1}^{n_M} \hat{\phi}_\ell(x) \, | 0 \rangle \right|^2 . \qquad (2.4)
\end{aligned}
$$

The above inner product containing our massless fields ϕ_ℓ, its complex conjugate, and the product of momentum integrations in Eq. (2.4) allow us to factor out n_M complete sets of momentum eigenstates, e.g. $\int d^3k \, |k\rangle \langle k| = 1$. The total transition probability is then given by

$$
\begin{aligned}
\mathcal{P} &= G^2 \frac{2}{\sigma\kappa} \int d^4x \sqrt{-g} \int d^4x' \sqrt{-g'} \times \\
&\quad \left| \langle 0 | \, \hat{\Psi}(x) \, | \Psi_i \rangle \right|^2 \prod_{j=1}^{n_M} \int d^3k_j \left| \langle \prod_{m=1}^{n_M} \mathbf{k}_m | \prod_{\ell=1}^{n_M} \hat{\phi}_\ell(x) \, | 0 \rangle \right|^2 \\
&= G^2 \frac{2}{\sigma\kappa} \int d^4x \sqrt{-g} \int d^4x' \sqrt{-g'} \times \\
&\quad \left| \langle 0 | \, \hat{\Psi}(x) \, | \Psi_i \rangle \right|^2 \prod_{\ell=1}^{n_M} \langle 0 | \, \hat{\phi}_\ell(x') \hat{\phi}_\ell(x) \, | 0 \rangle \, . \qquad (2.5)
\end{aligned}
$$

In examining the above equation, it serves to recall the expression $\langle 0 | \, \hat{\Psi}(x) \, | \Psi_i \rangle$ selects the positive frequency mode function $u_k(x, \tau)$ of the initial state Ψ. These positive frequency mode functions are eigenfunctions of the Rindler coordinate proper time τ such that $\partial_\tau u_k =$

$-i\omega u_k$. In the accelerated frame this particle is at rest and its energy is only the rest mass m. Letting $f_{\Psi_i}(x)$ denote the spatial variation of the particle, we find

$$\begin{aligned}
\langle 0|\,\hat{\Psi}(x)\,|\Psi_i\rangle &= \langle 0|\int d^3k'[\hat{a}_{k'}u_{k'}(x)+h.c]\,|\Psi_i\rangle \\
&= \int d^3k'\delta(k'-k)u_{k'}(x) \\
&= u_k(x) \\
&= f_{\Psi_i}[x(\tau)]e^{-im\tau}. \qquad (2.6)
\end{aligned}$$

Furthermore, each of the two-point functions $\langle 0|\,\hat{\phi}_\ell(x')\hat{\phi}_\ell(x)\,|0\rangle$ in Eq. (2.5) characterizes the probability amplitude for a field quanta to be created at the spacetime point x and propagate within the lightcone to the spacetime point x'. If $t' > t$ then the particle is traveling forward through time and has a postive frequency. This defines the appropriately named positive frequency Wightman function denoted $G^+(x',x)$. Similarly if $t > t'$ then this defines the negative frequency Wightman function, denoted $G^-(x',x)$, and describes a particle of negative frequency propagating backwards through time. The time ordered sum of the positive and negative frequency Wightman functions make up the more common Feynman propagator [33]. Denoting the general two point function $G^\pm(x',x)$, our probability can now be simplified to the following form:

$$\begin{aligned}
\mathcal{P} &= G^2\frac{2}{\sigma\kappa}\int d^4x\sqrt{-g}\int d^4x'\sqrt{-g'}\left|\langle 0|\,\hat{\Psi}(x)\,|\Psi_i\rangle\right|^2\prod_{\ell=1}^{n_M}\langle 0|\,\hat{\phi}_\ell(x')\hat{\phi}_\ell(x)\,|0\rangle \\
&= G^2\frac{2}{\sigma\kappa}\int d^4x\sqrt{-g}\int d^4x'\sqrt{-g'}f_{\Psi_i}(x)f^*_{\Psi_i}(x')e^{im(\tau'-\tau)}[G^\pm(x',x)]^{n_M}. \qquad (2.7)
\end{aligned}$$

The Wightman functions for the massless scalar field can be evaluated analytically by inserting the canonically normalized mode decomposition of our field operator $\hat{\phi} = \int \frac{d^3k}{(2\pi)^{3/2}\sqrt{2\omega}}[\hat{a}_{\mathbf{k}}e^{i(\mathbf{k}\cdot\mathbf{x}-\omega t)}+\hat{a}^\dagger_{\mathbf{k}}e^{-i(\mathbf{k}\cdot\mathbf{x}-\omega t)}]$. Thus,

$$
\begin{aligned}
G^{\pm}(x',x) &= \langle 0_\ell|\, \hat{\phi}_\ell(x')\hat{\phi}_\ell(x)\, |0_\ell\rangle \\
&= \frac{1}{2(2\pi)^3}\iint \frac{d^3k'd^3k}{\sqrt{\omega'\omega}} \times \\
&\quad \langle 0_\ell|\left[\hat{a}_{\mathbf{k}'}e^{i(\mathbf{k}'\cdot\mathbf{x}'-\omega't')} + \hat{a}^\dagger_{\mathbf{k}'}e^{-i(\mathbf{k}'\cdot\mathbf{x}'-\omega't')}\right]\left[\hat{a}_{\mathbf{k}}e^{i(\mathbf{k}\cdot\mathbf{x}-\omega t)} + \hat{a}^\dagger_{\mathbf{k}}e^{-i(\mathbf{k}\cdot\mathbf{x}-\omega t)}\right]|0_\ell\rangle \\
&= \frac{1}{2(2\pi)^3}\iint \frac{d^3k'd^3k}{\sqrt{\omega'\omega}}\, \langle 0_\ell|\, \hat{a}_{\mathbf{k}'}\hat{a}^\dagger_{\mathbf{k}}e^{i(\mathbf{k}'\cdot\mathbf{x}'-\mathbf{k}\cdot\mathbf{x}-\omega't'+\omega t)}\, |0_\ell\rangle \\
&= \frac{1}{2(2\pi)^3}\iint \frac{d^3k'd^3k}{\sqrt{\omega'\omega}} e^{i(\mathbf{k}'\cdot\mathbf{x}'-\mathbf{k}\cdot\mathbf{x}-\omega't'+\omega t)}\delta(\mathbf{k}'-\mathbf{k}) \\
&= \frac{1}{2(2\pi)^3}\int \frac{d^3k}{\omega} e^{i(\mathbf{k}\cdot\Delta\mathbf{x}-\omega\Delta t)}. \qquad (2.8)
\end{aligned}
$$

To facilitate the resultant integral we move into momentum space spherical coordinates and rotate until our momentum is aligned along the z axis. Recall that in the massless limit $\omega = k$ the integration simplifies further to

$$
\begin{aligned}
G^{\pm}(x',x) &= \frac{1}{2(2\pi)^3}\int \frac{d^3k}{\omega} e^{i(\mathbf{k}\cdot\Delta\mathbf{x}-\omega\Delta t)} \\
&= \frac{1}{2(2\pi)^3}\int_0^\infty\int_0^\pi\int_0^{2\pi} dkd\theta d\phi\; k\sin\theta e^{i(k\Delta x\cos\theta - k\Delta t)} \\
&= \frac{1}{2(2\pi)^2}\int_0^\infty\int_{-1}^1 dkd(\cos\theta)\; ke^{i(k\Delta x\cos\theta - k\Delta t)} \\
&= \frac{1}{2(2\pi)^2}\frac{i}{\Delta x}\int_0^\infty dk\left[e^{-ik(\Delta x+\Delta t)} - e^{-ik(-\Delta x+\Delta t)}\right]. \qquad (2.9)
\end{aligned}
$$

In order for the above integration to be well defined we must damp the oscillation at infinity via the introduction of a complex regulator to our time interval, e.g. $\Delta t \to \Delta t - i\epsilon$ with $\epsilon > 0$. Hence,

$$
\begin{aligned}
G^{\pm}(x',x) &= \frac{1}{2(2\pi)^2}\frac{i}{\Delta x}\int_0^\infty dk\left[e^{-ik(\Delta x+\Delta t)}-e^{-ik(-\Delta x+\Delta t)}\right] \\
&= \frac{1}{2(2\pi)^2}\frac{i}{\Delta x}\int_0^\infty dk\left[e^{-ik(\Delta x+(\Delta t-i\epsilon))}-e^{-ik(-\Delta x+(\Delta t-i\epsilon))}\right] \\
&= \frac{1}{2(2\pi)^2}\frac{i}{\Delta x}\left[\frac{1}{i(\Delta x+(\Delta t-i\epsilon))}-\frac{1}{i(-\Delta x+(\Delta t-i\epsilon))}\right] \\
&= \frac{1}{(2\pi)^2}\frac{1}{\Delta x^2-(\Delta t-i\epsilon)^2}. \qquad (2.10)
\end{aligned}
$$

Having determined the functional form of our massless Wightman function we return to the integrations over the spatial coordinates in our decay probability, Eq. (2.7). These can be dealt with by examining the covariant 4-volume element of Rindler space. The proper coordinates [34] $(\tau,\xi,\mathbf{x}_\perp)$ seen by a particle undergoing uniform proper acceleration a along the z axis are given by

$$
\begin{aligned}
\tau(t,z) &= \frac{1}{2a}\ln\frac{z+t}{z-t} \\
\xi(t,z) &= -\frac{1}{a}+\sqrt{z^2-t^2}. \qquad (2.11)
\end{aligned}
$$

The perpendicular coordinates $\mathbf{x}_\perp$ do not change in Rindler space. Note, the coordinate ξ parametrizes distances seen by the accelerated observer along the axis of acceleration and the point $\xi=0$ labels the origin of this axis and is defined to be the location of the uniformly accelerated particle. For an inertial observer, this point will then characterize the trajectory of the accelerated particle. In this coordinate chart, the metric takes the form

$$
ds^2 = (1+a\xi)^2 d\tau^2 - d\xi^2 - d\mathbf{x}_\perp^2. \qquad (2.12)
$$

The corresponding metric determinant of this spacetime used to covariantly scale our 4-volume of integration is $|g| = 1+a\xi$. Inverting our proper coordinate chart, Eq. (2.11),

and translating until $\xi = 0$ and $\mathbf{x}_\perp = 0$ yields the trajectory of our particle,

$$\begin{aligned} t &= \frac{1}{a}\sinh a\tau \\ z &= \frac{1}{a}\cosh a\tau \\ \mathbf{x}_\perp &= 0. \end{aligned} \tag{2.13}$$

It should be noted that under this trajectory our Wightman function, Eq. (2.10), depends only on the proper time τ and is therefore not affected by the spatial integrations. Returning to the decay probability, Eq. (2.7), we can handle the spatial components of the integration via

$$\begin{aligned} \mathcal{P} &= G^2\frac{2}{\sigma\kappa}\int d^4x\sqrt{-g}\int d^4x'\sqrt{-g'}f_\Psi(x)f^*_\Psi(x')e^{im(\tau'-\tau)}[G^\pm(x',x)]^{n_M} \\ &= G^2\frac{2}{\sigma\kappa}\int d^3x\sqrt{1+a\xi}\int d^3x'\sqrt{1+a\xi'}f_\Psi(x)f^*_\Psi(x')\iint d\tau d\tau' e^{im(\tau'-\tau)}[G^\pm(x',x)]^{n_M} \\ &= G^2\frac{2}{\sigma\kappa}\kappa\iint d\tau d\tau' e^{im(\tau'-\tau)}\left[G^\pm(x',x)\right]^{n_M} \\ &= G^2\frac{2}{\sigma}\mathcal{F}_{n_M}(m). \end{aligned} \tag{2.14}$$

The mode functions have the form $f_\Psi(x) \sim K_{i\omega/a}(\frac{m}{a}e^{a\xi})g(\mathbf{x}_\perp)$ where $g(\mathbf{x}_\perp)$ is an envelope function or wave packet describing the spatial distribution of our accelerated field in the directions perpendicular to the acceleration [22]. With the mode functions properly normalized [35], the expression $\kappa = \left|\int d^3x\sqrt{1+a\xi}f_\Psi(x)\right|^2$ will be of order unity. We see the probability of an acceleration induced transition is then given by the Fourier transform of the product of the n_M final state Wightman functions. This is known as the response function $\mathcal{F}_{n_M}(m)$. The effective coupling constant G^2 for the process being considered will be determined by taking the limit $a \to 0$ and matching the coefficient to the known inertial decay process. Note this compact form of the transition probability is valid for a more general

class of trajectories provided their parametrization only depends on the proper time. Using the trajectories from Eq. (2.13), the coordinate transformations $u = \frac{\tau' - \tau}{\rho}$ and $s = \frac{\tau' + \tau}{\sigma}$, and the inversion $\tau' = \frac{\rho u + \sigma s}{2}$ and $\tau = \frac{\sigma s - \rho u}{2}$ with arbitrary σ and ρ, we find the explicit form of the spacetime intervals in the massless Wightman function to be

$$\begin{aligned}
\Delta x^2 - (\Delta t - i\epsilon)^2 &= \frac{1}{a^2}\left\{[\cosh(a\tau') - \cosh(a\tau)]^2 - [\sinh(a\tau') - \sinh(a\tau) - i\epsilon]^2\right\} \\
&= \frac{1}{a^2}\left\{[2\sinh\left(\frac{a\rho u}{2}\right)\sinh\left(\frac{a\sigma s}{2}\right)]^2 - [2\sinh\left(\frac{a\rho u}{2}\right)\cosh\left(\frac{a\sigma s}{2}\right) - i\epsilon]^2\right\} \\
&= \frac{1}{a^2}[4\sinh^2\left(\frac{a\rho u}{2}\right)\sinh^2\left(\frac{a\sigma s}{2}\right) - 4\sinh^2\left(\frac{a\rho u}{2}\right)\cosh^2\left(\frac{a\sigma s}{2}\right) + \\
&\quad 4i\epsilon\sinh\left(\frac{a\rho u}{2}\right)\cosh\left(\frac{a\sigma s}{2}\right)] \\
&= \frac{1}{a^2}[4\sinh^2\left(\frac{a\rho u}{2}\right)\sinh^2\left(\frac{a\sigma s}{2}\right) - 4\sinh^2\left(\frac{a\rho u}{2}\right)\cosh^2\left(\frac{a\sigma s}{2}\right) \\
&\quad +8i\epsilon\sinh\left(\frac{a\rho u}{2}\right)\cosh\left(\frac{a\rho u}{2}\right)] \\
&= \frac{-4}{a^2}\sinh^2\left(\frac{a\rho u}{2} - i\epsilon\right). \qquad (2.15)
\end{aligned}$$

Note we have rescaled ϵ by the positive definite factor $2\cosh\left(\frac{a\rho u}{2}\right)/\cosh\left(\frac{a\sigma s}{2}\right)$ and used the Taylor expansion of $\sinh^2(x - i\epsilon)$ to combine the arguments. Thus we obtain

$$G^{\pm}(x', x) = -\frac{1}{(2\pi)^2}\frac{a^2}{4\sinh^2\left(\frac{a\rho u}{2} - i\epsilon\right)}. \qquad (2.16)$$

In changing the proper time integration variables we pick up the Jacobian $\frac{\sigma\rho}{2}$ and our transition probability induced by the uniformly accelerated trajectory then becomes

$$
\begin{aligned}
\mathcal{P} &= G^2 \frac{2}{\sigma} \mathcal{F}_{n_M}(m) \\
&= G^2 \frac{2}{\sigma} \iint d\tau d\tau' e^{im(\tau'-\tau)} \left[G^{\pm}(x', x) \right]^{n_M} \\
&= G^2 \frac{2}{\sigma} \iint d\tau d\tau' e^{im(\tau'-\tau)} \left[\frac{1}{(2\pi)^2} \frac{1}{\Delta x^2 - (\Delta t - i\epsilon)^2} \right]^{n_M} \\
&= G^2 \frac{2}{\sigma} \iint d\tau d\tau' e^{im(\tau'-\tau)} \left[-\frac{1}{(2\pi)^2} \frac{a^2}{4 \sinh^2 \left(\frac{a\rho u}{2} - i\epsilon \right)} \right]^{n_M} \\
&= G^2 (-1)^{n_M} \rho \left(\frac{a}{4\pi} \right)^{2n_M} \iint ds du \, \frac{e^{im\rho u}}{[\sinh \left(\frac{a\rho u}{2} - i\epsilon \right)]^{2n_M}}.
\end{aligned} \tag{2.17}
$$

By dividing out the infinite proper time interval $\int ds$ we obtain the probability of transition per unit proper time $\Gamma_{n_M}(m, a) = \frac{\mathcal{P}}{\Delta s}$. After rescaling $u \to \rho u$ we see that the result is independent of the parametrization of u. The parametrization of s yielded a factor of $\frac{\sigma}{2}$ which we absorbed by the initial rescaling of our coupling constant. The probability per unit time is thus given by

$$
\Gamma_{n_M}(m, a) = G^2 \left(\frac{ia}{4\pi} \right)^{2n_M} \int du \, \frac{e^{imu}}{[\sinh \left(\frac{au}{2} - i\epsilon \right)]^{2n_M}}. \tag{2.18}
$$

Focusing on the integration, we note that in the absence of the $i\epsilon$ prescription there will be poles of order $2n_M$ when $u = 2\alpha\pi i/a$ with α being any integer. To integrate over the real axis in the presence of the pole at $u = 0$ we will close our contour in the upper half plane to damp the oscillation at infinity. In doing so we also pick up the additional tower of poles along the imaginary axis. Furthermore, with the negative $i\epsilon$ prescription we will also capture the pole at $\alpha = 0$. We will now remove the regulator $\epsilon \to 0$ now that we understand the appropriate pole structure. The integrand can be cast into a simpler form via the change of variables $w = e^{au}$. Hence,

$$\begin{aligned}\int du\,\frac{e^{imu}}{[\sinh\left(\frac{au}{2}\right)]^{2n_M}} &= 2^{2n_M}\int_{-\infty}^{\infty} du\,\frac{e^{imu}}{\left[e^{\frac{au}{2}}-e^{-\frac{au}{2}}\right]^{2n_M}} \\ &= 2^{2n_M}\int_{-\infty}^{\infty} du\,\frac{e^{imu+aun_M}}{\left[e^{au}-1\right]^{2n_M}} \\ &= \frac{2^{2n_M}}{a}\int_0^{\infty} dw\,\frac{w^{im/a+n_M-1}}{\left[w-1\right]^{2n_M}}. \end{aligned} \tag{2.19}$$

We see that there are poles when $w=1$, i.e. $w=e^{i2\pi\alpha}$ where we keep the integer $\alpha\geq 0$. Evaluation of this integral may be accomplished via the residue theorem. Thus

$$\begin{aligned}\frac{2^{2n_M}}{a}\int_0^{\infty} dw\,\frac{w^{im/a+n_M-1}}{\left[w-1\right]^{2n_M}} &= \frac{2^{2n_M}}{a}\frac{2\pi i}{(2n_M-1)!}\sum_{\alpha=0}^{\infty}\frac{d^{2n_M-1}}{dw^{2n_M-1}}\left[\left[w-1\right]^{2n_M}\frac{w^{im/a+n_M-1}}{\left[w-1\right]^{2n_M}}\right]_{w=e^{i2\pi\alpha}} \\ &= \frac{2^{2n_M}}{a}\frac{2\pi i}{(2n_M-1)!}\sum_{\alpha=0}^{\infty}\left[\frac{w^{im/a-n_M}\Gamma(im/a+n_M)}{\Gamma(im/a+1-n_M)}\right]_{w=e^{i2\pi\alpha}} \\ &= \frac{2^{2n_M}}{a}\frac{2\pi i}{(2n_M-1)!}\frac{\Gamma(im/a+n_M)}{\Gamma(im/a+1-n_M)}\sum_{\alpha=0}^{\infty}e^{-2\pi\frac{m}{a}\alpha-2\pi i n_M\alpha} \\ &= \frac{2^{2n_M}}{a}\frac{2\pi i}{(2n_M-1)!}\frac{\Gamma(im/a+n_M)}{\Gamma(im/a+1-n_M)}\frac{1}{1-e^{-2\pi m/a}}. \end{aligned} \tag{2.20}$$

The presence of the factor of $[1-e^{-2\pi m/a}]^{-1}$ is indicative of the thermal nature of the vacuum associated with the Unruh effect. From our total rate, Eq. (2.18), for a uniformly accelerated particle of mass m to decay into n_M massless particles under the influence of a uniform acceleration is then found to be

$$\Gamma_{n_M}(m,a)=G^2\left(\frac{ia}{2\pi}\right)^{2n_M}\frac{1}{a}\frac{2\pi i}{(2n_M-1)!}\frac{\Gamma(im/a+n_M)}{\Gamma(im/a+1-n_M)}\frac{1}{1-e^{-2\pi m/a}}. \tag{2.21}$$

We can normalize the above expression by defining $\tilde{\Gamma}=\Gamma/\Gamma_0$, with $\Gamma_0=G^2$, to better analyze the normalized decay rate for an arbitrary n_M particle multiplicity final state. The

normalized decay rates $\tilde{\Gamma}_{n_M}$ for the first few integer values of n_M are given by

$$\begin{aligned}
\tilde{\Gamma}_1(m,a) &= \frac{m}{2\pi}\frac{1}{1-e^{-2\pi m/a}} \\
\tilde{\Gamma}_2(m,a) &= \frac{m^3}{48\pi^3}\frac{1+\left(\frac{a}{m}\right)^2}{1-e^{-2\pi m/a}} \\
\tilde{\Gamma}_3(m,a) &= \frac{m^5}{3840\pi^5}\frac{1+5\left(\frac{a}{m}\right)^2+4\left(\frac{a}{m}\right)^4}{1-e^{-2\pi m/a}} \\
\tilde{\Gamma}_4(m,a) &= \frac{m^7}{645120\pi^7}\frac{1+14\left(\frac{a}{m}\right)^2+49\left(\frac{a}{m}\right)^4+36\left(\frac{a}{m}\right)^6}{1-e^{-2\pi m/a}} \\
\tilde{\Gamma}_5(m,a) &= \frac{m^9}{185794560\pi^9}\frac{1+30\left(\frac{a}{m}\right)^2+273\left(\frac{a}{m}\right)^4+820\left(\frac{a}{m}\right)^6+576\left(\frac{a}{m}\right)^8}{1-e^{-2\pi m/a}}. \qquad (2.22)
\end{aligned}$$

Below, in Figs. 2.1 and 2.2, we plot both the normalized decay rates and lifetimes $\tilde{\tau} = 1/\tilde{\Gamma}$ for a particle of mass $m = 1$ to decay into n_M massless particle states as a function of the proper acceleration. It is clear from both Eq. (2.22) and the plots below that there exists a crossover scale of acceleration where the accelerated particle will preferentially choose the decay chain with the most final state products. This implies that an inertially decaying particle chooses the decay chain which contains the least allowable amount of end products and by imparting a sufficiently high acceleration on an unstable particle it will chose the decay chain which contains the most allowable final state products.

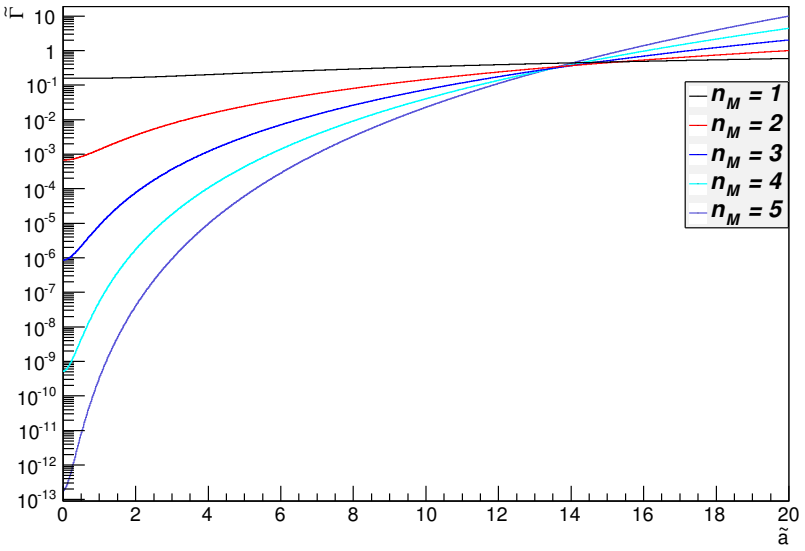

Figure 2.1: The normalized decay rates, Eq. (2.22), with $\tilde{a} = a/m$ and $m = 1$.

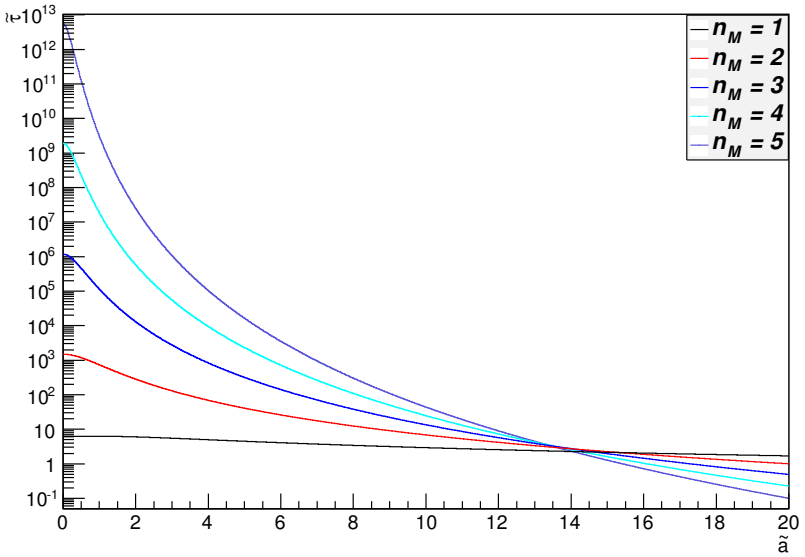

Figure 2.2: The normalized lifetimes, $\tilde{\tau}$, with $\tilde{a} = a/m$ and $m = 1$.

The prescription for this method of calculation can be seen by inspecting (2.14). In general, for n_M final state products, the response function is computed by taking the Fourier transform of the product of each of the Wightman functions of the n_M massless final states.

The number of final states determines the number of derivatives taken in calculating the residues of Eq. (2.20), which yields the gamma functions, and thus the number of terms in the decay rate polynomial as can be seen by Eq. (2.22). In the next chapter we will analyze the same situation utilizing an Unruh-DeWitt detector.

Chapter 3

Transition Rate of an Unruh-DeWitt Detector

In this chapter we utilize the formalism of Unruh-DeWitt detectors; see Ref. [16, 36]. As such, we form a two-level system consisting of two particles of arbitrary mass and determine the associated decay and excitation rates, accompanied by the simultaneous emission of n_M massless particles, of the system under uniform acceleration. These processes are illustrated schematically as

$$\Psi_1 \rightarrow_a \Psi_2 \phi_1 \phi_2 \cdots \phi_{n_M}. \tag{3.1}$$

The utility of this method is that it allows the inclusion of a massive final state in a rather uncomplicated fashion and, more importantly, allows for a description of acceleration induced excitation rather than just decay. To accomplish this, we will now promote the massive scalar fields Ψ_i to a two-level system, e.g. an Unruh-DeWitt detector. These fields, and their transitions, will now be characterized by the time evolved monopole moment operator [31],

$$\hat{m}(\tau) = e^{i\hat{H}\tau} \hat{m}_0 e^{-i\hat{H}\tau}. \tag{3.2}$$

The monopole moment operator $\hat{m}_0$ is assumed to be Hermitian. The operator $\hat{H}$ denotes the detectors or fields proper Hamiltonian with the property

$$\hat{H}\left|\Psi_i\right\rangle = m_i\left|\Psi_i\right\rangle,\ i=1,2 \tag{3.3}$$

since, in the proper frame, the total energy will be that of the rest mass of our field m_i. Utilizing this formalism, we define the interaction action as [31, 32],

$$\hat{S}_I = \int d\tau \sqrt{\frac{2}{\sigma}}\hat{m}(\tau)\prod_{\ell=1}^{n_M}\hat{\phi}_\ell. \tag{3.4}$$

Again we have pulled out the additional factor of $\sqrt{\frac{2}{\sigma}}$ to absorb the Jacobian of a proper time reparametrization. Furthermore, this action is only integrated over the detector proper time and not the full spatial extent of the accelerated field as in the previous section, Eq. (2.2), since we are considering the fields as a time-dependent two-level system with no spatial extent. In calculating matrix elements of the form $\left\langle\Psi_f\right|\hat{m}(\tau)\left|\Psi_i\right\rangle$ we define the effective coupling constant to be

$$G = \left\langle\Psi_f\right|\hat{m}_0\left|\Psi_i\right\rangle. \tag{3.5}$$

It is this effective coupling constant that encodes the physical characteristics of the particular transition under consideration. The probability amplitude for the process induced by the interaction, Eq. (3.4), is given by

$$\mathcal{A} = \langle\prod_{j=1}^{n_M}\mathbf{k}_j|\otimes\left\langle\Psi_f\right|\hat{S}_I\left|\Psi_i\right\rangle\otimes|0\rangle. \tag{3.6}$$

We again use the same notation for our Fock states and accommodate any complications due to the statistics or degeneracies of the final state products by rescaling our effective coupling. Utilizing the shorthand notation $\prod_{j=1}^{n_M} d^3k_j = D^3_{n_M}k$, the differential probability for the two-level system to undergo a transition and be accompanied by the emission of n_M

massless particles per unit momentum is given by

$$\begin{aligned}
\frac{d\mathcal{P}}{D^3_{n_M}k} &= |\mathcal{A}|^2 \\
&= \langle 0| \otimes \langle \Psi_i| \hat{S}_I |\Psi_f\rangle \otimes |\prod_{j'=1}^{n_M} \mathbf{k}_{j'}\rangle \langle \prod_{j=1}^{n_M} \mathbf{k}_j| \otimes \langle \Psi_f| \hat{S}_I |\Psi_i\rangle \otimes |0\rangle \\
&= \frac{2}{\sigma} \iint d\tau' d\tau \, \langle 0| \otimes \langle \Psi_i| \hat{m}(\tau') \prod_{\ell'=1}^{n_M} \hat{\phi}_{\ell'}(x') |\Psi_f\rangle \otimes |\prod_{j'=1}^{n_M} \mathbf{k}_{j'}\rangle \times \\
&\quad \langle \prod_{j=1}^{n_M} \mathbf{k}_j| \otimes \langle \Psi_f| \hat{m}(\tau) \prod_{\ell=1}^{n_M} \hat{\phi}_\ell(x) |\Psi_i\rangle \otimes |0\rangle \, . \qquad (3.7)
\end{aligned}$$

Operation of the time evolved monopole moment in the relevant inner product and recalling the definition of our effective coupling, Eq. (3.5), yields

$$\begin{aligned}
\langle \Psi_f| \hat{m}(\tau) |\Psi_i\rangle &= \langle \Psi_f| e^{i\hat{H}\tau} \hat{m}_0 e^{-i\hat{H}\tau} |\Psi_i\rangle \\
&= e^{i(m_f - m_i)\tau} \langle \Psi_f| \hat{m}_0 |\Psi_i\rangle \\
&= G e^{i\Delta m \tau}. \qquad (3.8)
\end{aligned}$$

Then our differential probability, Eq. (3.7), becomes

$$\begin{aligned}
\frac{d\mathcal{P}}{D^3_{n_M}k} &= \frac{2}{\sigma} \iint d\tau' d\tau \;\; \langle 0| \otimes \langle \Psi_i| \hat{m}(\tau') \prod_{\ell'=1}^{n_M} \hat{\phi}_{\ell'}(x') |\Psi_f\rangle \otimes |\prod_{j'=1}^{n_M} \mathbf{k}_{j'}\rangle \times \\
&\quad \langle \prod_{j=1}^{n_M} \mathbf{k}_j| \otimes \langle \Psi_f| \hat{m}(\tau) \prod_{\ell=1}^{n_M} \hat{\phi}_\ell(x) |\Psi_i\rangle \otimes |0\rangle \\
&= G^2 \frac{2}{\sigma} \iint d\tau' d\tau \; e^{-i\Delta m(\tau' - \tau)} \left| \langle \prod_{j=1}^{n_M} \mathbf{k}_j| \prod_{\ell=1}^{n_M} \hat{\phi}_\ell(x) |0\rangle \right|^2 . \qquad (3.9)
\end{aligned}$$

In this chapter we will endeavor to evaluate the above integral in a different way than in

the previous chapter. Originally we factored out the complete set of momentum eigenstates to yield the Wightman functions. We then showed that each massless Wightman function was, up to a constant, the inverse of the spacetime interval traversed along an arbitrary trajectory. The interval was then evaluated along the hyperbolic trajectory associated with uniform acceleration. Here, we evaluate the inner product without factoring out the complete set of momentum eigenstates. This allows us to insert the hyperbolic trajectory into the resultant mode functions then perform the integrations over momentum. In doing so, we gain insight into the physical properties of the emitted decay products. We also find, as expected, the end result to be identical to that of the previous section. Evaluation of the decay rate using these two different methods lends a greater understanding to the underlying character of these processes.

Operation on the vacuum with our massless fields in Eq. (3.9) will yield n_M momentum integrals of the negative frequency mode functions over their momentum. Hence the above inner product will reduce to

$$\begin{aligned}
\langle \prod_{j=1}^{n_M} \mathbf{k}_j | \prod_{\ell=1}^{n_M} \hat{\phi}_\ell(x) \, |0\rangle &= \langle \prod_{j=1}^{n_M} \mathbf{k}_j | \prod_{\ell=1}^{n_M} \frac{1}{(2\pi)^{\frac{3n_M}{2}}} \frac{1}{2^{\frac{n_M}{2}}} \int \frac{d^3k_\ell}{\sqrt{\omega_\ell}} \left[\hat{a}^\dagger_{\mathbf{k}_\ell} e^{-i(\mathbf{k}_\ell \cdot \mathbf{x} - \omega_{k_\ell} t)} + h.c. \right] |0\rangle \\
&= \frac{1}{(2\pi)^{\frac{3n_M}{2}}} \frac{1}{2^{\frac{n_M}{2}}} \prod_{\ell=1}^{n_M} \int \frac{d^3k_\ell}{\sqrt{\omega_\ell}} e^{-i(\mathbf{k}_\ell \cdot \mathbf{x} - \omega_{k_\ell} t)} \langle \prod_{j=1}^{n_M} \mathbf{k}_j | \mathbf{k}_\ell \rangle \\
&= \frac{1}{(2\pi)^{\frac{3n_M}{2}}} \frac{1}{2^{\frac{n_M}{2}}} \prod_{\ell=1}^{n_M} \int \frac{d^3k_\ell}{\sqrt{\omega_\ell}} e^{-i(\mathbf{k}_\ell \cdot \mathbf{x} - \omega_{k_\ell} t)} \prod_{j=1}^{n_M} \delta(\mathbf{k}_j - \mathbf{k}_\ell) \\
&= \frac{1}{(2\pi)^{\frac{3n_M}{2}}} \frac{1}{2^{\frac{n_M}{2}}} \frac{e^{-i \sum_{j=1}^{n_M} (\mathbf{k}_j \cdot \mathbf{x} - \omega_{k_j} t)}}{\sqrt{\prod_{j'=1}^{n_M} \omega_{j'}}}.
\end{aligned} \tag{3.10}$$

Utilizing the above expression, our differential probability becomes

$$\frac{d\mathcal{P}}{D^3_{n_M}k} = G^2\frac{2}{\sigma}\iint d\tau' d\tau\; e^{-i\Delta m(\tau'-\tau)}\left|\langle\prod_{j=1}^{n_M}\mathbf{k}_j|\prod_{\ell=1}^{n_M}\hat{\phi}_\ell(x)\,|0\rangle\right|^2$$
$$= G^2\frac{2}{\sigma}\frac{1}{(2\pi)^{3n_M}}\frac{1}{2^{n_M}}\iint d\tau' d\tau\; e^{-i\Delta m(\tau'-\tau)}\frac{e^{i\sum_{j=1}^{n_M}(\mathbf{k}_j\cdot(\mathbf{x}'-\mathbf{x})-\omega_{k_j}(t'-t))}}{\prod_{j'=1}^{n_M}\omega_{j'}}. \quad (3.11)$$

It should be noted that we are integrating over the accelerated particles proper time. As such, the position and time intervals in the above exponential need to be recast along the trajectory and expressed in terms of the proper time of the accelerated frame. Then, recalling the trajectory from the previous chapter, Eq. (2.13), we have

$$\frac{d\mathcal{P}}{D^3_{n_M}k} = G^2\frac{2}{\sigma}\frac{1}{(2\pi)^{3n_M}}\frac{1}{2^{n_M}}\iint d\tau' d\tau\; e^{-i\Delta m(\tau'-\tau)}\frac{e^{i\sum_{j=1}^{n_M}(\mathbf{k}_j\cdot(\mathbf{x}'-\mathbf{x})-\omega_{k_j}(t'-t))}}{\prod_{j'=1}^{n_M}\omega_{j'}}$$
$$= G^2\frac{2}{\sigma}\frac{1}{(2\pi)^{3n_M}}\frac{1}{2^{n_M}}\iint d\tau' d\tau\; e^{-i\Delta m(\tau'-\tau)}\times$$
$$\frac{e^{\frac{i}{a}\sum_{j=1}^{n_M}(k_{z_j}[\cosh(a\tau')-\cosh(a\tau)]-\omega_{k_j}[\sinh(a\tau')-\sinh(a\tau)])}}{\prod_{j'=1}^{n_M}\omega_{j'}}. \quad (3.12)$$

Again, utilizing the change of variables, $u=(\tau'-\tau)/\rho$ and $s=(\tau+\tau')/\sigma$, we recall

$$\cosh(a\tau')-\cosh(a\tau) = 2\sinh\left(\frac{a\rho u}{2}\right)\sinh\left(\frac{a\sigma s}{2}\right)$$
$$\sinh(a\tau')-\sinh(a\tau) = 2\sinh\left(\frac{a\rho u}{2}\right)\cosh\left(\frac{a\sigma s}{2}\right). \quad (3.13)$$

In changing variables we will again pick up the factor of $\frac{\rho\sigma}{2}$ due to the Jacobian. Using these proper time parametrizations the differential probability becomes

$$\begin{aligned}
\frac{d\mathcal{P}}{D^3_{n_M}k} &= G^2\frac{2}{\sigma}\frac{1}{(2\pi)^{3n_M}}\frac{1}{2^{n_M}}\iint d\tau' d\tau\; e^{-i\Delta m(\tau'-\tau)}\times \\
&\quad \frac{e^{\frac{i}{a}\sum_{j=1}^{n_M}(k_{z_j}[\cosh(a\tau')-\cosh(a\tau)]-\omega_{k_j}[\sinh(a\tau')-\sinh(a\tau)])}}{\prod_{j'=1}^{n_M}\omega_{j'}} \\
&= \frac{G^2}{(2\pi)^{3n_M}}\frac{\rho}{2^{n_M}}\iint ds du\; e^{-i\Delta m\rho u}\times \\
&\quad \frac{e^{\frac{2i}{a}\sum_{j=1}^{n_M}[k_{z_j}\sinh(\frac{a\sigma s}{2})-\omega_{k_j}\cosh(\frac{a\sigma s}{2})]\sinh(\frac{a\rho u}{2})}}{\prod_{j'=1}^{n_M}\omega_{j'}}.
\end{aligned} \tag{3.14}$$

Noting that our acceleration is along the z axis only, we can examine the 4-velocity of the accelerated particle using the new affine proper time parametrization $\tilde{s} = \frac{\sigma s}{2}$. Hence

$$\begin{aligned}
u^\mu(\tilde{s}) &= \frac{dx^\mu}{d\tilde{s}} \\
&= (\cosh(a\tilde{s}), 0, 0, \sinh(a\tilde{s})).
\end{aligned} \tag{3.15}$$

We can then read off the relativistic factors associated with this motion, $\gamma = \cosh(a\tilde{s})$ and $\beta\gamma = \sinh(a\tilde{s})$. Then, restricting our analysis to the 2-D subspace along the hyperbolic trajectory, we find that given a 2-momentum k^μ we can boost to the frame instantaneously at rest with the accelerated motion to find

$$
\begin{aligned}
\tilde{k}^{\nu} &= \Lambda^{\nu}_{\mu} k^{\mu} \\
&= \begin{pmatrix} \gamma & -\beta\gamma \\ -\beta\gamma & \gamma \end{pmatrix} \begin{pmatrix} \omega \\ k_z \end{pmatrix} \\
&= \begin{pmatrix} \cosh(a\tilde{s}) & -\sinh(a\tilde{s}) \\ -\sinh(a\tilde{s}) & \cosh(a\tilde{s}) \end{pmatrix} \begin{pmatrix} \omega \\ k_z \end{pmatrix} \\
\begin{pmatrix} \tilde{\omega} \\ \tilde{k}_z \end{pmatrix} &= \begin{pmatrix} \omega\cosh(a\tilde{s}) - k_z \sinh(a\tilde{s}) \\ -\omega\sinh(a\tilde{s}) + k_z\cosh(a\tilde{s}) \end{pmatrix}.
\end{aligned} \tag{3.16}
$$

Upon inspection of the exponential in Eq. (3.14), we see the argument in the sum is merely the frequency of the emitted particles as seen in the boosted frame instantaneously at rest with accelerated field, i.e. $\tilde{\omega}$. As such we may rewrite the exponential in terms of the boosted frequencies yielding

$$
\begin{aligned}
\frac{d\mathcal{P}}{D^3_{n_M} k} &= \frac{G^2}{(2\pi)^{3n_M}} \frac{\rho}{2^{n_M}} \iint ds du \; e^{-i\Delta m \rho u} \times \\
&\qquad \frac{e^{\frac{2i}{a}\sum_{j=1}^{n_M}[k_{z_j}\sinh(\frac{a\sigma s}{2}) - \omega_{k_j}\cosh(\frac{a\sigma s}{2})]\sinh(\frac{a\rho u}{2})}}{\prod_{j'=1}^{n_M}\omega_{j'}} \\
&= \frac{G^2}{(2\pi)^{3n_M}} \frac{\rho}{2^{n_M}} \iint du ds \; e^{-i\Delta m \rho u} \frac{e^{-\frac{2i}{a}[\sum_{j=1}^{n_M}\tilde{\omega}_{k_j}]\sinh(\frac{a\rho u}{2})}}{\prod_{j'=1}^{n_M}\omega_{j'}}.
\end{aligned} \tag{3.17}
$$

Note the integrand of our differential probability is now independent of the proper time parameter s. Therefore we can now divide out the total proper time interval $\int ds = \Delta s$ to obtain the transition probability per unit proper time, $\Gamma_{n_M}(\Delta m, a) = \mathcal{P}/\Delta s$. Furthermore, since we have the proper quantity $\tilde{\omega}$ in the exponent we will need to change the remaining momentum variables to the boosted frame as well. Upon inversion of the Lorentz transformations in Eq. (3.16) we obtain $k_z = \tilde{\omega}\sinh(a\tilde{s}) + \tilde{k}_z\cosh(a\tilde{s})$ and $\omega = \tilde{\omega}\cosh(a\tilde{s}) + \tilde{k}_z\sinh(a\tilde{s})$.

Recalling first that $\tilde{\mathbf{k}}_\perp = \mathbf{k}_\perp$, we then examine the quantity dk_z/ω. Hence

$$\begin{aligned}
\frac{dk_z}{\omega} &= \frac{dk_z}{d\tilde{k}_z}\frac{d\tilde{k}_z}{\omega} \\
&= \frac{d}{d\tilde{k}_z}[\tilde{\omega}\sinh(a\tilde{s}) + \tilde{k}_z\cosh(a\tilde{s})]\frac{d\tilde{k}_z}{\omega} \\
&= [\frac{\tilde{k}_z}{\tilde{\omega}}\sinh(a\tilde{s}) + \cosh(a\tilde{s})]\frac{d\tilde{k}_z}{\omega} \\
&= \frac{\tilde{k}_z\sinh(a\tilde{s}) + \tilde{\omega}\cosh(a\tilde{s})}{\tilde{\omega}}\frac{d\tilde{k}_z}{\omega} \\
&= \frac{d\tilde{k}_z}{\tilde{\omega}}. \qquad (3.18)
\end{aligned}$$

The recasting of our transition rate in terms of proper frame variables, accompanied by the rescaling of our proper time via $u \to \rho u$, yields the following more convenient expression:

$$\begin{aligned}
\Gamma_{n_M}(\Delta m, a) &= \frac{\mathcal{P}}{\Delta s} \\
&= \frac{G^2}{(2\pi)^{3n_M}}\frac{1}{2^{n_M}}\iint du D_{n_M}^3 k\, e^{-i\Delta m u}\frac{e^{-\frac{2i}{a}[\sum_{j=1}^{n_M}\tilde{\omega}_{k_j}]\sinh(\frac{au}{2})}}{\prod_{j'=1}^{n_M}\omega_{j'}} \\
&= \frac{G^2}{(2\pi)^{3n_M}}\frac{1}{2^{n_M}}\iint du \prod_{\ell=1}^{n_M} d^3k_\ell\, e^{-i\Delta m u}\frac{e^{-\frac{2i}{a}[\sum_{j=1}^{n_M}\tilde{\omega}_{k_j}]\sinh(\frac{au}{2})}}{\prod_{j'=1}^{n_M}\omega_{j'}} \\
&= \frac{G^2}{(2\pi)^{3n_M}}\frac{1}{2^{n_M}}\iint du \prod_{\ell=1}^{n_M} d^3\tilde{k}_\ell\, e^{-i\Delta m u}\frac{e^{-\frac{2i}{a}[\sum_{j=1}^{n_M}\tilde{\omega}_{k_j}]\sinh(\frac{au}{2})}}{\prod_{j'=1}^{n_M}\tilde{\omega}_{j'}}. \qquad (3.19)
\end{aligned}$$

The isotropy of the momentum of the emitted particles in the proper frame is apparent from the above expression. To further facilitate the calculation, we exploit this spherical symmetry by moving our momentum integrations into spherical coordinates. Thus

$$\begin{aligned}
\Gamma_{n_M}(\Delta m, a) &= \frac{G^2}{(2\pi)^{3n_M}} \frac{1}{2^{n_M}} \iint du \prod_{\ell=1}^{n_M} d^3\tilde{k}_\ell \; e^{-i\Delta m u} \frac{e^{-\frac{2i}{a}[\sum_{j=1}^{n_M} \tilde{\omega}_{k_j}] \sinh(\frac{au}{2})}}{\prod_{j'=1}^{n_M} \tilde{\omega}_{j'}} \\
&= \frac{G^2}{(2\pi)^{3n_M}} \frac{1}{2^{n_M}} \iint du \prod_{\ell=1}^{n_M} \tilde{k}_\ell^2 \sin(\tilde{\theta}_\ell) d\tilde{k}_\ell d\tilde{\theta}_\ell d\tilde{\phi}_\ell \; e^{-i\Delta m u} \frac{e^{-\frac{2i}{a}[\sum_{j=1}^{n_M} \tilde{\omega}_{k_j}] \sinh(\frac{au}{2})}}{\prod_{j'=1}^{n_M} \tilde{\omega}_{j'}} \\
&= \frac{(4\pi)^{n_M} G^2}{(2\pi)^{3n_M}} \frac{1}{2^{n_M}} \iint du \prod_{\ell=1}^{n_M} \tilde{k}_\ell^2 d\tilde{k}_\ell \; e^{-i\Delta m u} \frac{e^{-\frac{2i}{a}[\sum_{j=1}^{n_M} \tilde{\omega}_{k_j}] \sinh(\frac{au}{2})}}{\prod_{j'=1}^{n_M} \tilde{\omega}_{j'}}. \qquad (3.20)
\end{aligned}$$

Then, for the final state massless fields ϕ_i, we have $\tilde{\omega}_i = \tilde{k}_i$ and we may further simplify the above integrations to

$$\begin{aligned}
\Gamma_{n_M}(\Delta m, a) &= \frac{(4\pi)^{n_M} G^2}{(2\pi)^{3n_M}} \frac{1}{2^{n_M}} \iint du \prod_{\ell=1}^{n_M} \tilde{k}_\ell^2 d\tilde{k}_\ell \; e^{-i\Delta m u} \frac{e^{-\frac{2i}{a}[\sum_{j=1}^{n_M} \tilde{\omega}_{k_j}] \sinh(\frac{au}{2})}}{\prod_{j'=1}^{n_M} \tilde{\omega}_{j'}} \\
&= G^2 \frac{1}{(2\pi)^{2n_M}} \iint du \prod_{\ell=1}^{n_M} \tilde{k}_\ell^2 d\tilde{k}_\ell \; e^{-i\Delta m u} \frac{e^{-\frac{2i}{a}[\sum_{j=1}^{n_M} \tilde{k}_j] \sinh(\frac{au}{2})}}{\prod_{j'=1}^{n_M} \tilde{k}_{j'}} \\
&= G^2 \frac{1}{(2\pi)^{2n_M}} \iint du \prod_{\ell=1}^{n_M} \tilde{k}_\ell d\tilde{k}_\ell \; e^{-i\Delta m u} e^{-\frac{2i}{a}[\sum_{j=1}^{n_M} \tilde{k}_j] \sinh(\frac{au}{2})} \\
&= G^2 \frac{1}{(2\pi)^{2n_M}} \int du \; e^{-i\Delta m u} \left[\int d\tilde{k} \; \tilde{k} e^{-\frac{2i}{a}\tilde{k} \sinh(\frac{au}{2})} \right]^{n_M}. \qquad (3.21)
\end{aligned}$$

The integral over $\tilde{k}$ will require the use of a regulator to the ensure convergence of the integral. In order to damp the oscillation at infinity, we let $\sinh(\frac{au}{2}) \to \sinh(\frac{au}{2}) - i\epsilon \approx \sinh(\frac{au}{2} - i\epsilon)$ with $\epsilon > 0$. As such, the momentum integration yields

$$\begin{aligned}
\int d\tilde{k} \; \tilde{k} e^{-\frac{2i}{a}\tilde{k} \sinh(\frac{au}{2})} &= \int_0^\infty d\tilde{k} \; \tilde{k} e^{-\frac{2i}{a}\tilde{k}(\sinh(\frac{au}{2}) - i\epsilon)} \\
&= \left[e^{-\frac{2i}{a}\tilde{k}(\sinh(\frac{au}{2}) - i\epsilon)} \frac{(1 + \frac{2}{a}\tilde{k}(\sinh(\frac{au}{2}) - i\epsilon))}{(\frac{2}{a}(\sinh(\frac{au}{2}) - i\epsilon))^2} \right]_0^\infty \\
&= -\frac{a^2}{4} \frac{1}{\sinh^2(\frac{au}{2} - i\epsilon)}. \qquad (3.22)
\end{aligned}$$

It should be noted that, up to a multiplicative constant, we have reproduced the Wightman function for a massless scalar field in Rindler space, Eq. (2.16). We arrived at this expression by inserting the hyperbolic trajectory into the mode functions prior to evaluating the two point function rather than evaluating the two point function first and then inserting the trajectory as we did in the previous section. The fact that we obtained the same result serves as a self-consistency check. This method also served to shed light on the physics of the emission process in the proper frame. For a more comprehensive analysis of the physics of the proper frame we refer the reader to Ref. [24]. Our acceleration induced transition rate, Eq. (3.21), then takes the form

$$\begin{aligned}
\Gamma_{n_M}(\Delta m, a) &= G^2 \frac{1}{(2\pi)^{2n_M}} \int du\, e^{-i\Delta m u} \left[\int d\tilde{k}\, \tilde{k} e^{-\frac{2i}{a}\tilde{k}\sinh\left(\frac{au}{2}\right)} \right]^{n_M} \\
&= G^2 \frac{1}{(2\pi)^{2n_M}} \int du\, e^{-i\Delta m u} \left[-\frac{a^2}{4} \frac{1}{\sinh^2\left(\frac{au}{2} - i\epsilon\right)} \right]^{n_M} \\
&= G^2 \left(\frac{ia}{4\pi}\right)^{2n_M} \int du\, \frac{e^{-i\Delta m u}}{\left[\sinh\left(\frac{au}{2} - i\epsilon\right)\right]^{2n_M}}.
\end{aligned} \tag{3.23}$$

A similar integral, Eq. (2.18), was encountered in the previous chapter. By making the replacement in the integrand $m \to -\Delta m$ we can quote the result by inspection. Hence,

$$\Gamma_{n_M}(\Delta m, a) = G^2 \left(\frac{ia}{2\pi}\right)^{2n_M} \frac{1}{a} \frac{2\pi i}{(2n_M - 1)!} \frac{\Gamma(-i\Delta m/a + n_M)}{\Gamma(-i\Delta m/a + 1 - n_M)} \frac{1}{1 - e^{2\pi\Delta m/a}}. \tag{3.24}$$

To recast the above gamma functions into the same form as the previous chapter we recall the identity $\Gamma(z)\Gamma(1-z) = \frac{\pi}{\sin(\pi z)}$ to find

$$\frac{\Gamma(-i\Delta m/a + n_M)}{\Gamma(-i\Delta m/a + 1 - n_M)} = -\frac{\Gamma(i\Delta m/a + n_M)}{\Gamma(i\Delta m/a + 1 - n_M)}. \tag{3.25}$$

Thus, our total rate, Eq. (3.24), of our two-level system to undergo an acceleration induced transition and simultaneously emit n_M massless scalar fields is given by

$$\Gamma_{n_M}(\Delta m, a) = G^2 \left(\frac{ia}{2\pi}\right)^{2n_M} \frac{1}{a} \frac{2\pi i}{(2n_M - 1)!} \frac{\Gamma(i\Delta m/a + n_M)}{\Gamma(i\Delta m/a + 1 - n_M)} \frac{1}{e^{2\pi\Delta m/a} - 1}. \tag{3.26}$$

As expected, we have reproduced the same expression as in the previous chapter provided we made the appropriate identifications for m. The use of an Unruh-DeWitt detector has provided us with a relatively simple procedure for including a massive particle in the final state but at the expense of keeping it confined to Rindler space. This is due to one of the final state particles being locked in the detector. Again, normalizing the transition rate via $\tilde{\Gamma} = \Gamma/\Gamma_0$ with $\Gamma_0 = G^2$, we write out the first few normalized decay rates $\tilde{\Gamma}_{n_M}$. Hence,

$$\begin{aligned}
\tilde{\Gamma}_1(\Delta m, a) &= \frac{\Delta m}{2\pi} \frac{1}{e^{2\pi\Delta m/a} - 1} \\
\tilde{\Gamma}_2(\Delta m, a) &= \frac{(\Delta m)^3}{48\pi^3} \frac{1 + \left(\frac{a}{\Delta m}\right)^2}{e^{2\pi\frac{\Delta m}{a}} - 1} \\
\tilde{\Gamma}_3(\Delta m, a) &= \frac{(\Delta m)^5}{3840\pi^5} \frac{1 + 5\left(\frac{a}{\Delta m}\right)^2 + 4\left(\frac{a}{\Delta m}\right)^4}{e^{2\pi\Delta m/a} - 1} \\
\tilde{\Gamma}_4(\Delta m, a) &= \frac{(\Delta m)^7}{645120\pi^7} \frac{1 + 14\left(\frac{a}{\Delta m}\right)^2 + 49\left(\frac{a}{\Delta m}\right)^4 + 36\left(\frac{a}{\Delta m}\right)^6}{e^{2\pi\Delta m/a} - 1} \\
\tilde{\Gamma}_5(\Delta m, a) &= \frac{(\Delta m)^9}{185794560\pi^9} \times \\
&\quad \frac{1 + 30\left(\frac{a}{\Delta m}\right)^2 + 273\left(\frac{a}{\Delta m}\right)^4 + 820\left(\frac{a}{\Delta m}\right)^6 + 576\left(\frac{a}{\Delta m}\right)^8}{e^{2\pi\Delta m/a} - 1}.
\end{aligned} \tag{3.27}$$

Comparing with the previous rates from Eq. (2.22), the use of an Unruh-DeWitt detector to model particle decays produces a similar form for the decay rate but with a more general mass transition. This is due to the fact that the particle that is coupled into the two-level system with the initial accelerated particle remains in Rindler space. In the previous chapter all final state particles were emitted into Minkowski space and it was the Wightman functions

of these particles which contributed to the polynomial. Therefore one must take care when analyzing a system to ensure that the final state particles, i.e. fields, are expressed in terms of the mode functions of the appropriate spacetime.

By using the Unruh-DeWitt detector we can analyze not only acceleration induced decays but also excitations. By letting $\Delta m = -1$ we can reproduce the results of the previous chapter. Rather we set $\Delta m = 1$ to analyze an initially accelerated particle that excites into a more massive state. We can now look at normalized $\tilde{\Gamma}_{n_M}$ detector excitation rates with the simultaneous emission of n_M massless particles into Minkowski space. We focus this analysis for $a \geq \Delta m$ since the relevant plots rapidly diverge at low acceleration to reflect the infinite lifetimes for stable particles in inertial frames (see Figs. 3.1 and 3.2).

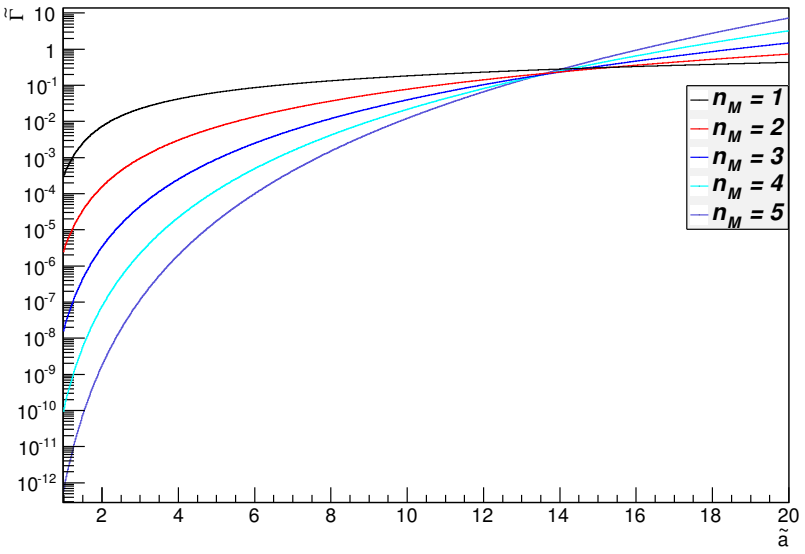

Figure 3.1: The normalized excitation rates, Eq. (3.27), with $\tilde{a} = a/\Delta m$ and $\Delta m = 1$.

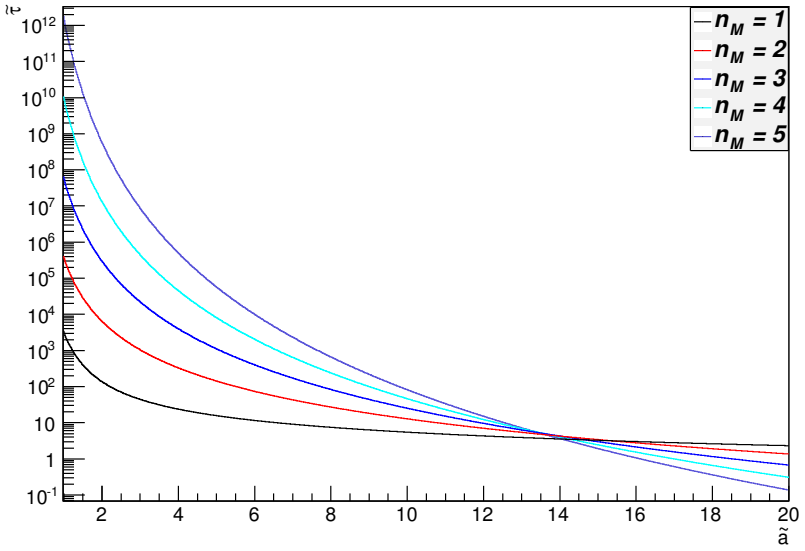

Figure 3.2: The normalized excitation lifetimes $\tilde{\tau} = 1/\tilde{\Gamma}$ with $\tilde{a} = a/\Delta m$ and $\Delta m = 1$.

We have found in this chapter that the use of an Unruh-DeWitt detector allows for a more general mass transition when examining the effect of acceleration on unstable particles. This is due to the coupling of one of the final state products into the accelerated detector which effectively keeps this particle in Rindler space. This situation arises, for example, when the acceleration mechanism is an electric field and an initial charged particle undergoes a transition into another charged particle with the simultaneous emission of two neutral particles. The final state charged particle remains in Rindler space on account of the acceleration due to the electric field while the neutral particles are unaffected by the electric field and are thus effectively in Minkowski space. A muon accelerated by an electric field and decaying into an electron and two neutrinos is an example of this type of process. This and the reverse process of electron excitation will be analyzed in a later chapter. In the next chapter we generalize the accelerated field transition process to arbitrary final state multiplicities in both Rindler and Minkowski spacetimes.

Chapter 4

Generalized N-Particle Transition Rates

In the previous chapters we evaluated the acceleration induced transition rate using two different methods. We now demonstrate the equivalence between the two methods and also show how to correctly interpret and make use of the overall formalism considering an initial particle in Rindler spacetime and allowing it to decay into n_R particles in Rindler space and n_M particles into Minkowski space. Schematically we are examining the process

$$\Psi_i \rightarrow_a \Psi_1 \Psi_2 \cdots \Psi_{n_R} \phi_1 \phi_2 \cdots \phi_{n_M} \tag{4.1}$$

We denote the initial accelerated massive field by Ψ_i, the final state Rindler particles of arbitrary mass by Ψ_j, and the massless final state Minkowski particles by ϕ_k. In order to analyze this process we consider the following more general interaction action [31, 32]:

$$\hat{S}_I = \int d^4x \sqrt{-g} \sqrt{\frac{2}{\sigma\kappa}} G \hat{\Psi}_i \prod_{r=1}^{n_R} \hat{\Psi}_r \prod_{m=1}^{n_M} \hat{\phi}_m. \tag{4.2}$$

As before, the coupling constant G will be determined by the inertial limit of the specific

interaction in question and the additional factor $\sqrt{\frac{2}{\sigma\kappa}}$ is defined for later convenience. The probability amplitude for the acceleration induced transition of our massive initial state into n total particles is given by

$$\mathcal{A} = \langle \prod_{\ell=1}^{n_M} \mathbf{k}_\ell | \otimes \langle \prod_{j=1}^{n_R} \Psi_j | \, \hat{S}_I \, | \Psi_i \rangle \otimes |0\rangle \, . \tag{4.3}$$

The Rindler states $|\Psi_j\rangle$ are labeled by the index j while the Minkowski states $|\mathbf{k}_\ell\rangle$ are labeled by their momenta. We again use the same notation for our Fock states and accommodate any complications due to the statistics or degeneracies of the final state products by rescaling our effective coupling. With the same notation $\prod_{n=1}^{n_M} d^3k_{n_M} = D^3_{n_M}k$ the differential probability for the accelerated field to decay and emit n_R particles into Rindler space and n_M particles into Minkowski space is given by

$$\begin{aligned}
\frac{d\mathcal{P}}{D^3_{n_M}k} &= |\mathcal{A}|^2 \\
&= G^2 \frac{2}{\sigma\kappa} \left| \int d^4x \sqrt{-g} \, \langle \prod_{\ell=1}^{n_M} \mathbf{k}_\ell | \otimes \langle \prod_{j=1}^{n_R} \Psi_j | \, \hat{\Psi}_i(x) \prod_{r=1}^{n_R} \hat{\Psi}_r(x) \prod_{m=1}^{n_M} \hat{\phi}_m(x) \, | \Psi_i \rangle \otimes |0\rangle \right|^2 \\
&= G^2 \frac{2}{\sigma\kappa} \left| \int d^4x \sqrt{-g} \, \langle \prod_{j=1}^{n_R} \Psi_j | \, \hat{\Psi}_i(x) \prod_{r=1}^{n_R} \hat{\Psi}_r(x) \, | \Psi_i \rangle \, \langle \prod_{\ell=1}^{n_M} \mathbf{k}_\ell | \prod_{m=1}^{n_M} \hat{\phi}_m(x) \, |0\rangle \right|^2 \\
&= G^2 \frac{2}{\sigma\kappa} \iint d^4x d^4x' \sqrt{-g}\sqrt{-g'} \times \\
&\quad \left| \langle \prod_{j=1}^{n_R} \Psi_j | \, \hat{\Psi}_i(x) \prod_{r=1}^{n_R} \hat{\Psi}_r(x) \, | \Psi_i \rangle \right|^2 \left| \langle \prod_{\ell=1}^{n_M} \mathbf{k}_\ell | \prod_{m=1}^{n_M} \hat{\phi}_m(x) \, |0\rangle \right|^2 .
\end{aligned} \tag{4.4}$$

We can now factor out the n_M complete set of momentum eigenstates. The result will give the product of Wightman functions of the massless Minkowski fields,

$$
\begin{aligned}
\mathcal{P} &= G^2 \frac{2}{\sigma\kappa} \iint d^4x d^4x' \sqrt{-g}\sqrt{-g'} \times \\
&\quad \left| \langle \prod_{j=1}^{n_R} \Psi_j | \, \hat{\Psi}_i(x) \prod_{r=1}^{n_R} \hat{\Psi}_r(x) \, |\Psi_i\rangle \right|^2 \prod_{n=1}^{n_M} \int d^3k_{n_M} \left| \langle \prod_{\ell=1}^{n_M} \mathbf{k}_\ell | \prod_{m=1}^{n_M} \hat{\phi}_m(x) \, |0\rangle \right|^2 \\
&= G^2 \frac{2}{\sigma\kappa} \iint d^4x d^4x' \sqrt{-g}\sqrt{-g'} \times \\
&\quad \left| \langle \prod_{j=1}^{n_R} \Psi_j | \, \hat{\Psi}_i(x) \prod_{r=1}^{n_R} \hat{\Psi}_r(x) \, |\Psi_i\rangle \right|^2 \prod_{m=1}^{n_M} \langle 0| \, \hat{\phi}_m(x') \hat{\phi}_m(x) \, |0\rangle \\
&= G^2 \frac{2}{\sigma\kappa} \iint d^4x d^4x' \sqrt{-g}\sqrt{-g'} \times \\
&\quad \left| \langle \prod_{j=1}^{n_R} \Psi_j | \, \hat{\Psi}_i(x) \prod_{r=1}^{n_R} \hat{\Psi}_r(x) \, |\Psi_i\rangle \right|^2 [G^{\pm}(x', x)]^{n_M}. \qquad (4.5)
\end{aligned}
$$

We now examine the remaining Rindler space inner products. As before, we have seen that each field operator serves to extract the appropriate mode function of each Rindler particle. The Rindler coordinate proper time of the initial field will again serve as our time coordinate. As such we can examine the above inner products. Hence

$$
\begin{aligned}
\langle \prod_{j=1}^{n_R} \Psi_j | \, \hat{\Psi}_i(x) \prod_{r=1}^{n_R} \hat{\Psi}_r(x) \, |\Psi_i\rangle &= f_{\Psi_i}[x(\tau)] e^{-im_i\tau} \prod_{r=1}^{n_R} f^*_{\Psi_r}[x(\tau)] e^{i\omega_r\tau} \\
&= \left[f_{\Psi_i}[x(\tau)] \prod_{r=1}^{n_R} f^*_{\Psi_r}[x(\tau)] \right] e^{i\Delta E_R \tau}. \qquad (4.6)
\end{aligned}
$$

The Rindler mode frequencies ω_r correspond to the energies of final state Rindler particles which may not necessarily be the appropriate rest masses. Also we have defined $\Delta E_R = \sum \omega_r - m_i$ to be the total energy difference between the final and initial Rindler space field configuration. Our total transition probability, Eq. (4.5), then becomes

$$
\begin{aligned}
\mathcal{P} &= G^2 \frac{2}{\sigma\kappa} \iint d^4x d^4x' \sqrt{-g}\sqrt{-g'} \times \\
&\quad \left| \langle \prod_{j=1}^{n_R} \Psi_j | \, \hat{\Psi}_i(x) \prod_{r=1}^{n_R} \hat{\Psi}_r(x) \, | \Psi_i \rangle \right|^2 [G^{\pm}(x', x)]^{n_M} \\
&= G^2 \frac{2}{\sigma\kappa} \iint d^4x d^4x' \sqrt{-g}\sqrt{-g'} \times \\
&\quad \left| \left[f_{\Psi_i}[x(\tau)] \prod_{r=1}^{n_R} f^*_{\Psi_r}[x(\tau)] \right] e^{i\Delta E_R \tau} \right|^2 [G^{\pm}(x', x)]^{n_M} \\
&= G^2 \frac{2}{\sigma\kappa} \iint d^4x d^4x' \sqrt{-g}\sqrt{-g'} \times \\
&\quad \left| f_{\Psi_i}[x(\tau)] \prod_{r=1}^{n_R} f^*_{\Psi_r}[x(\tau)] \right|^2 e^{-i\Delta E_R(\tau' - \tau)} [G^{\pm}(x', x)]^{n_M}. \qquad (4.7)
\end{aligned}
$$

We again define κ to be the overall normalization of the product of envelope functions f_Ψ, i.e.

$$
\kappa = \iint d^3x d^3x' \sqrt{-g}\sqrt{-g'} \left| f_{\Psi_i}[x(\tau)] \prod_{r=1}^{n_R} f^*_{\Psi_r}[x(\tau)] \right|^2 . \qquad (4.8)
$$

As such the total probability for our transition becomes

$$
\mathcal{P} = G^2 \frac{2}{\sigma} \iint d\tau d\tau' e^{-i\Delta E_R(\tau' - \tau)} [G^{\pm}(x', x)]^{n_M}. \qquad (4.9)
$$

In carrying out this analysis we see that one can consider having a transition involving an arbitrary number of final state particles in Rindler space to be equivalent to having an Unruh-DeWitt detector with the energy levels being the initial and final state energies of the Rindler space field configuration as seen in the proper frame of the initially accelerated field. Having evaluated this expression before we know the remaining procedures are to formulate

the transition rate and evaluate the Fourier transform of the product of the Minkowski final state Wightman functions evaluated along the accelerated trajectory of the initial Rindler particle state. We now quote the final form of the transition probability. Thus

$$\begin{aligned}\Gamma_{n_M}(\Delta E_R, a) &= G^2 \left(\frac{ia}{2\pi}\right)^{2n_M} \frac{1}{a} \frac{2\pi i}{(2n_M - 1)!} \times \\ &\quad \frac{\Gamma(i\Delta E_R/a + n_M)}{\Gamma(i\Delta E_R/a + 1 - n_M)} \frac{1}{e^{2\pi\Delta E_R/a} - 1}. \end{aligned} \tag{4.10}$$

This is the same form of the expression that we have arrived at previously but now we have a clearer understanding of the role each of the Rindler and Minkowski space fields plays in the transition rate. For the sake of completeness, we list the normalized decay rates $\tilde{\Gamma}_{n_M}(\Delta E_R, a)$, for the first few multiplicities. Hence,

$$\begin{aligned}
\tilde{\Gamma}_1(\Delta E_R, a) &= \frac{\Delta E_R}{2\pi} \frac{1}{e^{2\pi\Delta E_R/a} - 1} \\
\tilde{\Gamma}_2(\Delta E_R, a) &= \frac{\Delta E_R^3}{48\pi^3} \frac{1 + \left(\frac{a}{\Delta E_R}\right)^2}{e^{2\pi\Delta E_R/a} - 1} \\
\tilde{\Gamma}_3(\Delta E_R, a) &= \frac{\Delta E_R^5}{3840\pi^5} \frac{1 + 5\left(\frac{a}{\Delta E_R}\right)^2 + 4\left(\frac{a}{\Delta E_R}\right)^4}{e^{2\pi\Delta E_R/a} - 1} \\
\tilde{\Gamma}_4(\Delta E_R, a) &= \frac{\Delta E_R^7}{645120\pi^7} \frac{1 + 14\left(\frac{a}{\Delta E_R}\right)^2 + 49\left(\frac{a}{\Delta E_R}\right)^4 + 36\left(\frac{a}{\Delta E_R}\right)^6}{e^{2\pi\Delta E_R/a} - 1} \\
\tilde{\Gamma}_5(\Delta E_R, a) &= \frac{\Delta E_R^9}{185794560\pi^9} \times \\
&\quad \frac{1 + 30\left(\frac{a}{\Delta E_R}\right)^2 + 273\left(\frac{a}{\Delta E_R}\right)^4 + 820\left(\frac{a}{\Delta E_R}\right)^6 + 576\left(\frac{a}{\Delta E_R}\right)^8}{e^{2\pi\Delta E_R/a} - 1}.
\end{aligned} \tag{4.11}$$

The difficulty in measuring these effects is that the acceleration scale currently accessible in laboratory settings is significantly smaller than the energy scale of the transition. If, through some mechanism, we could not only control the acceleration but also the transition

energy scale we could bring the effects closer to our experimental reach. A mathematical analysis of the energy spectra of Rindler particles which have decay products in both Rindler and Minkowski spacetime has yet to be carried out but would provide a much clearer insight into the how any Rindler particle energies would be perceived in the proper frame of the accelerated field. With this in mind we plot, in Figs. 4.1 and 4.2, the normalized decay rates and lifetimes for a constant acceleration $a = 1$ while varying the energy scale ΔE_R.

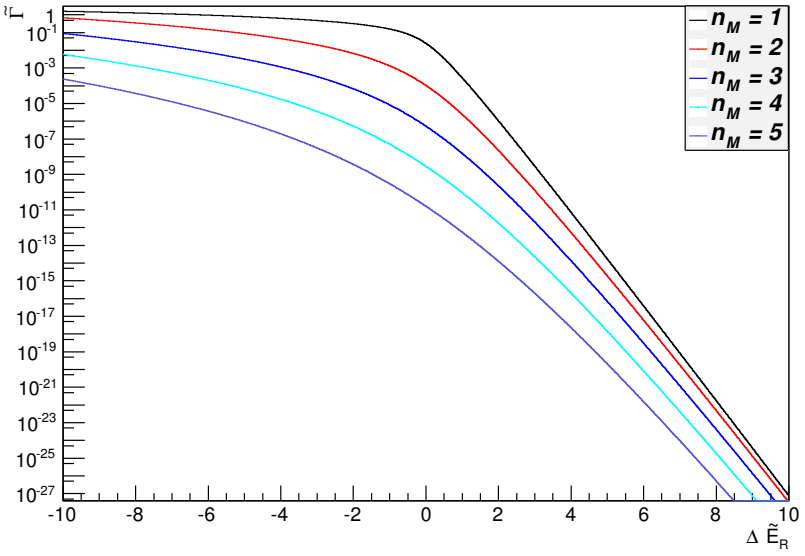

Figure 4.1: The normalized transition rates, Eq. (4.11), with $\Delta\tilde{E}_R = \Delta\tilde{E}_R/a$ and $a = 1$.

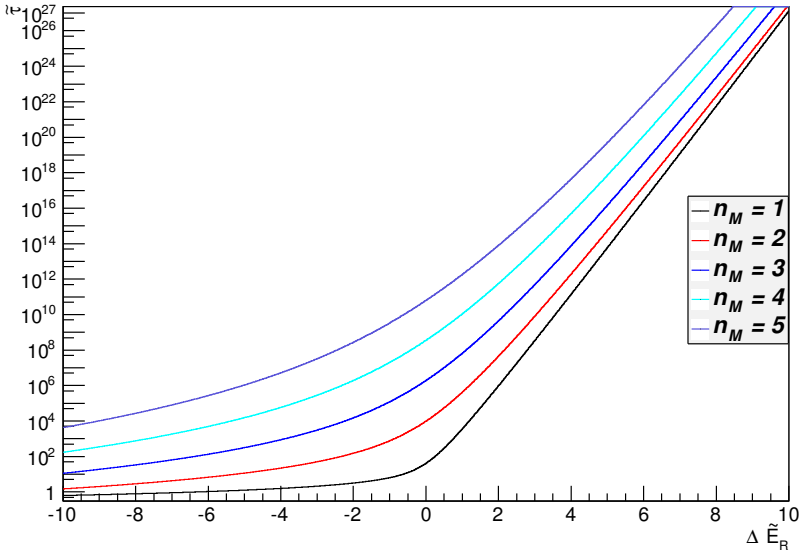

Figure 4.2: The normalized transition lifetimes $\tilde{\tau} = 1/\tilde{\Gamma}$ with $\Delta\tilde{E}_R = \Delta\tilde{E}_R/a$ and $a = 1$.

To better understand the role each spacetime field configuration has in the transition rate, we define the polynomial of multiplicity $\mathcal{M}_{n_M}(\Delta E_R, a)$ as follows:

$$\mathcal{M}_{n_M}(\Delta E_R, a) = \left(\frac{ia}{2\pi}\right)^{2n_M} \frac{1}{a} \frac{2\pi i}{(2n_M - 1)!} \frac{\Gamma(i\Delta E_R/a + n_M)}{\Gamma(i\Delta E_R/a + 1 - n_M)}. \tag{4.12}$$

We then find the general form for the decay rate to be

$$\Gamma_{n_M}(\Delta E_R, a) \quad = \quad G^2 \mathcal{M}_{n_M}(\Delta E_R, a) f(\Delta E_R, a). \tag{4.13}$$

We see that the rate factors into the inertial interaction specific coupling, the polynomial of multiplicity, and the thermal distribution $f(\Delta E_R, a)$ associated with the Unruh effect. The final state multiplicity in Minkowski space governs the number of terms in the polynomial while the total change of the energy in Rindler space sets the acceleration scale of the transition rate. The inertial interaction coupling constant sets the overall normalization of the transition rate.

In this chapter we generalized the analysis of acceleration induced field transitions to that of arbitrary Rindler and Minkowski space particle multiplicities. We determined the roles that each spacetime field configuration plays in the transition rate and examined how the rates evolve with the total energy change of Rindler space at constant acceleration. The next chapter focuses on the application of the above formalism to that of the electron and muon system.

Chapter 5

The Accelerated Electron and Muon System

The weak decay of muons into electrons could possibly provide a robust setting to investigate the effects of acceleration on certain aspects of the physics of unstable particles. We will apply the results of the previous section to model both muon decay as well as the reverse process of electron excitation utilizing the scalar field approximation. In addition to the standard decay/excitation rates, we will also compute the branching fractions of the muon decay chains as a function of proper acceleration. To model the muon and electron transitions we will assume the acceleration mechanism is something like an electric field so that both the muon and the electron are effectively in Rindler space, due to their charge, while the neutral neutrinos are emitted into Minkowski space. This setup more closely resembles an actual experimental setting which could, in principle, investigate this phenomena. Schematically we will analyze the following processes:

$$\mu^{\pm} \rightarrow_a e^{\pm} + \bar{\nu}_e + \nu_\mu, \quad e^{\pm} \rightarrow_a \mu^{\pm} + \bar{\nu}_\mu + \nu_e. \tag{5.1}$$

The transition rate which describes both of these processes is given by the $n_M = 2$ case

from Eq. (4.11),

$$\Gamma^{\mu\leftrightarrow e}(\Delta E_R, a) = G^2 \frac{(\Delta E_R)^3}{48\pi^3} \frac{1 + \left(\frac{a}{\Delta E_R}\right)^2}{e^{2\pi\Delta E_R/a} - 1}. \tag{5.2}$$

To determine the coupling constant G we compare the inertial limit of the above accelerated decay rate to that of the known inertial muon decay rate. The known decay rate of inertial muons, to lowest order in perturbation theory [37], is given by

$$\Gamma_i^\mu = \frac{G_f^2 m_\mu^5}{192\pi^3}, \tag{5.3}$$

where G_f is the Fermi coupling constant. Note we have disregarded higher order terms which contain powers of m_e/m_μ. As such, in our analysis of muon decay we may consider the electron, and of course the neutrinos, to be massless. In addition to considering the electron to be massless, we will also assume that the total energy of the electron emitted into Rindler space will be insignificant when compared to the muon mass. The spectra of the final state Minkowski particles has been calculated in Ref. [24] and indicates that each particle will have an energy distribution, as measured in the inertial frame instantaneously at rest with the initial accelerated particle, peaked about the proper acceleration. A computation of the energy spectra with the appropriate particles emitted into Rindler space has yet to be carried out. This would help more accurately determine the final state electron energy associated with the decay of accelerated muons. Recalling that $\Delta E_R = \sum \omega_R - m_i$, we will then have $\Delta E_R = -m_\mu$ for the current analysis. By taking the limit $a \to 0$ of the acceleration induced decay rate, Eq. (5.2), and equating it with the known inertial decay rate, Eq. (5.3), we can determine our effective coupling constant. Thus,

$$\begin{aligned}
\lim_{a\to 0}\Gamma^{\mu\to e}(\Delta E_R, a) &= \Gamma_i^{\mu} \\
\lim_{a\to 0} G^2 \frac{m_\mu^3}{48\pi^3}\frac{1+\left(\frac{a}{m_\mu}\right)^2}{1-e^{-2\pi m_\mu/a}} &= \frac{G_f^2 m_\mu^5}{192\pi^3} \\
\frac{G^2 m_\mu^3}{48\pi^3} &= \frac{G_f^2 m_\mu^5}{192\pi^3} \\
G &= \frac{1}{2} m_\mu G_f. \qquad (5.4)
\end{aligned}$$

As such, the properly normalized muon decay rate under the influence of acceleration is given by

$$\Gamma^{\mu\to e}(a) = \frac{G_f^2 m_\mu^5}{192\pi^3}\frac{1+\left(\frac{a}{m_\mu}\right)^2}{1-e^{-2\pi m_\mu/a}}. \qquad (5.5)$$

Our result differs from that of Mueller [22] by having a lower order polynomial due to our assumption of keeping the final state electron in Rindler space. Had we allowed the electron to be created in Minkowski space we would have recovered the same result as Mueller. Furthermore, the inclusion of fermions in the analysis would also yield a higher order polynomial due to the additional factors of frequency in the standard fermionic normalization [23, 24, 25]. This yields higher powers of frequency to be integrated over when summing over the final state momentum of the Minkowski particles. In either case, the resultant expressions are equivalent at low accelerations but also illustrate the fact that at high accelerations one needs to be precise in describing such processes. By recalling that $G_f = 1.166 \times 10^{-5}$ GeV^{-2} and $m_\mu = 105.7$ MeV, we can evaluate the canonical inertial muon lifetime $\frac{192\pi^3}{G_f^2 m_\mu^5} = \tau_\mu = 2.184$ μs which sets the overall scale of our transition rate. We need to also mention that the energy scale of the interaction is set by the acceleration. In this analysis we are using a scalar approximation of an effective Fermi interaction. The nonrenormalizability of this approximation necessitates the interaction energy to be less than the rest masses of the weak gauge bosons. With masses $m_W, m_Z \sim 1000$ GeV we have carried out all our analysis with

accelerations from 0 to 20 in muon mass units. With the muon system under consideration we have $\frac{20m_\mu}{m_W, m_Z} \sim .01 \ll 1$ and therefore our analysis remains valid. Plots of the acceleration-dependent muon decay rate and lifetime are shown below (see Figs. 5.1 and 5.2).

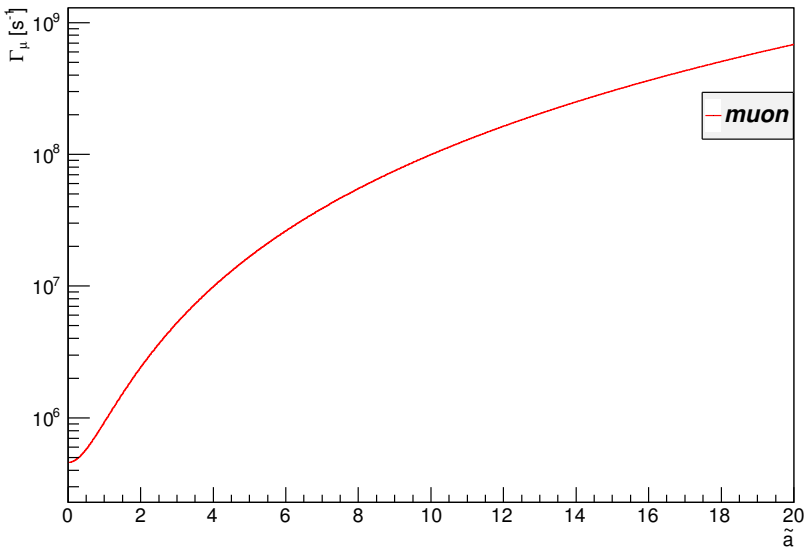

Figure 5.1: The muon decay rate, Eq. (5.5), as a function of $\tilde{a} = \frac{a}{m_\mu}$.

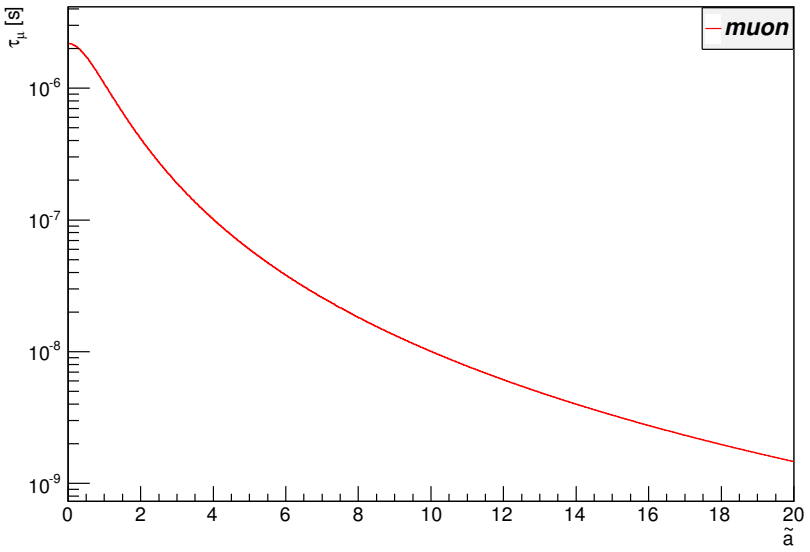

Figure 5.2: The muon lifetime $\tau_\mu = 1/\Gamma_\mu$ as a function of $\tilde{a} = \frac{a}{m_\mu}$.

We now apply the transition rate, Eq. (5.2), to the case of electron excitation. To do so, we use the detailed balance between the transitions $\Gamma^{e\to\mu} = e^{-2\pi\Delta E_R/a}\Gamma^{\mu\to e}$ at thermal equilibrium [35]. This is affected by merely reversing the sign $\Delta E_R \to -\Delta E_R$ or rather we take $m_\mu \to -m_\mu$ in Eq. (5.5). This also enables us to keep the overall coupling constant from the muon decay by using the symmetry between the two thermalized processes. Furthermore, this implies that the Rindler space energy of the created muon comprises mainly the mass with no appreciable momentum. Again we note that a better understanding of the energy spectra of all particles in all spacetimes is necessary to more accurately model these processes. With these considerations we can now estimate the acceleration induced excitation of electrons back into muons to be

$$\Gamma^{e\to\mu}(a) = \frac{G_f^2 m_\mu^5}{192\pi^3}\frac{1+\left(\frac{a}{m_\mu}\right)^2}{e^{2\pi m_\mu/a}-1}. \tag{5.6}$$

We can now plot, in Figs. 5.3 and 3.2, the excitation rate as well as the lifetime. Note the fact that the decay rate rapidly approaches zero as $a \to 0$, and thus causes the lifetime to diverge. This reflects the stability of inertial electrons.

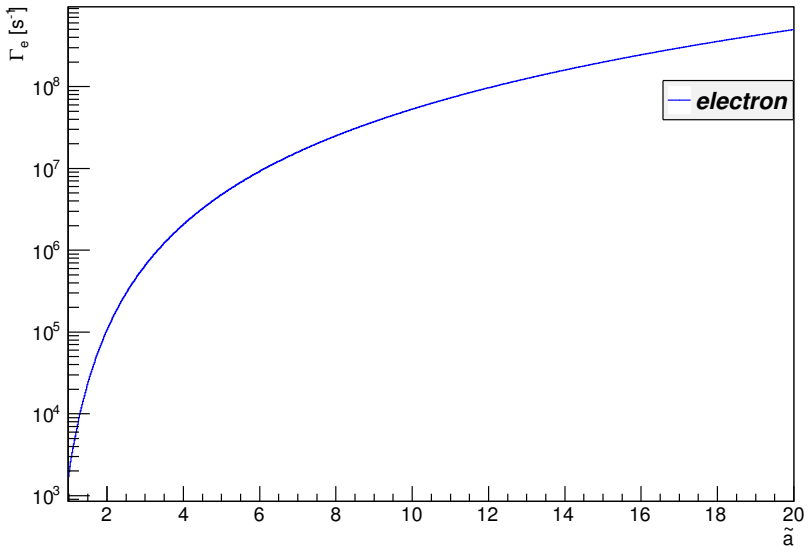

Figure 5.3: The electron excitation rate, Eq. (5.6), as a function of $\tilde{a} = \frac{a}{m_\mu}$.

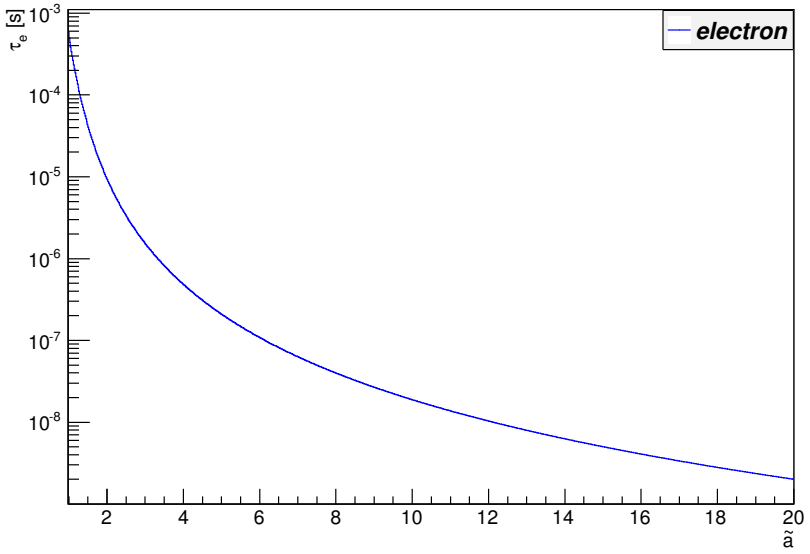

Figure 5.4: The electron lifetime $\tau_e = 1/\Gamma_e$ as a function of $\tilde{a} = \frac{a}{m_\mu}$.

This is a first estimate of the electron lifetime under the presence of uniform acceleration. A more accurate calculation would necessitate the inclusion of fermion fields as well as a weak or Fermi interaction Lagrangian. The use of fermions in the mathematically similar process of acceleration induced proton decay [24] yields a higher order polynomial of multiplicity in the decay rate due to additional factors of frequency in the fermionic normalization. This will not affect our result in the limit of low acceleration $a < m_\mu$. For higher accelerations, the difference between the scalar and fermionic description would be a higher order polynomial of multiplicity.

This analysis can be further utilized to investigate the various decay chains of accelerated muons. In this investigation we will assume all final state products to be massless and are emitted into Minkowski space, i.e. $\Delta E_R = -m_\mu$. This will allow us to get a better understanding of the overall conceptual properties of how the branching fractions of unstable particles change as a function of acceleration. Excluding any exotic or lepton number violating modes [38], there are three known decay channels for muons. These decay chains and their associated branching fractions are listed below:

$$\Gamma_1[\mu \to e\bar{\nu}_e\nu_\mu]: \quad Br_1 = 0.98599966$$
$$\Gamma_2[\mu \to e\bar{\nu}_e\nu_\mu\gamma]: \quad Br_2 = 0.014$$
$$\Gamma_3[\mu \to e\bar{\nu}_e\nu_\mu e\bar{e}]: \quad Br_3 = 0.000034. \tag{5.7}$$

We have seen in the previous chapters that the high acceleration limit favors the decay chain with the most final state products. Below we include the decay rate and lifetime plots of each decay channel, appropriately normalized to the inertial muon limit, for $n_M = 3, 4, 5$ final states from Eq. (4.11) weighted by their associated branching fractions (see Figs. 5.5 and 5.6). The crossover from the primary channel to the secondary and then tertiary takes place at approximately $a \sim 4m_\mu \sim 400$ MeV. We also include, for completeness, the various branching fractions as a function of proper acceleration given by

$$Br_i(a) = \frac{Br_i\Gamma_i(a)}{\sum_j Br_j\Gamma_j(a)}. \tag{5.8}$$

Rather than looking for direct evidence of acceleration induced decays it may be more experimentally tenable to measure these processes through the branching fractions of the decay chains and their dependence on proper acceleration (see Fig. 5.7). This may provide an easier method of discovering this or related phenomena.

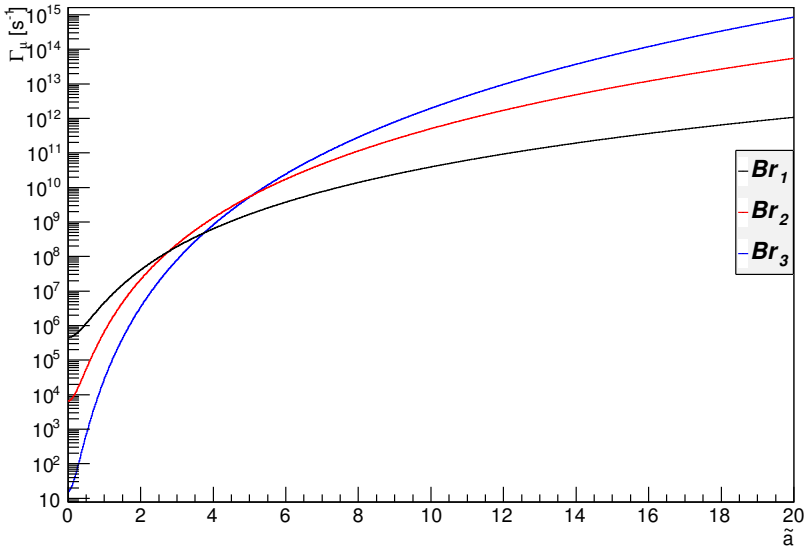

Figure 5.5: The muon decay rates for the three known branching ratios, Eq. (5.7), as a function of $\tilde{a} = \frac{a}{m_\mu}$.

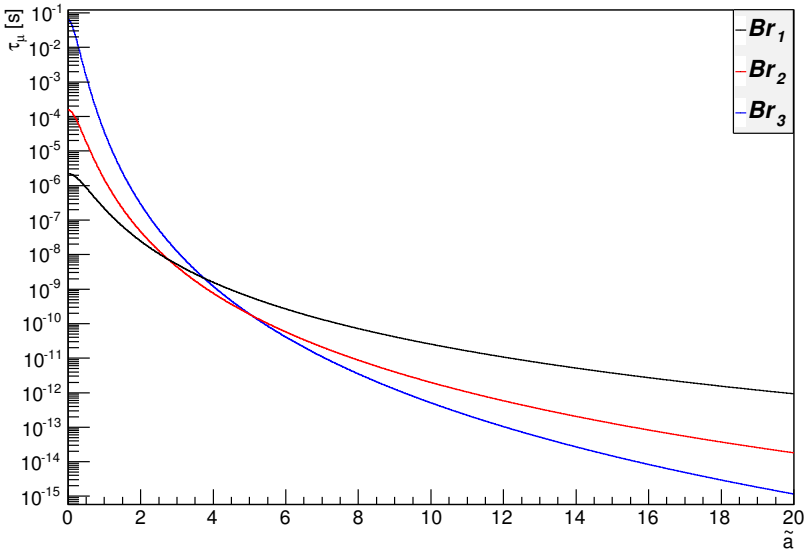

Figure 5.6: The muon lifetimes $\tau_\mu = 1/\Gamma_\mu$ for the three known branching ratios, Eq. (5.7), as a function of $\tilde{a} = \frac{a}{m_\mu}$.

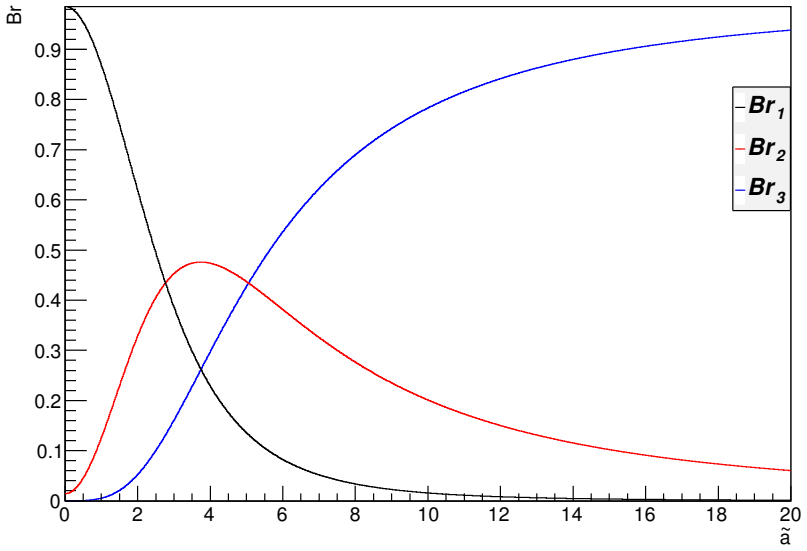

Figure 5.7: The muon decay branching fractions, Eq. (5.8), as a function of $\tilde{a} = \frac{a}{m_\mu}$.

Chapter 6

The Time-Dependent Response Function

In this chapter we set up a formalism capable of computing a wide class of particle transitions regardless of the number of final state products [22, 23, 24, 25, 29]. To facilitate the analysis, we consider all particles to be scalars. Consider an initial Rindler particle moving along an arbitrary time-dependent accelerated trajectory and decaying into a final state containing n_R Rindler particles and n Minkowksi particles. This process is schematically written as

$$\Psi_i \rightarrow_a \Psi_1 + \Psi_2 + \cdots + \Psi_{n_R} + \phi_1 + \phi_2 + \cdots + \phi_n. \tag{6.1}$$

The initial and final Rindler particles are denoted by Ψ_j and are used to describe any particle under acceleration. We consider the initial Rindler particle to be massive while the final state Rindler particles can be massless or massive in any combination. The massless Minkowski particles in the final state are denoted by ϕ_k and are used to describe any particles propagating along inertial trajectories. To describe these transitions, we consider their coupling to be described by the following general interaction action [29, 31, 32],

$$\hat{S}_I = \frac{G_n}{\sqrt{\kappa}} \int d^4x \sqrt{-g} \hat{\Psi}_i \prod_{r=1}^{n_R} \hat{\Psi}_r \prod_{m=1}^{n} \hat{\phi}_m. \tag{6.2}$$

The coupling constant G_n is labeled by the multiplicity and can be determined by fixing it to a known process in the inertial limit. We note that the coupling may be dimensionful depending on the transition in question. The $\frac{1}{\sqrt{\kappa}}$ term is included to absorb the overall normalization of our Rindler states. The domain of integration is confined to the right Rindler wedge where the modes of our accelerated fields are defined. We denote the Fock states of our Rindler particles $|\Psi_j\rangle$ with the index j characterizing their energies. As usual, we label our Minkowski states $|\mathbf{k}_\ell\rangle$ by their momenta. We use the notation $|\prod_i^n \mathbf{k}_i\rangle = |\mathbf{k}_1, \mathbf{k}_2, \cdots \mathbf{k}_n\rangle$ for the Fock states of both the Rindler and Minkowski fields. Note that we leave off subscripts denoting the Rindler and Minkowski Fock states and let the field operators imply the label, i.e. $|\Psi_j\rangle_R \to |\Psi_j\rangle$ and $|\mathbf{k}_i\rangle_M \to |\mathbf{k}_i\rangle$. Working in the interaction picture, the acceleration-induced probability amplitude for our massive initial state to transition into $N = n_R + n$ final state particles is given by,

$$\mathcal{A} = \langle \prod_{\ell=1}^{n} \mathbf{k}_\ell | \otimes \langle \prod_{j=1}^{n_R} \Psi_j | \, \hat{S}_I \, |\Psi_i\rangle \otimes |0\rangle \, . \tag{6.3}$$

The magnitude squared of the transition amplitude gives the differential probability per unit momenta of each Minkowski particle, i.e. $\frac{d\mathcal{P}}{D_n^3 k} = |\mathcal{A}|^2$. Note that we are using the more compact notation $\prod_{j=1}^n d^3k_j = D_n^3 k$. Moreover, since we are taking the magnitude squared of a complex integral, we remind the reader that there are two dummy variables in expressions such as $|\int f(x)dx|^2 = \iint dxdx' |f(x)|^2$, where $|f(x)|^2 \equiv f(x)f^*(x')$. Thus the differential probability of our N-particle acceleration-induced transition is given by

$$
\begin{aligned}
\frac{d\mathcal{P}}{D_n^3 k} &= \frac{G_n^2}{\kappa}\left|\int d^4x\sqrt{-g}\,\langle\prod_{\ell=1}^{n}\mathbf{k}_\ell|\otimes\langle\prod_{j=1}^{n_R}\Psi_j|\,\hat{\Psi}_i(x)\prod_{r=1}^{n_R}\hat{\Psi}_r(x)\prod_{m=1}^{n}\hat{\phi}_m(x)\,|\Psi_i\rangle\otimes|0\rangle\right|^2 \\
&= \frac{G_n^2}{\kappa}\left|\int d^4x\sqrt{-g}\,\langle\prod_{j=1}^{n_R}\Psi_j|\,\hat{\Psi}_i(x)\prod_{r=1}^{n_R}\hat{\Psi}_r(x)\,|\Psi_i\rangle\,\langle\prod_{\ell=1}^{n}\mathbf{k}_\ell|\prod_{m=1}^{n}\hat{\phi}_m(x)\,|0\rangle\right|^2 \\
&= \frac{G_n^2}{\kappa}\iint d^4xd^4x'\sqrt{-g}\sqrt{-g'}\,\times \\
&\quad \left|\langle\prod_{j=1}^{n_R}\Psi_j|\,\hat{\Psi}_i(x)\prod_{r=1}^{n_R}\hat{\Psi}_r(x)\,|\Psi_i\rangle\right|^2\left|\langle\prod_{\ell=1}^{n}\mathbf{k}_\ell|\prod_{m=1}^{n}\hat{\phi}_m(x)\,|0\rangle\right|^2. \qquad (6.4)
\end{aligned}
$$

By factoring out the n complete sets of momentum eigenstates we can further simplify the above expression. The resultant two-point functions, i.e. Wightman functions, characterize the probability for each Minkowski particle to propagate along the accelerated trajectory. The product of the n Wightman functions then characterizes the total probability that all of the n Minkowski particles simultaneously propagate together. Moreover, we will endow each Wightman function with the index m to label each of the Minkowski particles and also the relevant observables computed. Hence

$$
\begin{aligned}
\mathcal{P} &= \frac{G_n^2}{\kappa}\iint d^4xd^4x'\sqrt{-g}\sqrt{-g'}\,\times \\
&\quad \left|\langle\prod_{j=1}^{n_R}\Psi_j|\,\hat{\Psi}_i(x)\prod_{r=1}^{n_R}\hat{\Psi}_r(x)\,|\Psi_i\rangle\right|^2\prod_{n=1}^{n}\int d^3k_n\left|\langle\prod_{\ell=1}^{n}\mathbf{k}_\ell|\prod_{m=1}^{n}\hat{\phi}_m(x)\,|0\rangle\right|^2 \\
&= \frac{G_n^2}{\kappa}\iint d^4xd^4x'\sqrt{-g}\sqrt{-g'}\left|\langle\prod_{j=1}^{n_R}\Psi_j|\,\hat{\Psi}_i(x)\prod_{r=1}^{n_R}\hat{\Psi}_r(x)\,|\Psi_i\rangle\right|^2\prod_{m=1}^{n}\langle 0|\,\hat{\phi}_m(x')\hat{\phi}_m(x)\,|0\rangle \\
&= \frac{G_n^2}{\kappa}\iint d^4xd^4x'\sqrt{-g}\sqrt{-g'}\left|\langle\prod_{j=1}^{n_R}\Psi_j|\,\hat{\Psi}_i(x)\prod_{r=1}^{n_R}\hat{\Psi}_r(x)\,|\Psi_i\rangle\right|^2\prod_{m=1}^{n}G_m^{\pm}[x',x]. \qquad (6.5)
\end{aligned}
$$

The inner products over our Rindler fields in the above expression select the appropriate mode function of each particle. For Rindler particles [39], these mode functions can be

written as $f_\Psi[x(\tau)]e^{-i\omega\tau}$. Analyzing the transition process in a frame comoving with the initial accelerated particle allows us to parametrize the system with its proper time. This implies that its energy is just its rest mass, i.e. $\omega_i = m_i$, while the final particles have an arbitrary energy ω_r. The inner products then imply

$$\begin{aligned}\langle\prod_{j=1}^{n_R}\Psi_j|\,\hat{\Psi}_i(x)\prod_{r=1}^{n_R}\hat{\Psi}_r(x)\,|\Psi_i\rangle &= f_{\Psi_i}[x(\tau)]e^{-im_i\tau}\prod_{r=1}^{n_R}f^*_{\Psi_r}[x(\tau)]e^{i\omega_r\tau}\\ &= \left[f_{\Psi_i}[x(\tau)]\prod_{r=1}^{n_R}f^*_{\Psi_r}[x(\tau)]\right]e^{i\Delta E\tau}. \qquad (6.6)\end{aligned}$$

Note that we have defined the Rindler space transition energy $\Delta E = \sum_{r=1}^{n_R}\omega_r - m_i$ to be the total energy difference between the final and initial Rindler states. We then find our acceleration-induced transition probability, Eq. (6.5), to be

$$\begin{aligned}\mathcal{P} &= \frac{G_n^2}{\kappa}\iint d^4x d^4x'\sqrt{-g}\sqrt{-g'}\left|\langle\prod_{j=1}^{n_R}\Psi_j|\,\hat{\Psi}_i(x)\prod_{r=1}^{n_R}\hat{\Psi}_r(x)\,|\Psi_i\rangle\right|^2\prod_{m=1}^{n}G_m^{\pm}[x',x]\\ &= \frac{G_n^2}{\kappa}\iint d^4x d^4x'\sqrt{-g}\sqrt{-g'}\left|\left[f_{\Psi_i}[x(\tau)]\prod_{r=1}^{n_R}f^*_{\Psi_r}[x(\tau)]\right]e^{i\Delta E\tau}\right|^2\prod_{m=1}^{n}G_m^{\pm}[x',x]\\ &= \frac{G_n^2}{\kappa}\iint d^4x d^4x'\sqrt{-g}\sqrt{-g'}\times\\ &\quad\left|f_{\Psi_i}[x(\tau)]\prod_{r=1}^{n_R}f^*_{\Psi_r}[x(\tau)]\right|^2 e^{-i\Delta E(\tau'-\tau)}\prod_{m=1}^{n}G_m^{\pm}[x',x]. \qquad (6.7)\end{aligned}$$

We can now use the overall normalization associated with the overlap of the spatial waveforms κ [22, 29] to simplify the above expression. In experimental settings the initial accelerated particle will be described by a wave packet with mode functions of the form $f_\Psi(x) \sim K_{i\omega/a}(\frac{m}{a}e^{a\xi})g(\mathbf{x}_\perp)$. The spatial distribution of the initial particle, in the directions perpendicular to the acceleration, is assumed to be finite, e.g. Gaussian, and is given by $g(\mathbf{x}_\perp)$. With the mode functions properly normalized [35], κ will be of order unity. Hence

$$\kappa = \iint d^3x d^3x' \sqrt{-g}\sqrt{-g'} \left| f_{\Psi_i}[x(\tau)] \prod_{r=1}^{n_R} f^*_{\Psi_r}[x(\tau)] \right|^2 . \tag{6.8}$$

Having integrated over the spatial coordinates of the right Rindler wedge and noting that we still have to integrate over the proper times, it should be mentioned that the trajectories which characterize the Wightman functions must only depend on the proper time and have no spatial dependence. With this in mind, our transition probability becomes

$$\mathcal{P} \;=\; G_n^2 \iint d\tau d\tau' e^{-i\Delta E(\tau'-\tau)} \prod_{m=1}^{n} G_m^{\pm}[x', x]. \tag{6.9}$$

Upon inspection of the above transition probability we find that we have now effectively reproduced the formalism the would be obtained if we had used an Unruh-DeWitt detector provided we identify the energy gap of the detector with the initial and final state Rindler energies ΔE. To better incorporate the time dependence of our current analysis we will make the following change of variables to the rapidity variables u' and u defined by $u(\tau) = \int^{\tau} a(\tilde{\tau}) d\tilde{\tau}$. Hence

$$\begin{aligned} d\tau d\tau' &= du du' \frac{d\tau}{du}\frac{d\tau'}{du'} \\ &= du du' \frac{1}{a}\frac{1}{a'}. \end{aligned} \tag{6.10}$$

We dropped the proper time dependencies in terms of the more compact notation $a' = a(\tau')$ which we also apply for all other variables. In terms of the rapidity, the transition probability then takes the following form

$$\begin{aligned}\mathcal{P} &= G_n^2 \iint d\tau d\tau' e^{-i\Delta E(\tau'-\tau)} \prod_{m=1}^{n} G_m^{\pm}[x', x] \\ &= G_n^2 \iint du du' \frac{1}{a}\frac{1}{a'} e^{-i\Delta E(\tau'-\tau)} \prod_{m=1}^{n} G_m^{\pm}[x', x]. \end{aligned} \tag{6.11}$$

Finally we decouple the integrals by formulating the new variables in terms of the difference $\xi = u' - u$ and average $\eta = \frac{u'+u}{2}$ rapidities. The inversions of these transformations are given by $u' = \xi/2 + \eta$ and $u = -\xi/2 + \eta$. With this new rapidity parametrization, the transition probability takes the similar form

$$\mathcal{P} = G_n^2 \iint d\eta d\xi \frac{1}{a'}\frac{1}{a} e^{-i\Delta E(\tau'-\tau)} \prod_{m=1}^{n} G_m^{\pm}[x', x]. \tag{6.12}$$

For the sake of clarity we note that under this parametrization the primed and unprimed variables will all have dependencies such as $a' = a(\xi/2 + \eta)$ and $a = a(-\xi/2 + \eta)$. All components of the integrand depend on these variables in this manner. Moreover, we will eventually want to determine the transition rate, i.e. the probability per unit time $\Gamma = \frac{d\mathcal{P}}{d\tau}$. We shall choose the proper time parametrization τ_η that characterizes the rapidity variable η via the definition $d\eta = a(\tau_\eta)d\tau_\eta$ for this purpose. Finally, using the notation $a(\tau_\eta) = a_\eta$ we find the transition rate to be

$$\begin{aligned}\mathcal{P} &= G_n^2 \iint d\eta d\xi \frac{1}{a'a} e^{-i\Delta E(\tau'-\tau)} \prod_{m=1}^{n} G_m^{\pm}[x', x] \\ \Rightarrow \Gamma &= G_n^2 \int d\xi \frac{a_\eta}{a'a} e^{-i\Delta E(\tau'-\tau)} \prod_{m=1}^{n} G_m^{\pm}[x', x]. \end{aligned} \tag{6.13}$$

We mention as well the ability to compute the differential transition probability per unit rapidity $\Gamma_\eta = \frac{d\mathcal{P}}{d\eta}$ that follows along with this derivation as well. To develop the integrand into a more useful form, we Taylor expand the proper time interval about the point $\xi = 0$.

Recalling the form of the coordinate transformations used above, we find

$$\begin{aligned}
\tau' - \tau &\sim \tau_0 + \left.\frac{d\tau'}{du'}\frac{du'}{d\xi}\right|_{\xi=0}\xi - \left(\tau_0 + \left.\frac{d\tau}{du}\frac{du}{d\xi}\right|_{\xi=0}\xi\right) \\
&= \frac{1}{a_\eta}\frac{1}{2}\xi + \frac{1}{a_\eta}\frac{1}{2}\xi \\
&= \frac{\xi}{a_\eta}. \qquad (6.14)
\end{aligned}$$

Similarly, we expand the proper accelerations about the same point but we also disregard terms of order j_η/a_η^2 and higher. Hence

$$\begin{aligned}
a'(\xi/2+\eta) &\sim a_\eta + \left.\frac{da'}{d\tau'}\frac{d\tau'}{du'}\frac{du'}{d\xi}\right|_{\xi=0}\xi \\
&= a_\eta + \left. J'\frac{1}{a'}\frac{1}{2}\right|_{\xi=0}\xi \\
&= a_\eta + \frac{J_\eta}{a_\eta}\frac{1}{2}\xi \\
&= a_\eta[1 + \frac{J_\eta}{a_\eta^2}\frac{1}{2}\xi] \\
&\sim a_\eta. \qquad (6.15)
\end{aligned}$$

Similarly, we obtain $a(-\xi/2+\eta) \sim a_\eta$ as well. We must also recall that all other components of the integrand must be expanded to the appropriate order. As such, we employ the notation $G_m^{\pm}[x', x]_\eta$ to imply the necessary Taylor expansion of the Wightman function. Moreover, now that acceleration is a function of one variable only, we will drop the η subscript and define $a_\eta = a(\tau_\eta) \equiv a$. Thus our generalized response function takes the following form

$$\Gamma \;=\; G_n^2 \frac{1}{a} \int d\xi e^{-i\Delta E \xi/a} \prod_{m=1}^{n} G_m^{\pm}[x', x]_\eta. \tag{6.16}$$

This expression determines the transition rate for a Rindler, i.e. accelerated, particle to decay into n_R Rindler, i.e. accelerated, particles accompanied by the simultaneous emission of n Minkowski, i.e. inertial, particles. This is the process that is expressed schematically in Eq. (6.1). A conceptual depiction of the above acceleration-induced process is also illustrated in Fig. 6.1 for clarity. To finalize this section we comment on the relationship between the method of field operators, used in this manuscript, with the alternative method of detectors [29]. The method of fields enables a more general analysis via the inclusion of an arbitrary number of Rindler particles of varying energy in the final state. The energy difference, as measured in the proper frame of the initial accelerated particle, is given by $\Delta E = \sum_{r=1}^{n_R} \omega_r - m_i$; see e.g. Eq. (6.6) and the subsequent discussion. That is, the difference between the sum of all final state Rindler particle energies and the initial accelerated particle's mass. To map the analysis to the method of detectors, all one needs to do is identify this energy difference with the energy gap of the detector, i.e. a two-level system. In short, the initial and final state energies of the Rindler particles, as measured in the proper frame of the initial accelerated particle, define the two energy levels of the detector. For a more in-depth discussion of this correspondence we refer the reader to Ref. [29]. In the next chapter we develop the time-dependent formalism that will be used to compute the Wightman functions and their subsequent Taylor expansion used in Eq. (6.16) above.

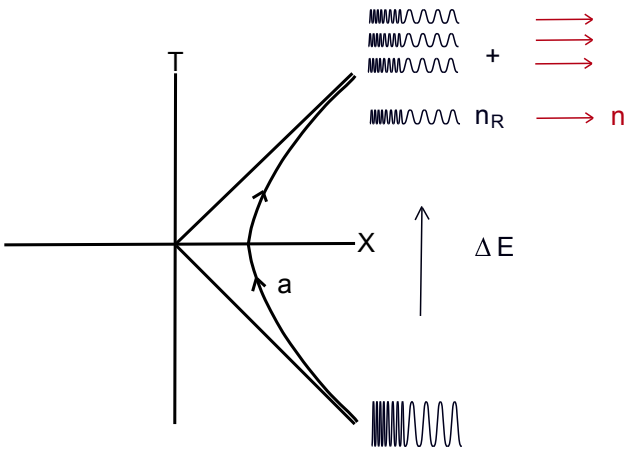

Figure 6.1: A pictorial representation of the acceleration-induced transition from Eq. (6.16).

Chapter 7

Time-Dependent Spacetime Trajectories

Prior to evaluating the Wightman functions we will need the time-dependent spacetime trajectories the Minkowski fields propagate along. For the time-dependent proper acceleration $a(\tau)$, we recall the rapidity is defined by $u(\alpha) = \int^{\alpha} a(\tau) d\tau$. Using the Rindler chart to characterize the resultant accelerated motion, see e.g. [34], we have

$$\begin{aligned} x(\tau) &= \int^{\tau} d\alpha \sinh\left[u(\alpha)\right] + x_0 \\ t(\tau) &= \int^{\tau} d\alpha \cosh\left[u(\alpha)\right] + t_0. \end{aligned} \tag{7.1}$$

In order to compute these, and related, integrals we shall make use of a simple variant of the method of steepest descent. Here, we will maintain the appropriate expansion and again disregard terms of order j/a^2. As such, the method utilized can accommodate general acceleration profiles quite easily but depending on the system additional care must be taken if the acceleration goes to zero within the interval. Thus we consider the following change of variables and integration by parts [40],

$$
\begin{aligned}
I &= \int_{\tau}^{\tau'} d\alpha e^{\pm u(\alpha)} \\
&= \int_{\tau}^{\tau'} \frac{1}{\pm a(\alpha)} \frac{d}{d\alpha}(e^{\pm u(\alpha)}) d\alpha \\
&= \left[\frac{1}{\pm a(\alpha)} e^{\pm u(\alpha)}\right]_{\tau}^{\tau'} \pm \int_{\tau}^{\tau'} \frac{j(\alpha)}{a^2(\alpha)} e^{\pm u(\alpha)} d\alpha \\
&\approx \left[\frac{1}{\pm a(\alpha)} e^{\pm u(\alpha)}\right]_{\tau}^{\tau'}. \qquad (7.2)
\end{aligned}
$$

Note that we used the fact that $u'(\tau) = a(\tau)$ and $u''(\tau) = j(\tau)$. Moreover we see that we obtained a solution to the integral to zeroth order in j/a^2 as required to be consistent with the development of the generalized response function in the previous chapter. We then have the general form of the integral to be applied to our spacetime intervals. Hence

$$
\int_{\tau}^{\tau'} d\alpha e^{\pm u(\alpha)} = \frac{1}{\pm a(\tau')} e^{\pm u(\tau')} - \frac{1}{\pm a(\tau)} e^{\pm u(\tau)}. \qquad (7.3)
$$

We now apply the above formula to compute all necessary spacetime quantities associated with our generalized hyperbolic trajectory. Considering first the spacelike interval $\Delta x = x' - x$, we find

$$
\begin{aligned}
\Delta x &= \int^{\tau'} d\alpha \sinh\left[u(\alpha)\right] + x_0 - \left(\int^{\tau} d\alpha \sinh\left[u(\alpha)\right] + x_0\right) \\
&= \int_{\tau}^{\tau'} d\alpha \sinh\left[u(\alpha)\right] \\
&= \frac{1}{2} \int_{\tau}^{\tau'} d\alpha [e^{u(\alpha)} - e^{-u(\alpha)}] \\
&= \frac{1}{a(\tau')} \cosh\left[u(\tau')\right] - \frac{1}{a(\tau)} \cosh\left[u(\tau)\right]. \qquad (7.4)
\end{aligned}
$$

Utilizing the same coordinate transformation, i.e. $u, u' \to \xi, \eta$ and Taylor expansion, i.e.

$a'(\xi,\eta), a(\xi,\eta) \to a_\eta = a$ as in Chp. 6, the above spacelike interval becomes

$$\begin{aligned}
\Delta x &= \frac{1}{a(\tau')}\cosh\left[u(\tau')\right] - \frac{1}{a(\tau)}\cosh\left[u(\tau)\right] \\
&= \frac{1}{a'(\eta,\xi)}\cosh\left[\xi/2+\eta\right] - \frac{1}{a(\eta,\xi)}\cosh\left[-\xi/2+\eta\right] \\
&= \frac{1}{a}(\cosh\left[\xi/2+\eta\right] - \cosh\left[-\xi/2+\eta\right]) \\
&= \frac{2}{a}\sinh\left[\xi/2\right]\sinh\left[\eta\right]. \qquad (7.5)
\end{aligned}$$

Note the use of the hyperbolic double angle formula to obtain the last line. Similarly, for the timelike interval $\Delta t = t' - t$ we find

$$\begin{aligned}
\Delta t &= \int^{\tau'} d\alpha \cosh\left[u(\alpha)\right] + t_0 - \left(\int^{\tau} d\alpha \cosh\left[u(\alpha)\right] + t_0\right) \\
&= \int_{\tau}^{\tau'} d\alpha \cosh\left[u(\alpha)\right] \\
&= \frac{1}{2}\int_{\tau}^{\tau'} d\alpha [e^{u(\alpha)} + e^{-u(\alpha)}] \\
&= \frac{1}{a(\tau')}\sinh\left[u(\tau')\right] - \frac{1}{a(\tau)}\sinh\left[u(\tau)\right]. \qquad (7.6)
\end{aligned}$$

The subsequent Taylor expansion to zeroth order in j/a^2 then yields

$$\begin{aligned}
\Delta t &= \frac{1}{a(\tau')}\sinh\left[u(\tau')\right] - \frac{1}{a(\tau)}\sinh\left[u(\tau)\right] \\
&= \frac{1}{a'(\eta,\xi)}\sinh\left[\xi/2+\eta\right] - \frac{1}{a(\eta,\xi)}\sinh\left[-\xi/2+\eta\right] \\
&= \frac{1}{a}(\sinh\left[\xi/2+\eta\right] - \sinh\left[-\xi/2+\eta\right]) \\
&= \frac{2}{a}\sinh\left[\xi/2\right]\cosh\left[\eta\right]. \qquad (7.7)
\end{aligned}$$

It should be noted that the addition of the complex regulator to the timelike interval can be added in without changing the computation. Next we compute the complex regulated square of the spacetime interval, $\Delta x^2 - (\Delta t - i\epsilon)^2$, more commonly found in Wightman functions. We can evaluate this quantity by substitution of the previously computed spacelike and timelike intervals; however, in the interest of further developing the time-dependent formalism, we shall first carry out a few more manipulations to obtain a more general form. Thus

$$\begin{aligned}
\Delta x^2 - (\Delta t - i\epsilon)^2 &= [x(\tau') - x(\tau)]^2 - [t(\tau') - t(\tau) - i\epsilon]^2 \\
&= \left[\int^{\tau'} d\alpha \sinh[u(\alpha)] - \int^{\tau} d\alpha \sinh[u(\alpha)]\right]^2 - \\
&\quad \left[\int^{\tau'} d\alpha \cosh[u(\alpha)] - \int^{\tau} d\alpha \cosh[u(\alpha)] - i\epsilon\right]^2 \\
&= \left[\int_{\tau}^{\tau'} d\alpha \sinh[u(\alpha)]\right]^2 - \left[\int_{\tau}^{\tau'} d\alpha \cosh[u(\alpha)] - i\epsilon\right]^2 \\
&= \iint_{\tau}^{\tau'} d\alpha d\beta \left(\sinh[u(\alpha)]\sinh[u(\beta)] - \cosh[u(\alpha)]\cosh[u(\beta)]\right) + \\
&\quad 2i\epsilon \int_{\tau}^{\tau'} d\alpha \cosh[u(\alpha)] \\
&= -\iint_{\tau}^{\tau'} d\alpha d\beta \cosh[u(\alpha) - u(\beta)] + 2i\epsilon\Delta t. \qquad (7.8)
\end{aligned}$$

Note in the last line that we used the hyperbolic double angle formula and rewrote the term on the complex regulator as Δt. Focusing on the integral, we break up the hyperbolic argument into exponentials to obtain a more convenient form. Hence

$$\begin{aligned}
\iint_{\tau}^{\tau'} d\alpha d\beta \cosh\left(u(\alpha)-u(\beta)\right) &= \frac{1}{2}\iint_{\tau}^{\tau'} d\alpha d\beta e^{u(\alpha)-u(\beta)} + e^{-(u(\alpha)-u(\beta))} \\
&= \frac{1}{2}\int_{\tau}^{\tau'} d\alpha e^{u(\alpha)} \int_{\tau}^{\tau'} d\beta e^{-u(\beta)} + \frac{1}{2}\int_{\tau}^{\tau'} d\alpha e^{-u(\alpha)} \int_{\tau}^{\tau'} d\beta e^{u(\beta)} \\
&= \int_{\tau}^{\tau'} d\alpha e^{u(\alpha)} \int_{\tau}^{\tau'} d\beta e^{-u(\beta)}. \qquad (7.9)
\end{aligned}$$

Note in the last line that we interchanged indices $\alpha \leftrightarrow \beta$ to combine the exponentials into one expression. We should also note a similar expression was obtained in [27]. Thus the square of the spacetime interval, along with its complex regulator, can be expressed in the following more compact form:

$$\Delta x^2 - (\Delta t - i\epsilon)^2 = \int_{\tau}^{\tau'} d\alpha e^{u(\alpha)} \int_{\tau}^{\tau'} d\beta e^{-u(\beta)} + 2i\epsilon\Delta t. \qquad (7.10)$$

In turning our task to evaluating the above integrals, we find

$$\begin{aligned}
\int_{\tau}^{\tau'} d\alpha e^{u(\alpha)} \int_{\tau}^{\tau'} d\beta e^{-u(\beta)} &= -\left[\frac{1}{a(\tau')}e^{u(\tau')} - \frac{1}{a(\tau)}e^{u(\tau)}\right]\left[-\frac{1}{a(\tau')}e^{-u(\tau')} + \frac{1}{a(\tau)}e^{-u(\tau)}\right] \\
&= \frac{-2}{a(\tau')a(\tau)}\cosh\left[u(\tau')-u(\tau)\right] + \frac{1}{a^2(\tau')} + \frac{1}{a^2(\tau)} \\
&= \frac{-4}{a(\tau')a(\tau)}\sinh^2\left[\frac{1}{2}(u(\tau')-u(\tau))\right] - \frac{2}{a(\tau')a(\tau)} + \frac{1}{a^2(\tau')} + \frac{1}{a^2(\tau)} \\
&= \frac{1}{a^2(\tau')a^2(\tau)} \times \\
&\quad \left[(a(\tau')-a(\tau))^2 - 4a(\tau')a(\tau)\sinh^2\left[\frac{1}{2}(u(\tau')-u(\tau))\right]\right]. \qquad (7.11)
\end{aligned}$$

Finally, performing the necessary change of variables and Taylor expanding the acceleration we obtain the final form of the $i\epsilon$ regularized square of the spacetime interval. Hence

$$
\begin{aligned}
\Delta x^2 - (\Delta t - i\epsilon)^2 &= \frac{1}{a^2(\tau')a^2(\tau)} \times \\
&\quad \left[(a(\tau') - a(\tau))^2 - 4a(\tau')a(\tau)\sinh^2\left[\frac{1}{2}(u(\tau') - u(\tau))\right]\right] + 2i\epsilon\Delta t \\
&= \frac{1}{a'^2(\eta,\xi)a^2(\eta,\xi)} \times \\
&\quad \left[(a'(\eta,\xi) - a(\eta,\xi))^2 - 4a'(\eta,\xi)a(\eta,\xi)\sinh^2\left[\xi/2\right]\right] + 2i\epsilon\Delta t \\
&= -\frac{4}{a^2}\sinh^2\left[\xi/2\right] + i\epsilon\frac{4}{a}\sinh\left[\xi/2\right]\cosh\left[\eta\right] \\
&= -\frac{4}{a^2}\sinh^2\left[\xi/2\right] + i\epsilon\frac{8a}{a^2}\sinh\left[\xi/2\right]\cosh\left[\xi/2\right] \\
&= -\frac{4}{a^2}\sinh^2\left[\xi/2 - ia\epsilon\right] \\
&= -\frac{4}{a^2}\sinh^2\left[\xi/2 - \mathrm{sgn}\,(a)i\epsilon\right]. \qquad (7.12)
\end{aligned}
$$

Note that, in the third to last line, we pulled the positive definite factor $\frac{2\cosh[\xi/2]}{\cosh[\eta]}$ out of the ϵ and in the last line we absorbed the magnitude of the acceleration into the regulator. We keep the overall sign of the acceleration so as to not change the direction of the shift along the imaginary axis by changing the sign of ϵ. To finalize the development of the components necessary to compute each of our Wightman functions, we also require the use of a Lorentz gamma to boost forward and backward between the proper and inertial lab frames. The Lorentz gamma can be computed by taking the derivative of the inertial time. We also parametrize our proper time here using the variable τ_η such that $u(\tau_\eta) = \eta$ as in the previous chapter. Recalling $dt = \gamma d\tau$ we have

$$
\begin{aligned}
\frac{d}{d\tau_\eta}t &= \frac{d}{d\tau_\eta}\int^{\tau_\eta} d\alpha\cosh\left[u(\alpha)\right] + t_0 \\
\Rightarrow \gamma &= \cosh\left[\eta\right]. \qquad (7.13)
\end{aligned}
$$

In the next chapter we will utilize the above dictionary of formulas to evaluate the

Wightman functions and its variants. The Wightman functions will then be used to compute the acceleration-induced transition rate, power emitted, and spectra of emitted particles.

Chapter 8

The Wightman Function and its Variants

In this chapter we compute the variants of the Wightman functions used for the computation of various observables. We will be working under the assumption that all Minkowski fields are massless. To evaluate the vacuum to vacuum two-point function [33], we use the canonically normalized field operator $\hat{\phi} = \int \frac{d^3k}{(2\pi)^{3/2}\sqrt{2\omega}}[\hat{a}_{\mathbf{k}}e^{i(\mathbf{k}\cdot\mathbf{x}-\omega t)} + \hat{a}^{\dagger}_{\mathbf{k}}e^{-i(\mathbf{k}\cdot\mathbf{x}-\omega t)}]$. Thus,

$$\begin{aligned} G^{\pm}_{m}[x',x] &= \langle 0|\, \hat{\phi}_m(x')\hat{\phi}_m(x)\, |0\rangle \\ &= \frac{1}{2(2\pi)^3}\iint \frac{d^3k'd^3k}{\sqrt{\omega'\omega}}\, \langle 0|\, \hat{a}_{\mathbf{k}'}\hat{a}^{\dagger}_{\mathbf{k}} e^{i(\mathbf{k}'\cdot\mathbf{x}'-\mathbf{k}\cdot\mathbf{x}-\omega' t'+\omega t)}\, |0\rangle \\ &= \frac{1}{2(2\pi)^3}\iint \frac{d^3k'd^3k}{\sqrt{\omega'\omega}} e^{i(\mathbf{k}'\cdot\mathbf{x}'-\mathbf{k}\cdot\mathbf{x}-\omega' t'+\omega t)}\delta(\mathbf{k}'-\mathbf{k}) \\ &= \frac{1}{2(2\pi)^3}\int \frac{d^3k}{\omega} e^{i(\mathbf{k}\cdot\Delta\mathbf{x}-\omega\Delta t)} \\ &= \frac{1}{2(2\pi)^3}\int \frac{d^3k}{\omega} e^{-ik^{\mu}\Delta x_{\mu}}. \end{aligned} \tag{8.1}$$

Since we are dealing with the emission of Minkowski particles by an accelerated field, it is advantageous to boost the momenta into the frame that is instantaneously at rest

with the accelerated field. The integration measure is Lorentz invariant, i.e. $\frac{d^3k}{\omega} = \frac{d^3\tilde{k}}{\tilde{\omega}}$. When boosting the momenta forward into the accelerated fields' instantaneous rest frame via $k^\mu \to \Lambda^\mu_\nu k^\nu = \tilde{k}^\mu$, the Lorentz scalar nature of the exponent necessitates the boosting of the spacetime interval back via $\Delta x^\mu \to (\Lambda^{-1})^\mu_\nu \Delta x^\nu = \Delta\tilde{x}^\mu$. It should be noted that each $\Delta\tilde{x}^\mu$ is a proper quantity that has just been boosted to the same velocity but in the opposite direction and therefore all of the relativistic effects, e.g. length contraction, remain the same. Also, here and throughout, we will denote all proper quantities with a tilde. Therefore, our Wightman function, evaluated in the proper frame, is given by

$$G^{\pm}_m[x', x] \equiv \frac{1}{2(2\pi)^3} \int \frac{d^3\tilde{k}}{\tilde{\omega}} e^{i(\tilde{\mathbf{k}}\cdot\Delta\tilde{\mathbf{x}} - \tilde{\omega}\Delta\tilde{t})}. \tag{8.2}$$

Integrals of this form are best evaluated in spherical coordinates. Without loss of generality we rotate the coordinate system until the momentum lies along the z-axis and then we enforce the condition that our Minkowski fields are massless, i.e. $\tilde{\omega} = \tilde{k}$. As such, the integral reduces to

$$\begin{aligned} G^{\pm}_m[x', x] &= \frac{1}{2(2\pi)^3} \int \frac{d^3\tilde{k}}{\tilde{\omega}} e^{i(\tilde{\mathbf{k}}\cdot\Delta\tilde{\mathbf{x}} - \tilde{\omega}\Delta\tilde{t})} \\ &= \frac{1}{2(2\pi)^3} \int_0^\infty \int_0^\pi \int_0^{2\pi} d\tilde{\omega} d\tilde{\theta} d\tilde{\phi}\ \tilde{\omega} \sin\tilde{\theta} e^{i(\tilde{\omega}\Delta\tilde{x}\cos\tilde{\theta} - \tilde{\omega}\Delta\tilde{t})} \\ &= \frac{1}{2(2\pi)^2} \int_0^\infty \int_{-1}^1 d\tilde{\omega} d(\cos\tilde{\theta})\ \tilde{\omega} e^{i(\tilde{\omega}\Delta\tilde{x}\cos\tilde{\theta} - \tilde{\omega}\Delta\tilde{t})} \\ &= \frac{1}{2(2\pi)^2} \frac{1}{i\Delta\tilde{x}} \int_0^\infty d\tilde{\omega} \left[e^{i\tilde{\omega}(\Delta\tilde{x} - \Delta\tilde{t})} - e^{-i\tilde{\omega}(\Delta\tilde{x} + \Delta\tilde{t})} \right]. \end{aligned} \tag{8.3}$$

The above Wightman function will be used to compute the acceleration-induced transition rate. To properly evaluate the integral we require an infinitesimal shift along the imaginary time axis to regulate the oscillations at infinity. This is accomplished by letting $\Delta\tilde{t} \to \Delta\tilde{t} - i\epsilon$ where $\epsilon > 0$. Thus,

$$
\begin{aligned}
G_m^{\pm}[x',x] &= \frac{1}{2(2\pi)^2}\frac{1}{i\Delta\tilde{x}}\int_0^{\infty} d\tilde{\omega}\left[e^{i\tilde{\omega}(\Delta\tilde{x}-(\Delta\tilde{t}-i\epsilon))}-e^{-i\tilde{\omega}(\Delta\tilde{x}+(\Delta\tilde{t}-i\epsilon))}\right] \\
&= -\frac{1}{2(2\pi)^2}\frac{1}{i\Delta\tilde{x}}\left[\frac{1}{i(\Delta\tilde{x}-(\Delta\tilde{t}-i\epsilon))}+\frac{1}{i(\Delta\tilde{x}+(\Delta\tilde{t}-i\epsilon))}\right] \\
&= \frac{1}{(2\pi)^2}\frac{1}{\Delta\tilde{x}^2-(\Delta\tilde{t}-i\epsilon)^2} \\
&= -\frac{1}{(2\pi)^2}\frac{1}{\Delta\tilde{x}^{\mu}\Delta\tilde{x}_{\mu}} \\
&= -\frac{1}{(2\pi)^2}\frac{1}{\Delta x^{\mu}\Delta x_{\mu}}. \qquad (8.4)
\end{aligned}
$$

Note in the last line we used the Lorentz invariance of the scalar product to boost the spacetime interval forward into the lab frame. This will facilitate later computations and also highlights the appropriate Lorentz invariance of the Wightman functions. It serves to also remember the presence of the complex regulator within the time component of the interval. Using the appropriately Taylor expanded spacetime interval derived in Eq. (7.12) of the previous chapter, we find the Taylor expanded Wightman function $G_m^{\pm}[x',x]_{\eta}$ to be

$$
\begin{aligned}
G_m^{\pm}[x',x]_{\eta} &= -\frac{1}{(2\pi)^2}\frac{1}{\Delta x^{\mu}\Delta x_{\mu}} \\
&= -\frac{1}{(2\pi)^2}\frac{1}{\frac{4}{a^2}\sinh^2\left[\xi/2-\mathrm{sgn}\,(a)i\epsilon\right]} \\
&= -\frac{a^2}{(4\pi)^2}\frac{1}{\sinh^2\left[\xi/2-\mathrm{sgn}\,(a)i\epsilon\right]}. \qquad (8.5)
\end{aligned}
$$

The Wightman function characterizes the probability for a particle to propagate along a given trajectory and is summed over all energies, i.e. integrated. Thus, by multiplying each probability by the energy (see e.g. [24]), and then integrating, we can effectively compute the average energy carried by the particle during the transition process, i.e. the power radiated. Denoting this energy weighted Wightman function as $\mathcal{G}_m^{\pm}[x',x]_{\eta}$, we then carry out its computation in a similar manner. Beginning with Eq. (8.3), we find

$$
\begin{aligned}
\mathcal{G}_m^{\pm}[x',x] &= \frac{1}{2(2\pi)^2}\frac{1}{i\Delta\tilde{x}}\int_0^\infty d\tilde{\omega}\tilde{\omega}\left[e^{i\tilde{\omega}(\Delta\tilde{x}-(\Delta\tilde{t}-i\epsilon))}-e^{-i\tilde{\omega}(\Delta\tilde{x}+(\Delta\tilde{t}-i\epsilon))}\right] \\
&= \frac{1}{2(2\pi)^2}\frac{1}{i\Delta\tilde{x}}\left[\frac{1}{[i(\Delta\tilde{x}-(\Delta\tilde{t}-i\epsilon))]^2}-\frac{1}{[i(\Delta\tilde{x}+(\Delta\tilde{t}-i\epsilon))]^2}\right] \\
&= -\frac{1}{2i\pi^2}\frac{\Delta\tilde{t}-i\epsilon}{[\Delta\tilde{x}^2-(\Delta\tilde{t}-i\epsilon)^2]^2} \\
&= -\frac{1}{2i\pi^2}\frac{\Delta\tilde{t}-i\epsilon}{[\Delta\tilde{x}^\mu\Delta\tilde{x}_\mu]^2} \\
&= -\frac{1}{2i\pi^2}\frac{\Delta t/\gamma-i\epsilon}{[\Delta x^\mu\Delta x_\mu]^2}.
\end{aligned}
\tag{8.6}
$$

Note that the presence of the proper frame timelike interval in the above quantity necessitated the use of the Lorentz gamma to boost it back to the lab frame via $\Delta\tilde{t}=\Delta\tau=\Delta t/\gamma$. Evaluation of this energy weighted Wightman function along the Taylor expanded hyperbolic trajectory yields

$$
\begin{aligned}
\mathcal{G}_m^{\pm}[x',x]_\eta &= -\frac{1}{2i\pi^2}\frac{\Delta\tilde{t}-i\epsilon}{[\Delta x^\mu\Delta x_\mu]^2} \\
&= -\frac{1}{2i\pi^2}\frac{\frac{2}{a}\sinh[\xi/2]-i\epsilon}{[-\frac{4}{a^2}\sinh^2[\xi/2-\mathrm{sgn}(a)i\epsilon]]^2} \\
&= -\frac{a^4}{i(4\pi)^2}\frac{\sinh[\xi/2]-i\frac{a}{2}\epsilon}{\sinh^4[\xi/2-\mathrm{sgn}(a)i\epsilon]} \\
&= -\frac{a^3}{i(4\pi)^2}\frac{\sinh[\xi/2]-i\,\mathrm{sgn}(a)\epsilon\cosh[\xi/2]}{\sinh^4[\xi/2-\mathrm{sgn}(a)i\epsilon]} \\
&= -\frac{a^3}{i(4\pi)^2}\frac{1}{\sinh^3[\xi/2-\mathrm{sgn}(a)i\epsilon]}.
\end{aligned}
\tag{8.7}
$$

Again we pulled a positive definite factor $2\cosh[\xi/2]$ out of the ϵ. We also absorbed the magnitude of the acceleration into the regulator and then recombined the numerator into the hyperbolic sine since it was the Taylor expansion about small ϵ. Finally, examining how the propagation, and thus emission probability, changes as we vary the energy enables us to compute the spectra. Taking the derivative of the Wightman function, Eq. (8.3), yields

$$\frac{d}{d\tilde{\omega}}G_m^{\pm}[x',x] \;=\; \frac{1}{2(2\pi)^2}\frac{1}{i\Delta\tilde{x}}\left[e^{i\tilde{\omega}(\Delta\tilde{x}-\Delta\tilde{t})}-e^{-i\tilde{\omega}(\Delta\tilde{x}+\Delta\tilde{t})}\right]. \tag{8.8}$$

Substitution of the relevant trajectories, along with the appropriate expansion, yields

$$\begin{aligned}
\frac{d}{d\tilde{\omega}}G_m^{\pm}[x',x]_\eta &= \frac{1}{2(2\pi)^2}\frac{1}{i\Delta\tilde{x}}\left[e^{i\tilde{\omega}(\Delta\tilde{x}-\Delta\tilde{t})}-e^{-i\tilde{\omega}(\Delta\tilde{x}+\Delta\tilde{t})}\right] \\
&= \frac{1}{(2\pi)^2}\frac{e^{-i\tilde{\omega}\Delta\tilde{t}}}{\Delta\tilde{x}}\sin\left(\tilde{\omega}\Delta\tilde{x}\right) \\
&= \frac{1}{(2\pi)^2}\frac{e^{-i\tilde{\omega}\Delta t/\gamma}}{\gamma\Delta x}\sin\left(\tilde{\omega}\gamma\Delta x\right) \\
&= \frac{a}{(2\pi)^2}\frac{e^{-i\tilde{\omega}\frac{2}{a}\sinh(\xi/2)}}{\sinh(\xi/2)\sinh(2\eta)}\sin\left(\frac{\tilde{\omega}}{a}\sinh(\xi/2)\sinh(2\eta)\right) \\
&\approx \frac{\tilde{\omega}}{(2\pi)^2}e^{-i\tilde{\omega}\xi/a}.
\end{aligned} \tag{8.9}$$

In the last line we expanded the arguments about small ξ. Note that we have kept, to first order, a dependence in the phase so we still encode the dynamics. Now that we have our catalog of the Wightman function and its variants, the next chapter will be devoted to the computation of the relevant observables of the theory.

Chapter 9

The Observables of Accelerated Quantum Dynamics

9.1 Transition Rate

The generalized response function developed previously will now be used to compute the acceleration-induced transition rate. This will enable us to analyze the decay of unstable particles as well as the excitation of stable particles into states of higher energy. We begin by recalling the functional form of the response function, Eq. (6.16),

$$\Gamma \;=\; G_n^2 \frac{1}{a} \int d\xi e^{-i\Delta E \xi/a} \prod_{m=1}^{n} G_m^{\pm}[x', x]_\eta. \tag{9.1}$$

To compute the transition rate we use all n of the Wightman functions in the above product over our final state particles. Recalling the form of the Wightman functions, Eq. (8.5), we find that the transition rate of n-particle multiplicity simplifies to

$$\begin{aligned}\Gamma &= G_n^2 \frac{1}{a}\int d\xi e^{-i\Delta E\xi/a}\prod_{m=1}^{n} G_m^{\pm}[x',x]_\eta \\ &= G_n^2 \frac{1}{a}\int d\xi e^{-i\Delta E\xi/a}\left[-\frac{a^2}{(4\pi)^2}\frac{1}{\sinh^2\left[\xi/2-\mathrm{sgn}\,(a)i\epsilon\right]}\right]^n \\ &= G_n^2\left(\frac{ia}{4\pi}\right)^{2n}\frac{\mathrm{sgn}\,(a)}{|a|}\int d\xi\frac{e^{-i\Delta E\xi/a}}{\sinh^{2n}\left[\xi/2-\mathrm{sgn}\,(a)i\epsilon\right]}. \end{aligned} \tag{9.2}$$

At this point we must focus the integral. Specifically we must note how the integration depends on the sign of the acceleration. By letting $\xi \to \mathrm{sgn}\,(a)\xi$ we see the integration is independent of the sign of the acceleration. As such we set $\mathrm{sgn}\,(a) = 1$, leaving the transition rate dependent only on the magnitude of the acceleration $|a|$. Hence,

$$\Gamma = G_n^2\left(\frac{ia}{4\pi}\right)^{2n}\frac{1}{|a|}\int d\xi\frac{e^{-i\Delta E\xi/|a|}}{\sinh^{2n}\left[\xi/2-i\epsilon\right]}. \tag{9.3}$$

We now see that the removal of the $i\epsilon$ yields a singularity structure with poles of order $2n$ at $\xi = 2\pi i\sigma$ with the integer $\sigma \geq 0$. Now that we know the pole structure, we rid ourselves of the complex regulator. Rewriting the denominator of the integrand in exponential form will yield a more useful form. Hence,

$$\begin{aligned}\Gamma &= G_n^2\left(\frac{ia}{4\pi}\right)^{2n}\frac{1}{|a|}\int d\xi\frac{e^{-i\Delta E\xi/|a|}}{\sinh^{2n}\left[\xi/2-i\epsilon\right]} \\ &= G_n^2\left(\frac{ia}{2\pi}\right)^{2n}\frac{1}{|a|}\int d\xi\frac{e^{-i\Delta E\xi/|a|}}{\left[e^{\xi/2}-e^{-\xi/2}\right]^{2n}}. \end{aligned} \tag{9.4}$$

Employing the more convenient change of variables $w = e^{\xi}$ we find

$$\begin{aligned}\Gamma &= G_n^2 \left(\frac{ia}{2\pi}\right)^{2n} \frac{1}{|a|} \int d\xi \frac{e^{-i\Delta E\xi/|a|}}{[e^{\xi/2} - e^{-\xi/2}]^{2n}} \\ &= G_n^2 \left(\frac{ia}{2\pi}\right)^{2n} \frac{1}{|a|} \int dw \frac{w^{-i\Delta E\xi/|a|+n-1}}{[w-1]^{2n}}. \end{aligned} \tag{9.5}$$

The above expression can be integrated using the residue theorem. The integral is of the form $\frac{w^{-i\beta+\gamma}}{[w-1]^{\delta}}$ with the appropriate identification for β, γ, and δ. Also note the added conditions that γ is an integer and δ is an even integer. Evaluation of this generalized integral yields

$$\begin{aligned}\int dw \frac{w^{-i\beta+\gamma}}{[w-1]^{\delta}} &= \frac{2\pi i}{(\delta-1)!} \sum_{\sigma=0}^{\infty} \frac{d^{\delta-1}}{dw^{\delta-1}} \left[[w-1]^{\delta} \frac{w^{-i\beta+\gamma}}{[w-1]^{\delta}} \right]_{w=e^{i2\pi\sigma}} \\ &= \frac{2\pi i}{(\delta-1)!} \frac{\Gamma(1-i\beta+\gamma)}{\Gamma(-i\beta+\gamma-\delta+2)} \sum_{\sigma=0}^{\infty} \left[w^{-i\beta+\gamma-\delta+1} \right]_{w=e^{i2\pi\sigma}} \\ &= \frac{2\pi i}{(\delta-1)!} \frac{\Gamma(1-i\beta+\gamma)}{\Gamma(-i\beta+\gamma-\delta+2)} \sum_{\sigma=0}^{\infty} e^{2\pi\sigma\beta+i2\pi\sigma(\gamma-\delta)} \\ &= \frac{2\pi i}{(\delta-1)!} \frac{\Gamma(1-i\beta+\gamma)}{\Gamma(-i\beta+\gamma-\delta+2)} \frac{1}{1-e^{2\pi\beta}} \\ &= \frac{2\pi i}{(\delta-1)!} \frac{\Gamma(i\beta-\gamma+\delta-1)}{\Gamma(i\beta-\gamma)} \frac{1}{e^{2\pi\beta}-1}. \end{aligned} \tag{9.6}$$

Note that we used the identity $\Gamma(z)\Gamma(1-z) = \pi/\sin(\pi z)$, along with the properties of γ and δ, in the last line. The sum in the above equation converges for $e^{2\pi\beta} < 1$ which is true for negative β. This corresponds to $\Delta E < 0$, i.e. decays. In order to evaluate the sum we may assume β to be negative to yield the closed form expression of the convergent sum. We can then relax the condition for $\Delta E > 0$ and we note that, in the zero acceleration limit, the transition rate appropriately diverges. This merely illustrates the fact that inertially stable particles have an infinite lifetime. Utilizing the above derived formula, we evaluate the integral in Eq. (9.5) to be

$$\int dw \frac{w^{-i\Delta E\xi/|a|+n-1}}{[w-1]^{2n}} = \frac{2\pi i}{(2n-1)!}\frac{\Gamma(i\Delta E/|a|+n)}{\Gamma(i\Delta E/|a|+1-n)}\frac{1}{e^{2\pi\Delta E/|a|}-1}. \tag{9.7}$$

The transition rate is then given by

$$\Gamma(\Delta E,\eta) = G_n^2\left(\frac{ia}{2\pi}\right)^{2n}\frac{1}{a}\frac{2\pi i}{(2n-1)!}\frac{\Gamma(i\Delta E/|a|+n)}{\Gamma(i\Delta E/|a|+1-n)}\frac{1}{e^{2\pi\Delta E/|a|}-1}. \tag{9.8}$$

We will take one final step in simplifying the above gamma functions using the Pochhammer symbol for rising factorials $(x)^a = \frac{\Gamma(x+a)}{\Gamma(x)} = \prod_{j=0}^{a-1}(x+j)$. This serves to better present the resultant polynomials of multiplicity. Applying the Pochhammer identity to the above expression, along with the identifications $x = i\Delta E/|a|+1-n$ and $a = 2n-1$, yields

$$\begin{aligned}
\frac{\Gamma(i\Delta E/|a|+n)}{\Gamma(i\Delta E/|a|+1-n)} &= \prod_{j=0}^{2n-2}(i\Delta E/|a|+1-n+j) \\
&= \prod_{k=-(n-1)}^{n-1}(i\Delta E/|a|+k) \\
&= \frac{|a|}{i\Delta E}\prod_{k=0}^{n-1}(i\Delta E/|a|+k)(i\Delta E/|a|-k) \\
&= (-1)^n\frac{|a|}{i\Delta E}\prod_{k=0}^{n-1}\left[(\Delta E/a)^2+k^2\right] \\
&= \left(\frac{i\Delta E}{|a|}\right)^{2n-1}\prod_{k=0}^{n-1}\left[1+k^2\left(\frac{a}{\Delta E}\right)^2\right].
\end{aligned} \tag{9.9}$$

Utilizing the above expression, along with the double factorial identity $(2x)!! = 2^x(x)!$, we finalize the computation of the acceleration-induced transition rate. Thus

$$\Gamma(\Delta E,\eta) = G_n^2\left(\frac{\Delta E}{\pi}\right)^{2n-1}\frac{1}{(4n-2)!!}\prod_{k=0}^{n-1}\left[1+k^2\left(\frac{a}{\Delta E}\right)^2\right]\frac{1}{e^{2\pi\Delta E/|a|}-1}. \tag{9.10}$$

The above transition rates are characterized by a bosonic distribution along with the integer indexed polynomial of multiplicity. Normalizing the rates to the multiplicity-dependent coupling via $\tilde{\Gamma} = \Gamma/G_n^2$, we explicitly compute the normalized rates for the first five multiplicities. Hence

$$\begin{aligned}
\tilde{\Gamma}_1(\Delta E, a) &= \frac{\Delta E}{2\pi}\frac{1}{e^{2\pi\Delta E/|a|}-1} \\
\tilde{\Gamma}_2(\Delta E, a) &= \frac{\Delta E^3}{48\pi^3}\frac{1+\left(\frac{a}{\Delta E}\right)^2}{e^{2\pi\Delta E/|a|}-1} \\
\tilde{\Gamma}_3(\Delta E, a) &= \frac{\Delta E^5}{3840\pi^5}\frac{1+5\left(\frac{a}{\Delta E}\right)^2+4\left(\frac{a}{\Delta E}\right)^4}{e^{2\pi\Delta E/|a|}-1} \\
\tilde{\Gamma}_4(\Delta E, a) &= \frac{\Delta E^7}{645120\pi^7}\frac{1+14\left(\frac{a}{\Delta E}\right)^2+49\left(\frac{a}{\Delta E}\right)^4+36\left(\frac{a}{\Delta E}\right)^6}{e^{2\pi\Delta E/|a|}-1} \\
\tilde{\Gamma}_5(\Delta E, a) &= \frac{\Delta E^9}{185794560\pi^9}\times \\
&\quad \frac{1+30\left(\frac{a}{\Delta E}\right)^2+273\left(\frac{a}{\Delta E}\right)^4+820\left(\frac{a}{\Delta E}\right)^6+576\left(\frac{a}{\Delta E}\right)^8}{e^{2\pi\Delta E/|a|}-1}.
\end{aligned} \tag{9.11}$$

The $n = 1$ case is the standard result for computing the transition rate of an Unruh-DeWitt detector. We should also mention that the acceleration-dependent lifetime is easily computed via $\tau = 1/\Gamma$. We plot (see Figs. 9.1 and 9.2) the transition rates for acceleration-induced decay and excitation respectively. The fact that the excitation rate rapidly goes to zero, in the inertial limit, reflects the infinite lifetime for such processes. Moreover, it should be noted that there is an acceleration-dependent crossover scale where one multiplicity dominates the transition process. The next section deals specifically with these crossovers.

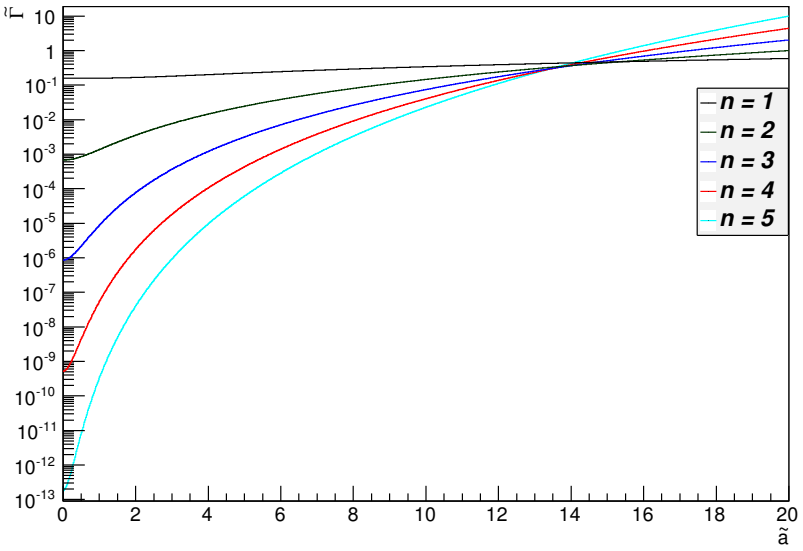

Figure 9.1: The normalized transition rates, Eq. (9.11), with $\tilde{a} = |a|/\Delta E$ and $\Delta E = -1$.

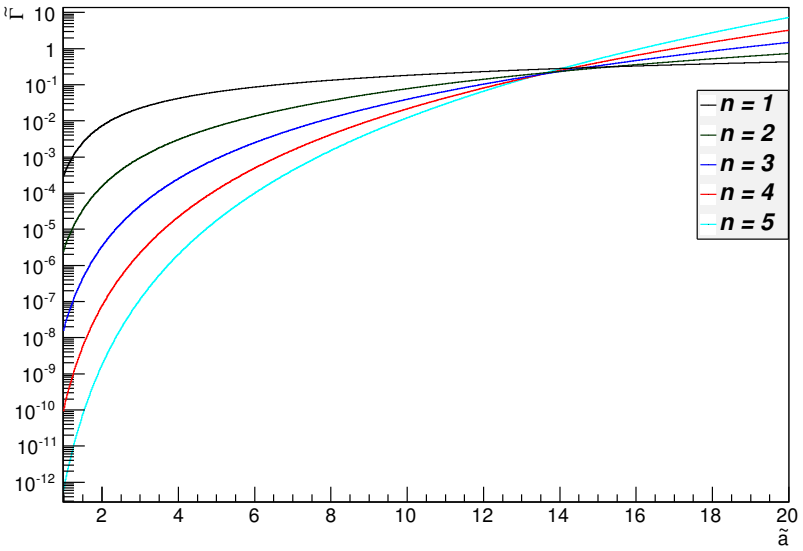

Figure 9.2: The normalized transition rates, Eq. (9.11), with $\tilde{a} = |a|/\Delta E$ and $\Delta E = 1$.

9.2 Multiplicity

In this section we compute the dominant multiplicity as a function of acceleration. Specifically, for final states which contain either n or m Minkowski particles, we ask when the transition rate for an n-particle final state is greater than an m-particle final state. This will enable us to characterize the acceleration scale which selects a specific transition when there are multiple decay pathways. Let us begin by computing the inertial limit of the decay rates. This enables us to fix the couplings G_n^2 to that of the inertial decay rate λ_n. For decays we have $\Delta E < 0$ and taking the limit $a \to 0$ of the transition rate, Eq. (9.10), yields

$$\begin{aligned} \lambda_n &= G_n^2 \left(\frac{\Delta E}{\pi}\right)^{2n-1} \frac{1}{(4n-2)!!} \\ \Rightarrow G_n^2 &= \lambda_n \left(\frac{\pi}{\Delta E}\right)^{2n-1} (4n-2)!!. \end{aligned} \tag{9.12}$$

In terms of the dimensionless acceleration $\tilde{a} = |a|/\Delta E$, the crossover scale, i.e. when $\Gamma_n = \Gamma_m$, can then be computed in terms of the inertial rates. Hence

$$\begin{aligned} \Gamma_n &= \Gamma_m \\ \lambda_n \prod_{k=0}^{n-1} \left[1 + k^2 \tilde{a}^2\right] &= \lambda_m \prod_{j=0}^{m-1} \left[1 + j^2 \tilde{a}^2\right]. \end{aligned} \tag{9.13}$$

The ratio of the inertial decay rates λ_m/λ_n is equivalent to the ratio of the branching fractions $Br_m/Br_n \equiv g$ of each decay pathway [38]. Assuming $n > m$ we find

$$\begin{aligned}
\lambda_n \prod_{k=0}^{n-1} \left[1 + k^2\tilde{a}^2\right] &= \lambda_m \prod_{j=0}^{m-1} \left[1 + j^2\tilde{a}^2\right] \\
\prod_{k=0}^{n-1} \left[1 + k^2\tilde{a}^2\right] &= g \prod_{j=0}^{m-1} \left[1 + j^2\tilde{a}^2\right] \\
\prod_{k=m}^{n-1} \left[1 + k^2\tilde{a}^2\right] &= g. \qquad (9.14)
\end{aligned}$$

The above equation defines the acceleration scale at which an n-particle multiplicity final state will dominate the m-particle multiplicity final state. We now examine in more detail the cases when $\tilde{a}k \gg 1$, $\tilde{a}k \ll 1$, $n = m+1$, and $n = m+2$. For the case of large acceleration, i.e. $\tilde{a}k \gg 1$, we find

$$\begin{aligned}
g &= \prod_{k=m}^{n-1} \left[1 + k^2\tilde{a}^2\right] \\
g &= \tilde{a}^{2(n-m)} \prod_{k=m}^{n-1} k^2 \\
g &= \tilde{a}^{2(n-m)} \left[\frac{(n-1)!}{(m-1)!}\right]^2 \\
\Rightarrow \tilde{a}_\uparrow &= \left[g \left[\frac{(m-1)!}{(n-1)!}\right]^2\right]^{1/(2(n-m))} . \qquad (9.15)
\end{aligned}$$

In the case of small acceleration, i.e. $\tilde{a}k \ll 1$, we make use of the properties of logarithms to simplify the computation. Hence

$$
\begin{aligned}
g &= \prod_{k=m}^{n-1}\left[1+k^2\tilde{a}^2\right] \\
\ln(g) &= \ln\left(\prod_{k=m}^{n-1}\left[1+k^2\tilde{a}^2\right]\right) \\
\ln(g) &= \sum_{k=m}^{n-1}\ln\left[1+k^2\tilde{a}^2\right] \\
\ln(g) &= \sum_{k=m}^{n-1}k^2\tilde{a}^2 \\
g &= 1+\tilde{a}^2\sum_{k=m}^{n-1}k^2
\end{aligned} \tag{9.16}
$$

The last line followed from Taylor expanding the resultant exponential. The sum of squares evaluates to $\sum_{k=m}^{n-1}k^2 = \frac{1}{6}(n-m)-\frac{1}{2}(n^2-m^2)+\frac{1}{3}(n^3-m^3)$. Thus the acceleration scale for multiplicity transitions at low acceleration is given by

$$
\tilde{a}_{\downarrow} = \sqrt{\frac{g-1}{\frac{1}{6}(n-m)-\frac{1}{2}(n^2-m^2)+\frac{1}{3}(n^3-m^3)}}. \tag{9.17}
$$

It should be noted that the above formula is most applicable for two decay pathways with nearly identical branching fractions, i.e. $g \sim 1$. The case when $n-m=1$ can be used to characterize the emission of an extra photon in the decay process. We can trivially solve for the acceleration in this case. Hence

$$
\tilde{a}_1 = \sqrt{\frac{g-1}{(n-1)^2}}. \tag{9.18}
$$

The case when $n-m=2$ can characterize the emission of an additional particle-antiparticle pair during the decay process. This case can also be solved exactly. Hence

$$
\begin{aligned}
g &= \prod_{k=n-2}^{n} \left[1 + k^2 \tilde{a}^2\right] \\
g &= \left[1 + (n-1)^2 \tilde{a}^2\right] \left[1 + (n-2)^2 \tilde{a}^2\right] \\
\Rightarrow \tilde{a}_2 &= \left[\frac{\sqrt{[(n-1)^2 + (n-2)^2]^2 + 4(g-1)(n-1)^2(n-2)^2} - [(n-1)^2 + (n-2)^2]}{2(n-1)^2(n-2)^2} \right]^{1/2}
\end{aligned} \tag{9.19}
$$

The above acceleration scales can be used to fine-tune a system to select a preferred decay pathway and also, if the acceleration of the system is known, predict the relevant branching fractions of the system under study. In the next section we shall analyze the power radiated away by an accelerated particle.

9.3 Power Radiated

In order to compute the power emitted by the ith particle $\mathcal{S}_i$ we use the energy weighted Wightman function $\mathcal{G}^{\pm}$ for that particle in the generalized transition rate from Eq. (6.16). Thus

$$
\begin{aligned}
\Gamma &= G_n^2 \frac{1}{a} \int d\xi e^{-i\Delta E \xi / a} \prod_{m=1}^{n} G_m^{\pm}[x', x]_\eta \\
\Rightarrow \mathcal{S}_i &= G_n^2 \frac{1}{a} \int d\xi e^{-i\Delta E \xi / a} \mathcal{G}_i^{\pm}[x', x]_\eta \prod_{m \neq i}^{n-1} G_m^{\pm}[x', x]_\eta .
\end{aligned} \tag{9.20}
$$

Note that we separated out the energy weighted Wightman function of the ith particle. Recalling the explicit forms of the appropriate Wightman functions, Eqs. (8.5) and (8.7), the power radiated away by the ith particle simplifies to

$$\begin{aligned}
\mathcal{S}_i &= G_n^2 \frac{1}{a} \int d\xi e^{-i\Delta E \xi/a} \mathcal{G}_i^{\pm}[x', x]_\eta \prod_{m \neq i}^{n-1} G_m^{\pm}[x', x]_\eta \\
&= G_n^2 \frac{1}{a} \int d\xi e^{-i\Delta E \xi/a} \left[-\frac{a^3}{i(4\pi)^2} \frac{1}{\sinh^3 [\xi/2 - \mathrm{sgn}\,(a) i\epsilon]} \right] \times \\
&\quad \left[-\frac{a^2}{(4\pi)^2} \frac{1}{\sinh^2 [\xi/2 - \mathrm{sgn}\,(a) i\epsilon]} \right]^{n-1} \\
&= -G_n^2 4\pi \left(\frac{ia}{4\pi} \right)^{2n+1} \frac{1}{a} \int d\xi \frac{e^{-i\Delta E \xi/a}}{\sinh^{2n+1} [\xi/2 - \mathrm{sgn}\,(a) i\epsilon]}. \qquad (9.21)
\end{aligned}$$

Again, with the same rescaling $\xi \to \mathrm{sgn}\,(a)\xi$, the integral is invariant under the change of sign of the acceleration. Thus we let $\mathrm{sgn}\,(a) = 1$ as before. Hence

$$\mathcal{S}_i = -G_n^2 4\pi \left(\frac{i|a|}{4\pi} \right)^{2n+1} \frac{1}{|a|} \int d\xi \frac{e^{-i\Delta E \xi/|a|}}{\sinh^{2n+1} [\xi/2 - i\epsilon]}. \qquad (9.22)$$

Note that we find a pole structure similar to the transition rate in the absence of the regulator, this time with poles of order $2n+1$ at $\xi = 2\pi i\sigma$ with integer $\sigma \geq 0$. Using the same computational machinery as before, we employ the change of variables as the previous section, $w = e^{\xi}$. Thus

$$\begin{aligned}
\mathcal{S}_i &= -G_n^2 4\pi \left(\frac{i|a|}{4\pi} \right)^{2n+1} \frac{1}{|a|} \int d\xi \frac{e^{-i\Delta E \xi/|a|}}{\sinh^{2n+1} [\xi/2 - i\epsilon]} \\
&= -G_n^2 4\pi \left(\frac{i|a|}{2\pi} \right)^{2n+1} \frac{1}{|a|} \int d\xi \frac{e^{-i\Delta E \xi/|a|}}{[e^{\xi/2} - e^{-\xi/2}]^{2n+1}} \\
&= -G_n^2 4\pi \left(\frac{i|a|}{2\pi} \right)^{2n+1} \frac{1}{|a|} \int dw \frac{w^{-i\Delta E/|a| + n - 1/2}}{[w-1]^{2n+1}}. \qquad (9.23)
\end{aligned}$$

Examining the above integral in a similar manner as in the last section we note that it is still of the form $\frac{w^{-i\beta+\gamma}}{[w-1]^{\delta}}$ but with odd integer δ and with γ being an odd integer multiple of $1/2$. Let us also note that $\gamma - \delta$ will also be an odd integer multiple of $1/2$. The effect

of this will be an alternating sign in the sum over the residues leading to a different thermal distribution. Hence

$$\begin{aligned}
\int dw \frac{w^{-i\beta+\gamma}}{[w-1]^{\delta}} &= \frac{2\pi i}{(\delta-1)!}\sum_{\sigma=0}^{\infty}\frac{d^{\delta-1}}{dw^{\delta-1}}\left[[w-1]^{\delta}\,\frac{w^{-i\beta+\gamma}}{[w-1]^{\delta}}\right]_{w=e^{i2\pi\sigma}} \\
&= \frac{2\pi i}{(\delta-1)!}\frac{\Gamma(1-i\beta+\gamma)}{\Gamma(-i\beta+\gamma-\delta+2)}\sum_{\sigma=0}^{\infty}\left[w^{-i\beta+\gamma-\delta+1}\right]_{w=e^{i2\pi\sigma}} \\
&= \frac{2\pi i}{(\delta-1)!}\frac{\Gamma(1-i\beta+\gamma)}{\Gamma(-i\beta+\gamma-\delta+2)}\sum_{\sigma=0}^{\infty}e^{2\pi\sigma\beta+i2\pi\sigma(\gamma-\delta)} \\
&= \frac{2\pi i}{(\delta-1)!}\frac{\Gamma(1-i\beta+\gamma)}{\Gamma(-i\beta+\gamma-\delta+2)}\frac{1}{e^{2\pi\beta}+1} \\
&= \frac{2\pi i}{(\delta-1)!}\frac{\Gamma(i\beta-\gamma+\delta-1)}{\Gamma(i\beta-\gamma)}\frac{1}{e^{2\pi\beta}+1}. \qquad (9.24)
\end{aligned}$$

Again we used the properties of δ and γ to manipulate the gamma functions in the last line. Then, utilizing the above formula, the integral in Eq. (9.23) yields

$$\int dw \frac{w^{-i\Delta E/|a|+n-1/2}}{[w-1]^{2n+1}} = \frac{2\pi i}{(2n)!}\frac{\Gamma(i\Delta E/|a|+n+1/2)}{\Gamma(i\Delta E/|a|+1/2-n)}\frac{1}{e^{2\pi\Delta E/|a|}+1} \qquad (9.25)$$

The expression for the power radiated by the ith particle is then given by

$$\mathcal{S}_i = -G_n^2 4\pi\left(\frac{i|a|}{2\pi}\right)^{2n+1}\frac{1}{|a|}\frac{2\pi i}{(2n)!}\frac{\Gamma(i\Delta E/|a|+n+1/2)}{\Gamma(i\Delta E/|a|+1/2-n)}\frac{1}{e^{2\pi\Delta E/|a|}+1}. \qquad (9.26)$$

We again use the Pochhammer identity $\frac{\Gamma(x+a)}{\Gamma(x)} = \prod_{j=0}^{a-1}(x+j)$ with the identifications $x = i\Delta E/|a| + 1/2 - n$ and $a = 2n$. As such, the above gamma functions yield a cleaner expression. Thus

$$\begin{aligned}
\frac{\Gamma(i\Delta E/|a|+n+1/2)}{\Gamma(i\Delta E/|a|+1/2-n)} &= \prod_{j=0}^{2n-1}(i\Delta E/|a|+1/2-n+j) \\
&= \prod_{\ell_{odd}=-(2n-1)}^{2n-1}(i\Delta E/|a|+\ell/2) \\
&= \prod_{\ell_{odd}=1}^{2n-1}(i\Delta E/|a|+\ell/2)(i\Delta E/|a|-\ell/2) \\
&= \left(\frac{i\Delta E}{|a|}\right)^{2n}\prod_{\ell_{odd}=1}^{2n-1}\left[1+(\ell/2)^2\left(\frac{a}{\Delta E}\right)^2\right] \\
&= \left(\frac{i\Delta E}{|a|}\right)^{2n}\prod_{k=0}^{n-1}\left[1+\left(\frac{2k+1}{2}\right)^2\left(\frac{a}{\Delta E}\right)^2\right]. \qquad (9.27)
\end{aligned}$$

Using the same double factorial identity $(2x)!! = 2^x(x)!$, we find that the power radiated by the ith particle is given by

$$\mathcal{S}_i = G_n^2 4\pi\left(\frac{\Delta E}{\pi}\right)^{2n}\frac{1}{(4n)!!}\prod_{k=0}^{n-1}\left[1+\left(\frac{2k+1}{2}\right)^2\left(\frac{a}{\Delta E}\right)^2\right]\frac{1}{e^{2\pi\Delta E/|a|}+1}. \qquad (9.28)$$

We see that the above power radiated is characterized by a fermionic distribution as well as the half-integer indexed polynomial of multiplicity. The root cause of this change in statistics is the fact that we had poles of odd integer order rather than even integer order as in the transition rate. The first few normalized power functions, $\tilde{\mathcal{S}} = \mathcal{S}/G_n^2$, are then given by

$$
\begin{aligned}
\tilde{\mathcal{S}}_1(\Delta E, a) &= \frac{\Delta E^2}{2\pi}\frac{1+\frac{1}{4}\left(\frac{a}{\Delta E}\right)^2}{e^{2\pi\Delta E/|a|}+1} \\
\tilde{\mathcal{S}}_2(\Delta E, a) &= \frac{\Delta E^4}{96\pi^3}\frac{1+\frac{5}{2}\left(\frac{a}{\Delta E}\right)^2+\frac{9}{16}\left(\frac{a}{\Delta E}\right)^4}{e^{2\pi\Delta E/|a|}+1} \\
\tilde{\mathcal{S}}_3(\Delta E, a) &= \frac{\Delta E^6}{11520\pi^5}\frac{1+\frac{35}{4}\left(\frac{a}{\Delta E}\right)^2+\frac{259}{16}\left(\frac{a}{\Delta E}\right)^4+\frac{225}{64}\left(\frac{a}{\Delta E}\right)^6}{e^{2\pi\Delta E/|a|}+1} \\
\tilde{\mathcal{S}}_4(\Delta E, a) &= \frac{\Delta E^8}{2580480\pi^7}\times \\
&\quad \frac{1+21\left(\frac{a}{\Delta E}\right)^2+\frac{987}{8}\left(\frac{a}{\Delta E}\right)^4+\frac{3229}{16}\left(\frac{a}{\Delta E}\right)^6+\frac{11025}{256}\left(\frac{a}{\Delta E}\right)^8}{e^{2\pi\Delta E/|a|}+1}.
\end{aligned}
\tag{9.29}
$$

We note that the $n = 1$ case, along with $\Delta E = 0$ as determined in [41], reproduces the known a^2 dependence for the power emitted by bremsstrahlung. The plots of the power radiated for both transitions downn and up in Rindler energy can be found in Figs. 9.3 and 9.4 respectively. Note that the power radiated diverges in the case of a positive energy transitions. This reflects that inertially stable particles do not transition up in energy and radiate energy away.

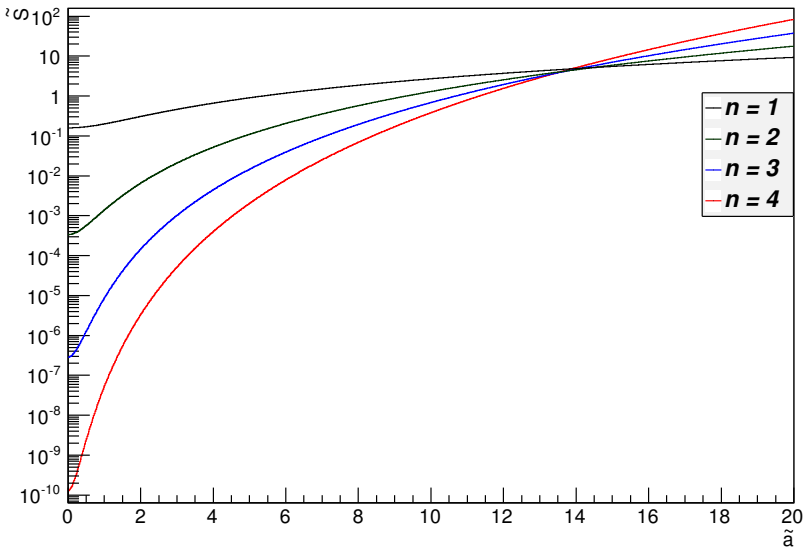

Figure 9.3: The normalized power radiated, Eq. (9.29), with $\tilde{a} = a/\Delta E$ and $\Delta E = -1$.

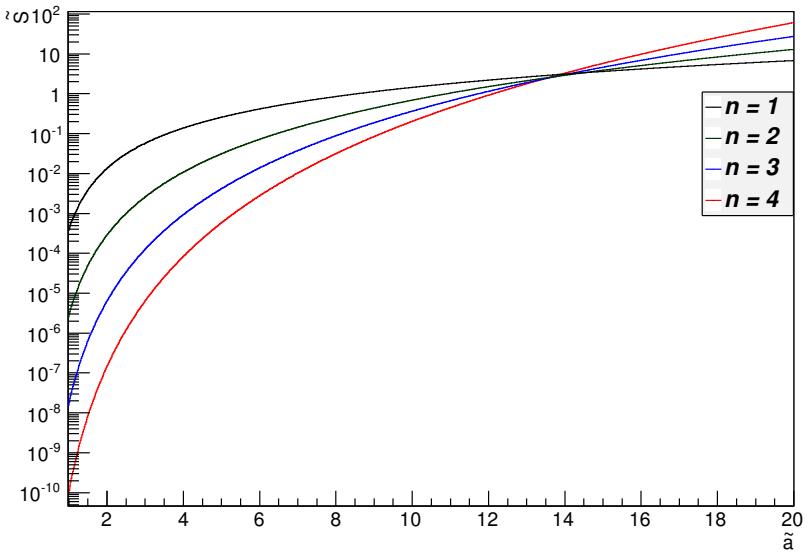

Figure 9.4: The normalized power radiated, Eq. (9.29), with $\tilde{a} = a/\Delta E$ and $\Delta E = 1$.

9.4 Energy Spectra

Utilizing the same prescription, we now endeavor to compute the energy spectrum of the ith Minkowski particle emitted in the transition process. The transition rate from Eq. (6.16) characterizes the probability per unit time that a transition will occur. The differential transition per unit energy then characterizes how the probability of emission changes with energy, i.e. the spectra. Therefore we begin by taking the derivative with respect to the ith particle's proper energy. Hence

$$\begin{aligned}\frac{d\Gamma}{d\tilde{\omega}_i} &= \frac{d}{d\tilde{\omega}_i} G_n^2 \frac{1}{a} \int d\xi e^{-i\Delta E\xi/a} \prod_{m=1}^{n} G_m^{\pm}[x', x]_\eta \\ &= G_n^2 \frac{1}{a} \int d\xi e^{-i\Delta E\xi/a} \frac{d}{d\tilde{\omega}_i} G_i^{\pm}[x', x]_\eta \prod_{m\neq i}^{n} G_m^{\pm}[x', x]_\eta. \end{aligned} \tag{9.30}$$

Again, we have separated out the relevant variant of the Wightman function for the

observable we are calculating. Referring to Eqs. (8.5) and (8.9) for the Wightman function and its derivative respectively, the above energy spectra reduce to a more convenient form. Hence

$$\begin{aligned}
\frac{d\Gamma}{d\tilde{\omega}_i} &= G_n^2 \frac{1}{a} \int d\xi e^{-i\Delta E\xi/a} \frac{d}{d\tilde{\omega}_i} G_i^{\pm}[x', x]_\eta \prod_{m\neq i}^{n} G_m^{\pm}[x', x]_\eta \\
&= G_n^2 \frac{1}{a} \int d\xi e^{-i\Delta E\xi/a} \frac{\tilde{\omega}}{(2\pi)^2} e^{-i\tilde{\omega}a\xi} \left[-\frac{a^2}{(4\pi)^2} \frac{1}{\sinh^2\left[\xi/2 - \mathrm{sgn}\,(a) i\epsilon\right]} \right]^{n-1} \\
&= G_n^2 \frac{\tilde{\omega}}{(2\pi)^2} \left(\frac{ia}{4\pi} \right)^{2(n-1)} \frac{1}{|a|} \int d\xi \frac{e^{-i(\Delta E+\tilde{\omega})\xi/|a|}}{\sinh^{2(n-1)}\left[\xi/2 - i\epsilon\right]}. \qquad (9.31)
\end{aligned}$$

Note in the last line that we enforced the invariance of the above integral under a change in sign of the acceleration. We have encountered similar integrals for both the transition rate and the power radiated. It is worth noting that the difference is that the frequency variable which we are Fourier transforming with respect to has shifted via $\Delta E \to \Delta E + \tilde{\omega}$. We can evaluate the $n = 1$ case quite easily at this point. Hence

$$\begin{aligned}
\left(\frac{d\Gamma}{d\tilde{\omega}} \right)_{n=1} &= G_1^2 \frac{\tilde{\omega}}{(2\pi)^2} \frac{1}{|a|} \int d\xi e^{-i(\Delta E+\tilde{\omega})\xi/|a|} \\
&= G_1^2 \frac{\tilde{\omega}}{2\pi} \delta(\Delta E + \tilde{\omega}). \qquad (9.32)
\end{aligned}$$

The above expression is merely a statement analogous to Fermi's golden rule. Note that the presence of the delta function serves to enforce conservation of energy in the case of one particle emission. This implies that when there is only one Minkowski particle emitted that the radiated particle, as measured in an inertial frame instantaneously at rest with the accelerated particle, carries away the total change in the Rindler space energy. For the higher multiplicity cases we rid ourselves of the regulator and note the similar pole structure of order $2(n-1)$ when $\xi = 2\pi i\sigma$ with integer $\sigma \geq 1$. Finally, we make the same change of

variables $w = e^{i\xi}$ to obtain

$$\begin{aligned}
\frac{d\Gamma}{d\tilde{\omega}} &= G_n^2 \frac{\tilde{\omega}}{(2\pi)^2} \left(\frac{ia}{4\pi}\right)^{2(n-1)} \frac{1}{|a|} \int d\xi \frac{e^{-i(\Delta E+\tilde{\omega})\xi/|a|}}{\sinh^{2(n-1)}\left[\xi/2 - i\epsilon\right]} \\
&= G_n^2 \frac{\tilde{\omega}}{(2\pi)^2} \left(\frac{ia}{2\pi}\right)^{2(n-1)} \frac{1}{|a|} \int d\xi \frac{e^{-i(\Delta E+\tilde{\omega})\xi/|a|}}{\left[e^{\xi/2} - e^{-\xi/2}\right]^{2(n-1)}} \\
&= G_n^2 \frac{\tilde{\omega}}{(2\pi)^2} \left(\frac{ia}{2\pi}\right)^{2(n-1)} \frac{1}{|a|} \int dw \frac{w^{-i(\Delta E+\tilde{\omega})/|a|+n-2}}{\left[w-1\right]^{2(n-1)}}. \qquad (9.33)
\end{aligned}$$

The above integral can be evaluated using the integration formula from Eq. (44) provided we make the relevant identification of the indices β, γ, and δ. Moreover, since the γ is an integer and δ is an even integer, the Pochhammer identity holds as well. Thus, by making the identification of $n \to n-1$ from the transition rate, we may merely quote the final form of the spectra. Hence

$$\begin{aligned}
\frac{d\Gamma}{d\tilde{\omega}} &= \frac{G_n^2 \tilde{\omega}}{(2\pi)^2} \left(\frac{\Delta E + \tilde{\omega}}{\pi}\right)^{2n-3} \frac{1}{(4n-6)!!} \times \\
&\prod_{k=0}^{n-2} \left[1 + k^2 \left(\frac{a}{\Delta E + \tilde{\omega}}\right)^2\right] \frac{1}{e^{2\pi(\Delta E+\tilde{\omega})/|a|} - 1}. \qquad (9.34)
\end{aligned}$$

Here we find a bosonic thermal distribution with a chemical potential and a polynomial of multiplicity characterized by an integer index. It is interesting to note that the total change in Rindler space energy is identified as the chemical potential of the thermal bath. Recalling the above spectra gives the probability of emission per unit energy per unit time, we note that it needs to be normalized via $\frac{1}{\Gamma}\frac{d\Gamma}{d\tilde{\omega}} = \mathcal{N}$. This serves to scale the overall spectra and remove the effective differential time averaging. Below we write out the first few spectra normalized to the coupling via $\frac{1}{G_n^2}\frac{d\Gamma}{d\tilde{\omega}} = \tilde{\mathcal{N}}$ as in the previous sections. Hence

$$
\begin{aligned}
\tilde{\mathcal{N}}_1(\Delta E, a, \tilde{\omega}) &= \frac{\tilde{\omega}}{2\pi}\delta(\Delta E + \tilde{\omega}) \\
\tilde{\mathcal{N}}_2(\Delta E, a, \tilde{\omega}) &= \frac{\tilde{\omega}(\Delta E + \tilde{\omega})}{8\pi^3}\frac{1}{e^{2\pi(\Delta E+\tilde{\omega})/|a|}-1} \\
\tilde{\mathcal{N}}_3(\Delta E, a, \tilde{\omega}) &= \frac{\tilde{\omega}(\Delta E + \tilde{\omega})^3}{192\pi^5}\frac{1+\left(\frac{a}{\Delta E+\tilde{\omega}}\right)^2}{e^{2\pi(\Delta E+\tilde{\omega})/|a|}-1} \\
\tilde{\mathcal{N}}_4(\Delta E, a, \tilde{\omega}) &= \frac{\tilde{\omega}(\Delta E + \tilde{\omega})^5}{15360\pi^7}\frac{1+5\left(\frac{a}{\Delta E+\tilde{\omega}}\right)^2+4\left(\frac{a}{\Delta E+\tilde{\omega}}\right)^4}{e^{2\pi(\Delta E+\tilde{\omega})/|a|}-1} \\
\tilde{\mathcal{N}}_5(\Delta E, a, \tilde{\omega}) &= \frac{\tilde{\omega}(\Delta E + \tilde{\omega})^7}{2580480\pi^9}\frac{1+14\left(\frac{a}{\Delta E+\tilde{\omega}}\right)^2+49\left(\frac{a}{\Delta E+\tilde{\omega}}\right)^4+36\left(\frac{a}{\Delta E+\tilde{\omega}}\right)^6}{e^{2\pi(\Delta E+\tilde{\omega})/|a|}-1}. \quad (9.35)
\end{aligned}
$$

In Figs. 9.5 and 9.6 we show the spectra normalized by the transition rate, i.e. $\mathcal{N}_i$, of the ith particle emitted for both transitions down and up in Rindler energy respectively. It is interesting to note that regardless of the sign of the transition energy, we find Planck-like spectra for all multiplicities greater than 1.

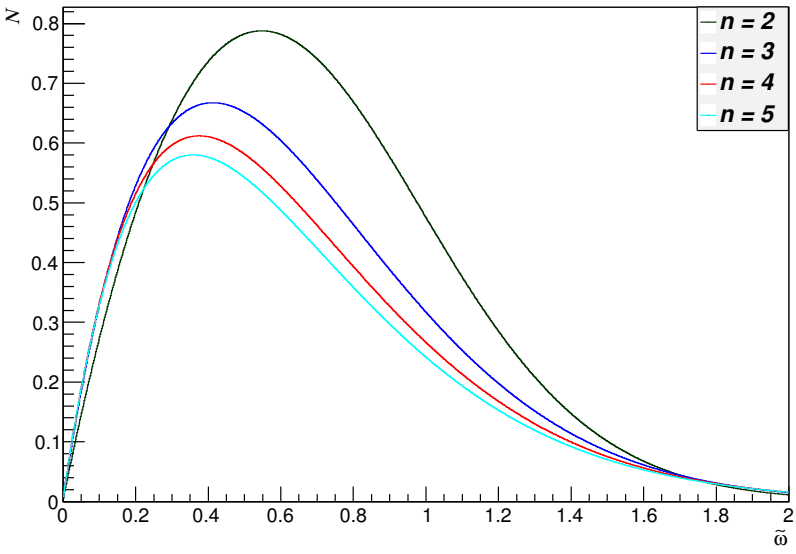

Figure 9.5: The normalized spectra, $\mathcal{N}_i = \frac{1}{\Gamma}\frac{d\Gamma}{d\tilde{\omega}_i}$, with $a = 1$ and $\Delta E = -1$.

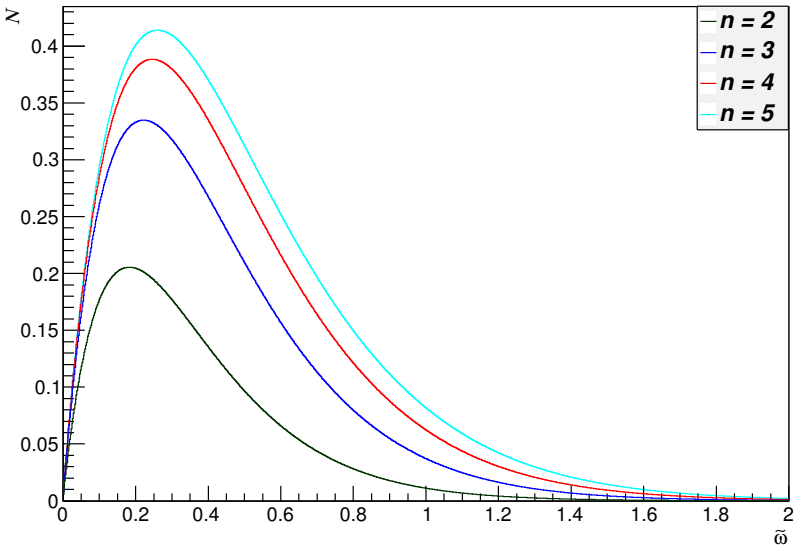

Figure 9.6: The normalized spectra, $\mathcal{N}_i = \frac{1}{\Gamma}\frac{d\Gamma}{d\tilde{\omega}_i}$, with $a = 1$ and $\Delta E = 1$.

9.5 Displacement Law

To better characterize the spectra, we can also look at the peak energy of the emitted Minkowski particle for each multiplicity greater than 1. In the interest of determining the maximum of each peak via setting the derivative equal to zero, we can drop all prefactors and focus only on the energy dependence. Labeling the spectra polynomial of multiplicity $\mathcal{M}_n = \prod_{k=0}^{n-2}\left[1 + k^2\left(\frac{a}{\Delta E+\tilde{\omega}}\right)^2\right]$ we have

$$\tilde{\mathcal{N}} \sim \frac{\tilde{\omega}(\Delta E + \tilde{\omega})^{2n-3}\mathcal{M}_n}{e^{2\pi(\Delta E+\tilde{\omega})/|\tilde{a}_\eta|} - 1}. \tag{9.36}$$

Then, by taking the derivative with respect to $\tilde{\omega}$ and setting it equal to zero, we find

$$\left[(\Delta E+\tilde{\omega})+\tilde{\omega}(2n-3)+\tilde{\omega}(\Delta E+\tilde{\omega})\frac{\mathcal{M'}_n}{\mathcal{M}_n}\right]\left(e^{2\pi(\Delta E+\tilde{\omega})/|\tilde{a}_\eta|}-1\right)$$
$$-\tilde{\omega}(\Delta E+\tilde{\omega})\frac{2\pi}{|a|}e^{2\pi(\Delta E+\tilde{\omega})/|\tilde{a}_\eta|} = 0$$
$$\frac{xe^x}{e^x-1}-\left[\frac{1}{1-\frac{2\pi\Delta E}{|a|x}}+(2n-3)+\frac{|a|x}{2\pi}\frac{\mathcal{M'}_n}{\mathcal{M}_n}\right] = 0. \qquad (9.37)$$

Note in the last line that we defined the dimensionless parameter $x=\frac{2\pi}{|a|}(\Delta E+\tilde{\omega})$. Now we must evaluate the logarithmic derivative of the polynomial of multiplicity. Hence

$$\begin{aligned}
\frac{\mathcal{M'}_n}{\mathcal{M}_n} &= \frac{d}{d\tilde{\omega}}\ln\mathcal{M}_n \\
&= \frac{d}{d\tilde{\omega}}\ln\prod_{k=0}^{n-2}\left[1+k^2\left(\frac{a}{\Delta E+\tilde{\omega}}\right)^2\right] \\
&= \frac{d}{d\tilde{\omega}}\sum_{k=0}^{n-2}\ln\left[1+k^2\left(\frac{a}{\Delta E+\tilde{\omega}}\right)^2\right] \\
&= -\frac{2a^2}{(\Delta E+\tilde{\omega})^3}\sum_{k=0}^{n-2}\frac{k^2}{1+k^2\left(\frac{a}{\Delta E+\tilde{\omega}}\right)^2} \\
&= -\frac{2}{|a|}\left(\frac{2\pi}{x}\right)^3\sum_{k=0}^{n-2}\frac{k^2}{1+k^2\left(\frac{2\pi}{x}\right)^2}. \qquad (9.38)
\end{aligned}$$

Then, combining the logarithmic derivative with the Eq. (9.37), we obtain our numerically solvable displacement law which allows us to determine the peak energy of the emitted Minkowski particles. Hence

$$\frac{xe^x}{e^x-1}-\left[\frac{1}{1-\frac{2\pi\Delta E}{|a|x}}+(2n-3)-2\left(\frac{2\pi}{x}\right)^2\sum_{k=0}^{n-2}\frac{k^2}{1+k^2\left(\frac{2\pi}{x}\right)^2}\right] = 0. \qquad (9.39)$$

Then, in terms of the numerically solved x, we find that the peak energy is given by

$$\tilde{\omega} = x\frac{|a|}{2\pi} - \Delta E. \tag{9.40}$$

Thus we have shown that the emitted particle's energy, in the limit of high acceleration or zero change in the Rindler space energy, is directly proportional to the accelerated temperature, i.e. $\tilde{\omega} = xt_a$. This is in agreement with Wien's displacement law but now with a more general transcendental equation to determine the displacement constant. Moreover, this establishes the fact that acceleration has an energy associated with it that is quantum mechanical in nature. By reinserting all relevant physical constants, we find the energy of acceleration E_a is given by

$$E_a = \frac{xa\hbar}{2\pi c}. \tag{9.41}$$

The acceleration dependence of the energy of the emitted particles would have a clear signature at sufficiently high accelerations. Advanced experimental systems could be coming online in the coming years that may be able to verify these effects [35].

Chapter 10

Conclusions

In this dissertation we have established a computational framework capable of computing various observables of a wide range of acceleration-induced particle physics processes. We utilized methods of field operators and Unruh-DeWitt detectors to carry out the analysis. Generalized analytic results of n-particle multiplicities into both Rindler and Minkowski spacetimes were obtained. To better analyze physically realistic settings, a time-dependent formalism was developed to compute the spacetime quantities that go into the Wightman functions and its variants. These were then used to compute the transition rate, multiplicity, power radiated, energy spectra, and displacement law for accelerated decays and excitations of arbitrary final state multiplicity. We found the transition rate, power, and spectra are characterized by integer and half-integer indexed polynomials and thermal distributions of both bosonic and fermionic statistics. The multiplicity showed that high accelerations favor the decay chain with the most amount of Minkowski space final state products and was applied to the electron-muon system. In computing the power, we were also able to recover the Larmor formula in the appropriate limit. For the spectra, we found the total change in Rindler space energy plays the role of a chemical potential of the thermal bath. The displacement law for the spectra predicts the peak energy of the emitted Minkowski particles have a proper energy proportional to the accelerated temperature; in direct analogy with

Wein's displacement law. To finalize, the combination of results presented here strengthens the idea that highly accelerated systems are inherently thermal and we have developed a framework to compute a wide range of experimental observables in anticipation of upcoming experiments.

Bibliography

[1] L. Parker and D. Toms, *Quantum Field Theory in Curved Spacetime: Quantized Fields and Gravity* (Cambridge University Press, Cambridge, England, 1982).

[2] L. H. Ford, *Quantum Field Theory in Curved Spacetime*, arXiv:gr-qc/9707062, (1997).

[3] R. M. Wald, *Quantum Field Theory in Curved Spacetime and Black Hole Thermodynamics* (Chicago Lectures in Physics, Chicago, United States, 1994).

[4] L. Parker, The Creation of Particles by the Expanding Universe, Ph.D. thesis, Harvard University, 1966; Nature (London) **261**, 20 (1976).

[5] L. Parker, Phys. Rev. **183**, 1075 (1969); Phys. Rev. D **3**, 346 (1971).

[6] L. Parker and I. Agullo, Phys. Rev. D **83**, 063526 (2011).

[7] I. Agullo, J. Navarro-Salas, G. J. Olmo, L. Parker, Phys. Rev. Lett. **103**, 061301 (2009); Gen. Relativ. Gravit. **41**, 2301 (2009).

[8] P. A. R. Ade et al. (BICEP2 Collaboration), Phys. Rev. Lett. **112**, 241101 (2014).

[9] C. L. Bennet et al. (WMAP Collaboration) arXiv:1212.5225 [astro-ph.CO]

[10] S. W. Hawking, Nature (London) **248**, 30 (1974); Commun. Math. Phys. **43**, 199 (1975).

[11] J.D. Bekenstein, Lettere al Nuovo Cimento, **4**, 737 (1972).

[12] B.P. Abbott et al. (LIGO Scientific Collaboration and Virgo Collaboration), Phys. Rev. Lett. **116**, 061102 (2016).

[13] M. D. Johnson et al. Science **350**, 6265 (2015).

[14] S. Weinfurtner et al. Phys. Rev. Lett. **106**, 021302 (2011).

[15] J. Steinhauer, Nature Physics **12**, 959 (2016).

[16] W. G. Unruh, Phys. Rev. D **14**, 870 (1976).

[17] S. A. Fulling, Phys. Rev. D **7**, 2850 (1973).

[18] P. C. W. Davies, Journal of Physics A. **8**, 609 (1975).

[19] G. Cozzella et al. arXiv:1701.03446 [gr-qc] (2017).

[20] P. Chen and T. Tajima, Phys. Rev. Lett. **83**, 256 (1999).

[21] I. Kaminer et al. Nature (London) **11**, 261 (2015).

[22] R. Muller, Phys. Rev. D **56**, 953 (1997).

[23] G. E. A. Matsas and D. A. T. Vanzella, Phys. Rev. D **59**, 094004 (1999).

[24] D. A. T. Vanzella and G. E. A. Matsas, Phys. Rev. D **63**, 014010 (2000)

[25] D. A. T. Vanzella and G. E. A. Matsas, Phys. Rev. Lett. **87**, 151301 (2001).

[26] N. Obadia and M. Milgrom, Phys. Rev. D **75**, 065006 (2007).

[27] D. Kothawala and T. Padmanabhan, Phys. Lett. B **690**, 201 (2010).

[28] L. C. Barbado and M. Visser, Phys. Rev. D **86**, 084011 (2012).

[29] M. H. Lynch, Phys. Rev. D **90**, 024049 (2014).

[30] M. H. Lynch, Phys. Rev. D **92**, 024019 (2015).

[31] B. S. DeWitt, Phys. Rept. **19**, 295 (1975).

[32] S. Takagi, Progress of Theoretical Physics Supplement **88**, 1 (1986).

[33] N. D. Birrell and P. C. W. Davies, *Quantum Field Theory in Curved Space* (Cambridge University Press, Cambridge, England, 1982).

[34] V. F. Mukhanov and S. Winitzki, *Introduction to Quantum Effects in Gravity* (Cambridge University Press, Cambridge, England, 2010).

[35] L. C. B. Crispino, A. Higuchi, and G. E. A. Matsas, Rev. Mod. Phys. **80**, 787 (2008).

[36] W. G. Unruh and R. M. Wald, Phys. Rev. D **29**, 1047 (1984).

[37] A. Lahiri and P. B. Pal, *A First Book in Quantum Field Theory* (Narosa Publishing House, New Delhi, India, 2000), 1st ed.

[38] J. Beringer *et al.* (Particle Data Group), Phys. Rev. D **86**, 010001 (2012).

[39] U. H. Gerlach, Phys. Rev. D **38**, 514 (1988).

[40] Simon J.A. Malham, *An Introduction to Asymptotic Analysis* (Heriot-Watt University, Edinburgh, UK, 2005).

[41] A Higuchi, G. E. A. Matsas, and D. Sudarsky, Phys. Rev. D. **45**, R3308 (1992); **46** 3450 (1992).

Curriculum Vitae

Education

- **2017** Ph.D. The University of Wisconsin-Milwaukee, Milwaukee, WI.
- **2011** M.A. SUNY Stony Brook, Stony Brook, NY.
- **2008** B.S. Angelo State University, San Angelo, TX.

Academic Experience

- **2015 - 2016** Visiting Graduate Fellow, Perimeter Institute for Theoretical Physics.
- **2012 - 2017** Graduate Teaching Assistant, The University of Wisconsin-Milwaukee.
- **2013 - 2014** Graduate Research Assistant, The University of Wisconsin-Milwaukee.
- **2010 - 2012** Graduate Research Assistant, SUNY Stony Brook.
- **2009 - 2010** Graduate Teaching Assistant SUNY Stony Brook.
- **2007** REU, Vanderbilt University.
- **2006** REU, The University of North Texas.
- **2006 - 2008** Undergraduate Researcher, Angelo State University.
- **2006 - 2008** Mathematics Dept. Tutor, Angelo State University.

Awards & Achievements

- **2017** Eli Lubkin Award, The University of Wisconsin-Milwaukee.
- **2016** Papastamatiou Award, The University of Wisconsin-Milwaukee.
- **2015** Visiting Graduate Fellowship, Perimeter Institute of Theoretical Physics.
- **2013** Summer Research Scholarship, The University of Wisconsin-Milwaukee.

- **2008** Presidential Award, Angelo State University.
- **2008** Mathematics MFT Perfect Score, Angelo State University.
- **2007** Carr Research Fellow, Angelo State University.
- **2007** Outstanding Student Presentation Award, Angelo State University.
- **2006** Outstanding Student Poster Award, Angelo State University.